Differential Regulation of Genes and Transcription Factors in Vascular Endothelial Cells Exposed to Uniform and Disturbed Laminar Shear Stress

by

Tobi Elaine Nagel

Bachelor of Science with Distinction, Stanford University, 1989

Submitted to the Harvard-MIT Division of Health Sciences and Technology
in Partial Fulfillment of the Requirements for the Degree of

DOCTOR OF PHILOSOPHY IN MEDICAL ENGINEERING

at the

Massachusetts Institute of Technology

June, 1997

Signature of Author_____
Harvard-MIT Division of Health Science and Technology
May, 1997

Certified by_____
Michael A. Gimbrone, Jr.
Professor of Pathology, Harvard Medical School
Thesis Supervisor

Certified by_____
Robert Langer
Professor of Chemical and Biomedical Engineering, MIT
Chairman, Thesis Committee

Accepted by_____
Martha L. Gray
Associate Professor of Electrical Engineering and Computer Science, MIT
Interim Co-Director, Harvard-MIT Division of Health Sciences and Technology

DIFFERENTIAL REGULATION OF GENES AND TRANSCRIPTION FACTORS IN VASCULAR ENDOTHELIAL CELLS EXPOSED TO UNIFORM AND DISTURBED LAMINAR SHEAR STRESS

by

Tobi Elaine Nagel

Submitted to the Harvard-MIT Division of Health Sciences and Technology
on May 23, 1997, in Partial Fulfillment of the Requirements for the Degree of
Doctor of Philosophy in Medical Engineering

ABSTRACT

Hemodynamic shear stress has been shown to induce various functional changes in vascular endothelium, many of which reflect alterations at the level of gene expression. We have utilized a class of endothelial-leukocyte adhesion molecules, including Intercellular Adhesion Molecule-1 (ICAM-1), Vascular Cell Adhesion Molecule-1 (VCAM-1), and E-selectin (ELAM-1) -- which are coordinately induced by soluble stimuli such as cytokines -- as model genes with which to investigate the shear stress parameters which regulate endothelial gene expression. These studies indicate that ICAM-1, but not VCAM-1 or E-selectin, is upregulated in endothelial cells exposed to uniform laminar shear stress, and this induction occurs at the levels of transcriptional activation, steady state message, and functional cell surface protein. In addition, using a disturbed laminar shear stress model -- designed to mimic *in vivo* flow patterns at sites predilected for atherosclerotic development, such as arterial bifurcations and curvatures -- we have shown that cytokine induction of VCAM-1, in contrast to ICAM-1 or E-selectin, is inhibited by preconditioning with disturbed, but not uniform laminar shear stress. Thus, this differential regulation of adhesion molecule expression by fluid shear stresses, in contrast to the coordinate pattern of induction by humoral stimuli, indicates that regional differences in biomechanical forces may represent important local modulators of endothelial gene regulation.

Work in our laboratory and others has identified several "shear stress response elements" within the promoters of certain endothelial genes which mediate the shear stress induction of those genes by functionally interacting with previously identified transcription factors, including nuclear factor-κB (NF-κB), early growth response-1 (Egr-1), and activator protein-1 (AP-1, comprised of c-Jun/c-Jun and c-Jun/c-Fos protein dimers). With the aid of newly developed image analysis techniques, we have demonstrated that endothelial cells exposed to disturbed laminar shear stress exhibit increased levels of nuclear localized NF-κB, Egr-1, c-Jun, and c-Fos, as compared with cells subjected to uniform flow and static conditions. Taken together, these data suggest that the spectrum of biomechanical forces encountered in the circulatory system may represent important stimuli that are relevant to both the physiology and pathology of vascular endothelium.

Thesis Committee:
Michael A. Gimbrone, Jr., Professor of Pathology, Harvard Medical School (Adviser)
Robert Langer, Professor of Chemical & Biomedical Engineering, MIT (Committee Chairman)
C. Forbes Dewey, Jr., Professor of Mechanical Engineering, MIT
Rakesh K. Jain, Professor of Tumor Biology, Harvard Medical School

ACKNOWLEDGMENTS

As I complete the chapters of this thesis, I also complete a significant chapter in my life, and it has been a very rich one, mostly because of the people in my life. I am indebted to my adviser, Dr. Michael Gimbrone, for guiding me in my development as a scientist and for providing me with a wealth of resources, in terms of both laboratory supplies and outstanding colleagues with whom to interact. I am also deeply grateful to Dr. Nitzan Resnick, who served as my direct mentor during the first few years of my thesis research and who taught me so much about bench-top science as well as how to balance that science with other aspects of life. Dr. Forbes Dewey, in his co-advisory role, provided me with guidance from an engineering perspective, which helped to round out my training in this interdisciplinary field. Dr. Bob Langer served as both my academic adviser and thesis committee chairman, and I have greatly appreciated the counsel he has given me throughout my graduate career. I am also thankful to Dr. Rakesh Jain for his encouragement and insights as a member of my thesis committee.

Many members of the Vascular Research Division at Brigham and Women's Hospital have helped to make my experiments possible and the work enjoyable at the same time. Bill Atkinson worked side-by-side with me during my initial shear stress experiments and the development of the image analysis system, and I have also appreciated his serving as a great sounding board in my various decision-making processes. Kay Case provided me with endothelial cell cultures too numerous to count, especially single cord preparations, and I am thankful to both Kay and Bill for letting me take temporary residence in their laboratory and office during the final stages of my research. I am grateful to Alice Callahan for her diligence and sense of humor in helping me with all of the administrative paperwork that comes with being an MIT student conducting research at Brigham and Women's Hospital. Dick Fenner (as a consultant from MIT), together with Keith Anderson, provided invaluable assistance in maintaining the shear stress apparatuses. Dr. Jamie Topper allowed me to bounce numerous questions and ideas off of him, and I enjoyed working closely with both him and Scott Wasserman on our related shear stress projects. It was also a delight to share the laboratory for several years with Jeanne Kiely, Dr. Tony Rosenzweig, and Dr. Masayuki Yoshida. George Stravrakis was helpful with many of my staining protocols. I am thankful to Dr. Tucker Collins for educating me regarding the intricacies of gene regulation. Dr. Margaret Read was particularly helpful in teaching me about NF-κB regulatory mechanisms, as well as serving as an unofficial mentor.

I have been amazed at the personal support I have received from many friends throughout my graduate school experience. I have appreciated hours of laughter and encouragement shared with Anita Erler, and I am glad that she was a medical resident during the past few years, so that I could page her anytime of the day or night. Chi Huang has been particularly supportive during the final stages of my thesis, helping to keep me going during some long work days and boosting my spirits with his sense of humor. I have also appreciated the support of Don and Mary Martin, Anne O'Donnell, Lois Barndt, and Andrea Kirazian (with whom I will celebrate the completion of this thesis with a trip to Greece!), and many other friends too numerous to list. In addition, I have enjoyed the camaraderie of fellow HST students, especially Ann Celi, Chris Chen, Brian Benda, and Edwin Ozawa.

My family members have been a constant source of support for me. When I was in fifth grade, my parents stood at the edge of the soccer field and cheered their hearts out, and they have remained my greatest cheerleaders throughout this period of my life. I have appreciated the support and strength of my grandmother and, together with her, I wish my grandfather could have been here to share the final few years of my graduate experience. I am also thankful for my relationships with my aunt Coletta and uncle John, who have been like paternal grandparents to me.

Finally, I believe that the presence of all of these wonderful people in my life has not been just a chance occurrence, and I am thankful to God who has blessed me with these relationships and given me the opportunity to pursue this significant life experience exploring the intricacies of biological systems.

TABLE OF CONTENTS

Chapter 1

INTRODUCTION: REGULATION OF ENDOTHELIAL CELL STRUCTURE AND FUNCTION BY FLUID SHEAR STRESS

Hemodynamics and the Endothelium

The pulsatile blood flow through the mammalian vascular network imparts several different forms of biomechanical stresses on the vascular wall, including hydrostatic pressure, cyclic stretch, and tangential fluid shear stress [1]. The pressure and stretch components are borne by cellular and matrix constituents throughout the full thickness of the vessel wall. In contrast, the fluid shear stresses are borne primarily by the endothelium, which comprises the monolayer of cells lining the luminal wall of the vessel. Indeed, the endothelium appears uniquely positioned to sense variations in the shear stress patterns and transduce those signals into biological responses through its production of an impressive repertoire of soluble effector molecules and the display of various cell surface-associated receptors [2]. While these hemodynamically induced responses can have significant physiologic and pathophysiologic implications, the mechanisms through which endothelial cells sense and respond to their biomechanical environment have yet to be fully elucidated.

Initial studies by Fry and colleagues in 1968 demonstrated that extreme elevations in shear stress levels can lead to physical disruption of the endothelial monolayer [3]. However, subsequent analyses have shown that more subtle shear stress variations, within the physiological range, can significantly alter endothelial cell structure and function, in the absence of frank injury. Under physiologic conditions, blood flow patterns and shear stress levels vary along the arterial tree, and regional differences in endothelial cell shape reflect these local hemodynamic differences [4, 5]. In relatively straight, unbranched regions of the vasculature, the blood flow is primarily unidirectional, and endothelial cells are elongated and aligned in the direction of flow. Near bifurcations and curves, complex disturbed flow patterns prevail, with the endothelial cells displaying less aligned, more polygonal shapes. These morphological patterns can be replicated by surgical modifications leading to changes in blood flow patterns, indicating that the endothelium can truly act as a flow sensor of the local fluid mechanical environment [6-8].

While the direct transmission of fluid shear stresses is limited to the endothelial monolayer, alterations in blood flow patterns, mediated through the endothelium, can affect the entire vessel wall. Thus, alterations in blood velocity lead to both acute (vasodilation or vasoconstriction) and chronic (vascular remodeling) endothelial-dependent adaptations within the vessel wall which serve to return the wall shear stress levels to original values [9]. These vascular responses involve several different cell types and are likely mediated through the shear-induced elaboration of various endothelial-derived vasoactive substances (histamine, prostacyclin, endothelin-1, nitric oxide) and growth factors (platelet derived growth factors-A and -B, basic fibroblast growth factor, transforming growth factor) [10-17]. In addition, sites predilected for atherosclerotic development

in vivo -- including arterial bifurcations, curves and ostial openings -- are associated with the presence of a unique flow pattern, identified as disturbed laminar shear stress [18]. Since endothelial dysfunction is considered an initiating event in atherogenesis [2], endothelial cell responses to the local fluid mechanical environment may play pivotal roles in the focal development of this disease. Undoubtedly, hemodynamically-induced alterations in the endothelium are important in many other physiologic and pathophysiologic processes, including development, angiogenesis, inflammation, and metastatic progression. Many of these processes may reflect a complex balance of shear stress-mediated alterations in gene expression within the endothelial cell.

In vitro Responses of Endothelial Cells to Shear Stress

In order to more precisely analyze the shear stress parameters (e.g., amplitude, duration and spectral properties of the applied force) which regulate endothelial cell structure and function, different types of *in vitro* apparatuses have been developed. The two most common designs are the cone and plate device, described by Dewey *et al.* in 1981 [19], and the parallel plate flow system, first utilized by Eskin *et al.* in 1984 [20]. Both can generate defined fluid flow over cultured monolayers of endothelial cells isolated from animal or human blood vessels. The cone-plate system, utilized in the studies reported here, is comprised of a rotating cone over a stationary base plate which supports the endothelial monolayer (**Figure 1.1**). By adjusting cone angle, medium viscosity, and cone rotation speed, a broad dynamic range of shear stresses can be generated, in both laminar and turbulent flow regimes [21]. Endothelial monolayers may be plated either on multiple small coverslips mounted at different positions in the base plate -- which allows for analysis of replicate samples -- or on a single large plastic plate, providing ample numbers of cells for molecular biological analyses. Addition of a barrier in the flow streamline, in the form of a small step on each coverslip, results in regions of disturbed laminar shear stress downstream. The regions of flow reversal and reattachment thus created have large spatial shear stress gradients which mimic disturbed flow patterns that occur *in vivo* [22, 23]. Similar uniform and disturbed laminar shear stress patterns may be produced within a parallel plate apparatus [22, 24]. Also, by coupling a parallel plate device to a microscopic image analysis system, live-time analyses of endothelial cell responses to shear stress may be performed. However, unlike the cone and plate apparatus, parallel plate systems generally allow analysis on only one coverslip at a time and require constant recirculation of culture medium.

Initial experiments with these *in vitro* flow apparatuses confirmed *in vivo* shear stress-associated endothelial cell shape changes [25-28] and analyzed alterations in other complex cell functions, such as cytoskeletal reorganization [29, 30], cell stiffness [31], proliferation [32-34],

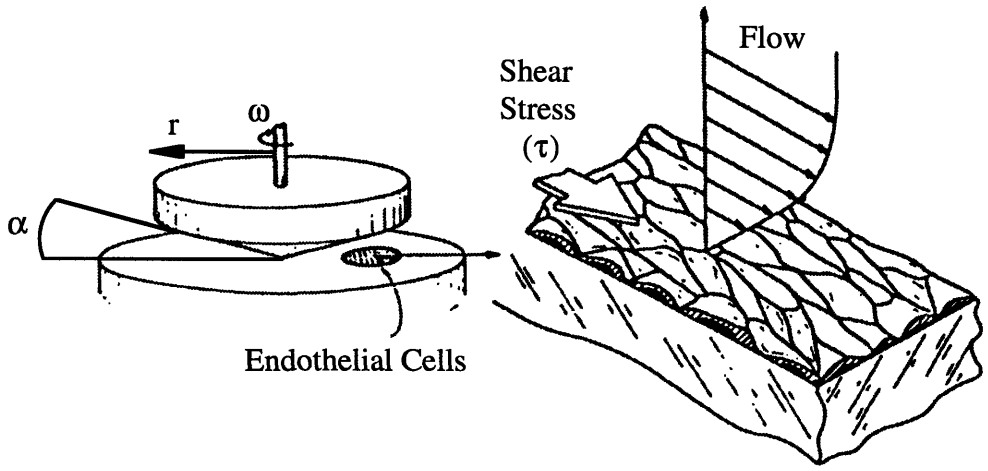

ω = cone angular velocity
r = radial position
α = cone angle
μ = viscosity
ν = kinematic viscosity

$$\tau = \frac{\mu\omega}{\alpha}\left(1 - 0.4743\tilde{R}^2\right)$$

$$\tilde{R} \equiv \frac{r^2\omega\alpha^2}{12\nu}$$

Figure 1.1. **The *in vitro* cone and plate shear stress apparatus.** Endothelial monolayers are exposed to defined fluid mechanical conditions within the cone and plate system. Flow is created by rotating the cone over the stationary base plate, and the shear stress, τ, is a function of the viscosity of the culture medium contained between the cone and plate, the cone angle and rotation speed, and the dimensionless parameter, $\tilde{R}$.

[Adapted from Davies *et al*, 1984, *J Clin Invest*, 73:1121-1129.]

migration [33], and pinocytosis [35]. In 1985 Frangos *et al.* and Grabowski *et al.* demonstrated the enhanced secretion of a distinct endothelial-derived molecule, prostacyclin, by endothelial monolayers exposed to laminar shear stress [12, 36]. Subsequent analyses by several groups revealed the shear stress regulation of other endothelial-derived effector molecules, including coagulation factors (tissue plasminogen activator, thrombomodulin) [37-40], vasoactive substances (histamine, endothelin-1, nitric oxide) [11, 13, 14, 41, 42], cytokines (interleukin-1 and -6) [43], and growth factors (platelet-derived growth factors-A and -B, heparin-binding EGF-like growth factor, basic fibroblast growth factor) [15, 16, 44]. Certain of the acutely regulated events involve alterations in substrate availability and rate-limiting enzymatic activities in metabolic pathways. Other more chronic effects reflect direct alterations in gene expression, due to transcriptional as well as post-transcriptional events. The variety of shear stress responses in endothelial cells may involve a growing number of intracellular signal transduction mediators that are also modulated by shear stress (intracellular Ca^{++}, arachidonic acid and phosphoinositide metabolites, G-proteins, mitogen-activated protein kinases, reactive oxygen intermediates) [45-51].

Mechanisms of Endothelial Gene Regulation by Shear Stress

In 1993, Resnick and colleagues in our laboratory provided the first evidence of a specific transcriptional mechanism through which shear stress can regulate endothelial gene expression [52]. Transfection of deletional promoter constructs of the platelet-derived growth factor-B (PDGF-B) gene into endothelial cells exposed to uniform laminar shear stress led to the identification of a six base pair nucleotide sequence (GAGACC), termed the "shear stress response element" (SSRE), within the promoter of PDGF-B that was required for the shear stress induction of this gene. Subsequent studies revealed that nuclear factor-κB (NF-κB), a DNA-binding transcription factor, could functionally interact with the SSRE within the PDGF-B promoter [53]. Recent data from our laboratory and others have identified three additional "SSREs" which mediate the shear stress induction of other endothelial cell genes by binding specific, previously defined transcription factors. A TPA (tetra-decanoyl phorbol acetate) response element (TRE) mediates the upregulation of the monocyte chemotactic protein-1 gene by interacting with activator protein-1 (AP-1), a transcription factor composed of protein dimers of c-Jun and c-Fos [54]. The shear-induction of the platelet-derived growth factor-A (PDGF-A) gene requires functional interactions between another transcription factor, early growth response-1 (Egr-1), and its DNA binding sequence in the PDGF-A promoter [55]. Finally, upregulation of the tissue factor gene by shear stress involves activation of the transcription factor, Sp1, by phosphorylation [56]. The diversity

of molecular mechanisms through which these SSREs and associated transcription factors exert their regulatory effects suggest that the local promoter architecture and regional associations between distinct transcription factors may be important variables in the shear stress activation of different endothelial genes.

Objectives

One of the best studied paradigms of endothelial cell gene activation is the cytokine induction of a class of cell surface receptors, the endothelial-leukocyte adhesion molecules, which includes Intercellular Adhesion Molecule-1 (ICAM-1), Vascular Cell Adhesion Molecule-1 (VCAM-1), and E-selectin (ELAM-1). All three genes are coordinately upregulated, with varying kinetics, in endothelial cells exposed to soluble cytokines such as interleukin-1ß (IL-1ß) and tumor necrosis factor-α (TNFα), and elevated expression levels have been detected in a number of disease states, particularly inflammation and atherosclerosis [2]. The molecular regulatory mechanisms through which cytokines induce ICAM-1, VCAM-1, and E-selectin have been extensively studied and involve several transcription factors and DNA binding sites, certain of which have been identified as shear responsive in other genes [57]. However, at the time the work presented here was initiated, the potential shear stress regulation of endothelial adhesion molecules had not yet been examined. As such, the specific aims of this research were as follows:

- ***Investigate the potential regulatory effects of uniform laminar shear stress on ICAM-1, VCAM-1, and E-selectin expression in cultured human endothelial cells.***

  This regulation was explored at multiple levels, including cell surface protein, functional interactions with leukocytes, steady state mRNA, and transcriptional activation.

- ***Extend these findings on adhesion molecule regulation by uniform laminar shear stress to a disturbed laminar shear stress model, which incorporates regions of both uniform and disturbed flow.***

  The disturbed flow model also was utilized to examine the effects of shear stress pre-conditioning on subsequent cytokine induction of ICAM-1, VCAM-1, and E-selectin.

- ***Examine the effects of uniform and disturbed laminar shear stress on the induction and nuclear localization of transcription factors (NF-κB, Egr-1, c-Jun, c-Fos) which bind to identified SSREs.***
  These analyses required the assemblage of a customized image analysis system and the development of specialized image analysis algorithms.

The results of these investigations will be described in Chapters 2, 3, and 4, respectively.

Chapter 2

DIFFERENTIAL REGULATION OF ENDOTHELIAL-LEUKOCYTE ADHESION MOLECULES BY UNIFORM LAMINAR SHEAR STRESS

INTRODUCTION: ENDOTHELIAL-LEUKOCYTE ADHESION MOLECULES IN VASCULAR BIOLOGY

The adhesive properties of the endothelium are central to its role in physiological and pathophysiological processes. Of particular importance are its adhesive interactions with blood-borne leukocytes, since leukocytes must emigrate from the bloodstream through the endothelial lining of blood vessels in order to perform their functions in host defense at extravascular sites. Endothelial cells coordinate leukocyte recruitment via the regulated expression of a number of cell surface adhesion molecules (endothelial-leukocyte adhesion molecules, ELAMs) which bind to specific counter-receptors on leukocytes (**Table 2.1**). A large body of both *in vivo* and *in vitro* experimental evidence has identified a sequence of adhesive interactions in this process [58, 59]. First, a loose attachment is initiated between the two cell types, which serves to decelerate leukocyte velocity and results in their rolling along the endothelial surface. This process, which is generally mediated by adhesion molecules of the selectin family (E-selectin and P-selectin on endothelial cells) interacting with sialylated counter-receptors (expressed on different leukocyte types), involves rapid bond formation at the leading edge of the leukocyte together with bond dissociation at the trailing edge [60-63]. Cell rolling is followed by leukocyte activation mediated by a variety of factors (cytokines, chemokines, chemoattractants), with resulting upregulation of secondary adhesion molecules. Firm attachment is then established via the interaction of these secondary adhesion molecules, such as $ß_1$ and $ß_2$ integrins expressed by leukocytes (e.g., very late antigen-4/VLA-4, leukocyte function-associated antigen-1/LFA-1, Mac-1) with members of the immunoglobulin gene superfamily (VCAM-1, ICAM-1) on the activated endothelial surface. Finally, the leukocyte migrates through cell-cell junctions in the endothelial monolayer and into the extravascular tissue. Thus, the regulation of expression of ELAMs, such as E-selectin, VCAM-1, and ICAM-1, constitutes an important control mechanism in leukocyte recruitment.

The significance of ELAMs in inflammatory processes is emphasized by the complications encountered by patients with the Type 1 Leukocyte Adhesion Deficiency Syndrome. These patients have reduced levels of functional $ß_2$ integrin subunits and experience recurrent bacterial infections and impaired wound healing [66]. ELAMs also play significant roles in pathophysiologic processes other than inflammation. A number of disease-associated cells utilize adhesion receptors for pathologic functions. For example, ICAM-1 has been identified as the major cell surface receptor for at least two pathogens: rhinovirus and *Plasmodium falciparum* (the microorganism responsible for malaria) [67-70]. Certain malignant cells, including carcinomas, melanomas and lymphomas, express LFA-1, VLA-4, and ligands for E-selectin, and increased expression of ICAM-1 on endothelial cells has been correlated with metastatic spread [59, 71-75].

Table 2.1

Endothelial Adhesion Molecules and Their Leukocyte Counter-Receptors [64, 65]

Endothelial Cell	Leukocyte
ICAM-1	$ß_2$- integrins: LFA-1 (CD11a/CD18) Mac-1 (CD11b/CD18) p150 (CD11c/CD18)
VCAM-1	$ß_1$- and $ß_7$ - integrins: VLA-4 ($\alpha_4ß_1$) $\alpha_4ß_7$
E-selectin	Sialyl-Lewis^x

Thus, the adhesive properties of ELAMs are important in a diverse set of disease processes, including inflammation, infection, and metastatic progression. In addition, many adhesive interactions are intimately associated with signaling mechanisms, transducing information linking intracellular and extracellular events. For example, ICAM-1 functions as a costimulatory molecule to activate T-cells, and upregulated endothelial expression of ICAM-1 and VCAM-1 has been demonstrated in a number of autoimmune diseases, including Graves' disease, Hashimoto's thyroiditis, and experimental autoimmune neuritis [76-78]. Recent evidence from our laboratory has indicated that leukocyte binding to E-selectin on the endothelial cell surface induces transmembrane cytoskeletal linkage of this adhesion molecule, a process which may have important implications for cell-cell signaling as well as mechanical anchoring during leukocyte binding [79]. Therefore, both the adhesive and signaling functions of ELAMs may be important mechanisms in pathophysiologic processes.

Atherosclerosis, the leading cause of death in the United States, involves alterations in ELAM expression. One of the earliest morphologically detectable events in atherogenesis is the adherence of circulating blood monocytes to the endothelial wall [80-82]. These cells then migrate across the endothelium and into the arterial intima where they transform into resident macrophages and accumulate cholesterol esters to become "foam cells" [83]. In addition to accumulating lipids, foam cells elaborate a number of soluble effector molecules such as cytokines, growth factors, chemotactic factors, and reactive oxygen species. Many of these products result in the recruitment and proliferation of additional monocytes from the lumen as well as smooth muscle cells from the media. The resulting intimal hyperplasia, together with depositions of extracellular matrix proteins synthesized by intimal smooth muscle cells, characterizes the developing atherosclerotic plaque [66].

The first *in vivo* demonstration of lesion-selective ELAM expression showed enhanced endothelial VCAM-1 covering aortic atherosclerotic lesions at various stages of development in atherogenic rabbit models [84]. Several subsequent studies have revealed elevated levels of VCAM-1, ICAM-1, E-selectin, and P-selectin on endothelium in histologic sections of advanced human atherosclerotic plaques [85-87]. What is most striking, in terms of hemodynamics factors, is the recent finding that ICAM-1 expression, but not VCAM-1 or E-selectin, was significantly upregulated on histologic sections from the lateral walls of carotid sinuses, both in normal (lesion-free) and advanced atherosclerotic vessels [85]. This anatomic position is the frequent site of atherosclerotic development, a finding correlated with its exposure to disturbed shear stress patterns.

Given the roles that both shear stress and ELAMs appear to play in atherogenesis, as well

as other disease processes, we chose to investigate the potential regulation of ICAM-1, VCAM-1, and E-selectin in endothelial cells exposed to laminar shear stress. Endothelial activation by soluble mediators (e.g., cytokines and bacterial endotoxins), most commonly detected as enhanced ELAM expression, has been extensively examined. Indeed, biochemical stimulation constitutes a well-established model of endothelial cell activation. In contrast, biomechanical forces are now being recognized as an emerging paradigm of endothelial activation [88] and, at the time the work presented here was initiated, no comparative study of endothelial-leukocyte adhesion molecule regulation by hemodynamic forces had been reported.

METHODS

Cell Culture. Pooled primary cultures of human umbilical vein endothelial cells (HUVEC) were established from normal term human umbilical cords as previously described [89]. For experimental use, second passage cells were plated on tissue culture treated polystyrene (Costar, Cambridge, MA; and Modern Plastics, Peabody, MA) coated with 0.1% gelatin (Difco Laboratories, Detroit, MI), and grown to confluence in Medium 199 (with 25 mM HEPES; Gibco Laboratories, Gaithersburg, MD) supplemented with 10% fetal bovine serum (FBS) (Gibco Laboratories), 2 mM glutamine, 100 U/ml penicillin, 100 µg/ml streptomycin, 25 mg/ml endothelial cell growth supplement (Collaborative Research, Bedford, MA), 50 mg/ml heparin (Sigma Chemical Company, St. Louis, MO), and 250 ng/ml amphotericin B (Fungizone®, Gibco Laboratories). Bovine aortic endothelial cells (BAEC) were isolated from calf descending thoracic aortas as previously described [89], and were cultured in Dulbecco's modified Eagles' medium (Gibco Laboratories) supplemented with 10% bovine serum (BioWhittaker, Walkersville, MD), 2 mM glutamine, 100 U/ml penicillin, and 100 µg/ml streptomycin. Suspension cultures of human JY lymphocytic cells [90], kindly provided by Dr. T. Springer (Center for Blood Research, Boston, MA), were maintained in RPMI-1640 medium (with 25 mM HEPES; BioWhittaker) supplemented with 10% FBS, 20 mM glutamine, 100 U/ml penicillin, and 100 mg/ml streptomycin. In certain experiments, endothelial cells were activated by treatment with recombinant human interleukin-1ß (IL-1ß; Biogen, Cambridge, MA), as indicated.

Shear Stress Apparatus. The cone and plate flow apparatus used to expose cultured endothelial monolayers to defined fluid shear stresses has been described in detail previously [19, 21]. The essential components consist of a stainless steel cone rotating over a stationary base plate, which supports either twelve 12 mm diameter polystyrene coverslips or a single 17.8 cm diameter polystyrene plate (see **Figure 1.1**). The culture medium present between the cone and base plate (15 ml total volume) is gradually exchanged (0.5 ml/min) without recirculation. The

entire apparatus is maintained at 37°C in a humidified 5% CO_2 and 95% air atmosphere. The shear stress on the surface of the plate, τ, can be described by:

$$\tau = \frac{\mu\omega}{\alpha}\left(1 - 0.4743\tilde{R}^2\right),$$

where

$$\tilde{R} = \frac{r^2\omega\alpha^2}{12\nu},$$

and where μ is medium viscosity, ω is angular velocity of the cone, α is cone angle, r is radial location on the plate, and ν is kinematic viscosity of the medium. The flow is laminar for $\tilde{R} << 1$ [21]. For the experiments reported here, fluid mechanical parameters were adjusted such that endothelial monolayers were subjected to laminar shear stress of 2.5 - 46 dynes/cm^2 for variable time intervals. Dextran (476,000 MW, 1% w/v; Sigma Chemical Company) was utilized to alter the medium viscosity, when required, and the viscosity was measured with a coaxial cylinder viscometer at 37°C (Haake, Berlin, Germany). Shear stressed and static monolayers were cultured in the same medium for each experiment. Control monolayers on coverslips were maintained in cell culture dishes (Costar) under static (no flow) conditions at 37°C in a humidified 5% CO_2 and 95% air atmosphere for equivalent time intervals.

Fluorescence Immunobinding Assay (FIA). Endothelial monolayers were incubated on ice for 1 hour in RPMI plus 10% FBS with saturating concentrations of monoclonal antibodies (mAbs) specific for human endothelial-leukocyte adhesion molecules (Hu 5/3, purified IgG, anti-human ICAM-1; E 1/6, ascites, anti-human VCAM-1; H18/7, purified IgG, anti-human E-selectin), followed by a FITC-labeled $F(ab')_2$ anti-mouse IgG (14 µg/ml in PBS plus 1% FBS, 1 hour; Caltag Laboratories, South San Francisco, CA), then lysed with a 0.01% NaOH/0.1% SDS solution and the fluorescence was measured in a Pandex plate reader (Travenol Laboratories, Mundelein, IL).

Immunocytochemistry. For microscopic visualization of cell surface associated proteins, endothelial monolayers were fixed in 2% paraformaldehyde at 4°C, and incubated for 1 hour with specific mAbs directed to human endothelial-leukocyte adhesion molecules, as described above, followed by biotinylated anti-mouse IgG (15 µg/ml in PBS plus 2% bovine serum, 1 hour; Vector Laboratories, Burlingame, CA), a peroxidase conjugated biotin-avidin complex (Vectastain Elite ABC Kit, 1 hour; Vector Laboratories), and finally an amino-ethyl-carbazole developing reagent (Peroxidase Substrate Kit, 8 minutes; Vector Laboratories). All incubations were performed at ambient temperature (25°C).

Northern Blot Analysis. Total cellular RNA was extracted from endothelial monolayers by the acid guanidinium thiocyanate-phenol-chloroform method (Cinna/Biotecx Laboratories International, Inc., Friendswood, TX). Samples (15 mg each) were electrophoresed through 1% agarose gels containing formaldehyde, transferred to nitrocellulose membranes (Schleicher & Schuell, Inc., Keene, NH) and hybridized with human ICAM-1, VCAM-1, or E-selectin cDNA probes labeled by [α-^{32}P] dCTP (Amersham Corporation, Arlington Heights, IL), using random hexanucleotide primers (Pharmacia, Inc., Piscataway, NJ). The cDNA fragments used were as follows: a 1.8 kb SalI-KpnI fragment of ICAM-1 cDNA from pGEM4, kindly provided by Dr. T. Springer (Center for Blood Research, Boston, MA); a 1.0 kb EcoRI/BamHI fragment of VCAM-1 cDNA from pBSM13, kindly provided by Dr. T. Collins (Brigham and Women's Hospital, Boston, MA); and a 1.0 kb XbaI fragment of E-selectin cDNA from pCDM8.

Leukocyte Adhesion Assay. Endothelial monolayers on 12 mm coverslips were coincubated for 15 minutes at room temperature under static conditions in 24-well cell culture plates (Costar) with JY cells (1.5 x 10^5 cells/ml), a human lymphocytic cell line which expresses an ICAM-1 ligand, LFA-1 (CD11a/CD18) [90], in 75 ml of RPMI-1640 plus 10% FBS. To remove unattached JY cells, each coverslip was washed by immersion three times in RPMI-1640 plus 1% FBS, then once in phosphate buffered saline (PBS), and fixed in 2% paraformaldehyde at 4°C. After staining with hematoxylin, adherent JY cells were counted in 5 randomly selected high power microscopic fields (100X) on each of 2 coverslips for each controlled variable.

Plasmid Vectors. The ICAM-1 deletional promoter constructs were kindly provided by Dr. M. Gerritsen (Bayer Corporation, West Haven, CN) and were made by cloning sequences (-716 to -12 bp or -617 to -12 bp) from the ICAM-1 promoter into the KpnI and BglII sites of the luciferase reporter vector pGL2-Basic (Promega, Madison, WI). CMV-CAT and CMV-ß-gal (the kind gifts of Dr. T. Collins, Brigham and Women's Hospital) contain the human cytomegalovirus (CMV) immediate-early enhancer/promoter coupled to the chloramphenical acetyl transferase (CAT) and ß-galactosidase (ß-gal) genes, respectively, and are constitutively expressed, non-shear-regulated reporter genes which were utilized for normalization of transfection efficiency and cell number.

Transient Transfections. BAEC (passages 2-5) grown on 100 mm culture dishes (Corning Glass Works, Corning, NY) at 70% confluence were transiently co-transfected by the calcium phosphate precipitation method with either of the ICAM-1 reporter gene constructs (22.5 - 26.25 µg) and either CMV-CAT or CMV-ß-gal (3.75 - 7.5 µg). The cells were then incubated in a 3% CO_2 humidified atmosphere at 37°C for at least 16 hours, washed three times with fresh culture medium, allowed to recover 6 - 10 hours in a 5% CO_2 atmosphere, washed again, then replicate-plated at 100% confluence (1.2 x 10^5 cell/ml) onto 12 mm diameter coverslips. Approximately 24

hours later, the confluent monolayers of BAEC were exposed to laminar shear stress or were maintained under static conditions. For the CMV-CAT experiments, each sample was split for separate luciferase (Enhanced Luciferase Assay Kit, Analytical Luminescence Laboratory, San Diego, CA) and CAT (as previously described) assays [91]. In the CMV-ß-gal experiments, luciferase and ß-galactosidase assays were performed consecutively on the same sample (Dual-Light Kit, Tropix, Inc., Bedford, MA) using a Monolight 2010 luminometer (Analytical Luminescence Laboratory).

RESULTS

Shear stress upregulates ICAM-1 surface expression in a time-dependent and force-independent manner. ICAM-1 expression on the surface of HUVEC monolayers which had been either incubated under static (no flow) conditions or subjected to laminar shear stress of 10 dynes/cm^2 for 4, 8, 24, and 48 hours was measured quantitatively by a fluorescence immunobinding assay (FIA). **Table 2.2** summarizes the results obtained from a total of 12 separate experiments in which confluent endothelial monolayers on multiple coverslips were simultaneously exposed to the same fluid shear stress or static conditions. Significant elevations in cell surface immunoreactive ICAM-1 were observed as early as 8 hours after the onset of shear stress, and increased progressively up to 48 hours. It is important to note the significant variability in basal expression of ICAM-1 in different HUVEC cultures. In particular, in cultures with high basal levels, shear stress induction of ICAM-1 was seldom observed. The maximum level of ICAM-1 expression induced by shear stress was comparable to that observed in HUVEC activated with a maximally effective concentration of recombinant human interleukin-1ß (10 U/ml) (see **Figure 2.3** below). Conditioned effluent medium collected from the shear stress apparatus, at intervals ranging from 15 minutes to 24 hours, failed to induce ICAM-1 upregulation when incubated with static HUVEC monolayers for 3 and 24 hours (data not shown).

As illustrated in **Figure 2.1**, immunocytochemical staining of paraformaldehyde-fixed HUVEC monolayers subjected to laminar shear stress of 10 dynes/cm^2 also demonstrated the progressive upregulation of cell surface ICAM-1 at 24 and 48 hours. Morphological responses of cells, namely elongation and alignment in the flow direction, were clearly evident in these shear stressed monolayers at both time points. However, HUVEC monolayers exposed to a lower level of shear stress (3 dynes/cm^2) for 24 hours displayed a similar increase in surface ICAM-1 expression, without any detectable elongation or alignment of the cells. In both of these relatively high (10 dynes/cm^2) and low (3 dynes/cm^2) shear stress conditions, ICAM-1 induction was not uniform across the monolayer. To further investigate the potential force-dependence of ICAM-1

Table 2.2

Shear Stress Induces Cell Surface Expression of ICAM-1 in Cultured Human Umbilical Vein Endothelial Cells

Experiment Duration (hours)	Cell Surface Immunobinding (Fluorescence Units)		
	Static	Shear Stress	Shear Stress / Static
4	1974 ± 109	2259 ± 545	1.1
4	886 ± 180	838 ± 88	1.0
8	2819 ± 116	3689 ± 223	1.3*
8	1618 ± 319	1590 ± 160	1.0
24	599 ± 48	1427 ± 327	2.4‡
24	673 ± 98	1333 ± 268	2.0‡
24	2443 ± 371	2753 ± 597	1.1
48	207 ± 144	3413 ± 406	16.5*
48	767 ± 154	2419 ± 111	3.2*
48	395 ± 132	1080 ± 71	2.7‡
48	997 ± 72	2474 ± 283	2.5*
48	944 ± 19	941 ± 637	1.0

Confluent HUVEC monolayers were either exposed to shear stress (10 dynes/cm^2) or maintained under static conditions for the times indicated. Cell surface expression of ICAM-1 was measured using a fluorescence immunobinding assay, as described in Methods. Data are expressed as mean ± standard deviation; n = 2-4 replicate coverslips in each separate experiment; *$p < 0.01$ and ‡$p < 0.05$ shear stress versus static control (Student's t-test).

Figure 2.1. **Immunocytochemistry of ICAM-1 surface expression on HUVEC exposed to shear stress (following page).** HUVEC monolayers were either maintained under static conditions or subjected to high (10 dynes/cm^2) or low (3 dynes/cm^2) laminar shear stress for variable time periods: (A) static, (B) high shear stress, 24 hours, (C) high shear stress, 48 hours, or (D) low shear stress, 24 hours. The monolayers were then fixed with 2% paraformaldehyde and immunocytochemically stained using an ICAM-1-specific mAb, as described in Methods. Original magnification = 45X.

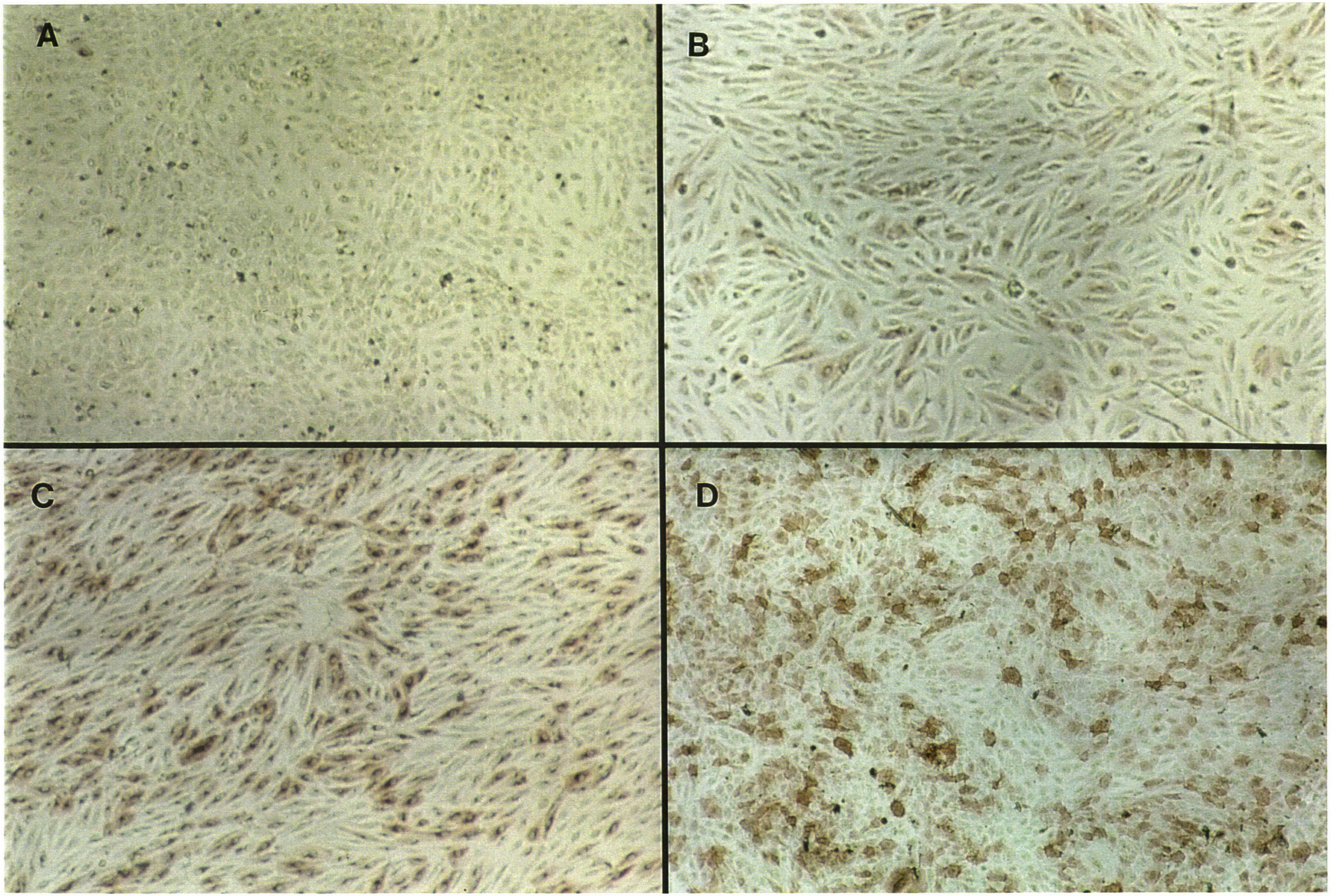
A
B
C
D

induction, confluent HUVEC monolayers were exposed for 24 hours to a broad range of laminar shear stresses (2.5 - 46 dynes/cm^2), comparable to those encountered *in vivo* in large vessels [92]. In a series of 12 experiments, as illustrated in **Figure 2.2**, significant increases in immunoreactive surface ICAM-1 expression, measured by FIA, were observed at each level of shear stress tested; however, the amount of induction appeared to be independent of the magnitude of the applied force.

E-selectin and VCAM-1 are not upregulated in HUVEC by shear stress. In contrast to the induction of ICAM-1 by shear stress, no significant changes were observed in either E-selectin or VCAM-1 expression, as measured by cell surface FIA, at any time point (4 - 48 hours) or shear stress level (2.5 - 46 dynes/cm^2) studied (data not shown). In particular, as seen in **Figure 2.3**, at time points when IL-1ß treated HUVEC cultures displayed peak levels of E-selectin (4 hours) and VCAM-1 (24 hours), no changes in the cell surface expression of these molecules were observed in HUVEC cultures subjected to 10 dynes/cm^2 of laminar shear stress.

In order to test whether shear stressed endothelial cells were still responsive to other activating stimuli, such as cytokines, we subjected HUVEC monolayers to 24 hours of laminar shear stress (10 dynes/cm^2) followed by a 4 or 24 hour treatment with IL-1ß (10 U/ml) under static conditions. Immunocytochemical staining revealed marked upregulation of E-selectin (after 4 hours) and VCAM-1 (after 24 hours) comparable to that observed in HUVEC that were not exposed to shear stress (data not shown).

Laminar shear stress selectively upregulates ICAM-1 mRNA. Northern blot analysis of RNA extracted from HUVEC revealed a marked increase in ICAM-1 transcript levels as early as 2 hours after the onset of shear stress, which was sustained at 8 hours and still elevated above static HUVEC at 24 hours (**Figure 2.4**). Rehybridization of the membrane with cDNA probes for VCAM-1 and E-selectin did not show induction of these genes at any time point examined, consistent with the FIA measurements of cell surface protein (see **Figure 2.3**).

Enhanced leukocyte adhesion to shear stressed HUVEC monolayers. The shear stress-induced surface expression of immunoreactive ICAM-1 suggested that HUVEC monolayers subjected to laminar shear stress might be more adhesive for leukocytes expressing ligands for ICAM-1. To test this hypothesis, HUVEC were exposed to 48 hours of shear stress and then coincubated in a standard monolayer adhesion assay with JY cells, a human lymphoblastoid cell line which expresses the ICAM-1 ligand, LFA-1 (CD11a/CD18), as measured by flow cytometry (data not shown). A 3-fold increase in JY cell adhesion was observed to shear stressed HUVEC versus static monolayers, which was comparable to the upregulated ICAM-1 expression detected by FIA. These increases in leukocyte adhesion were comparable in magnitude

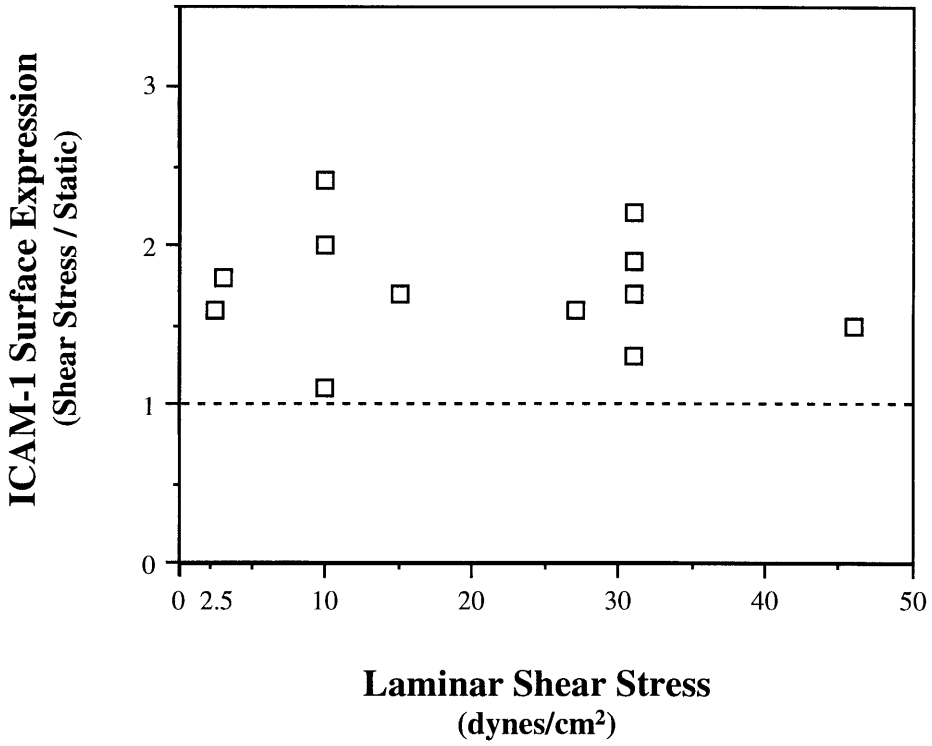

Figure 2.2. **Upregulation of ICAM-1 by a range of laminar shear stress levels (2.5 - 46 dynes/cm^2).** HUVEC monolayers were either maintained under static conditions or subjected to various levels of laminar shear stress, as indicated, for 24 hours. Cell surface protein was determined using a fluorescence immunobinding assay, as described in Methods, and displayed as the ratio (shear stress / static) for each experiment.

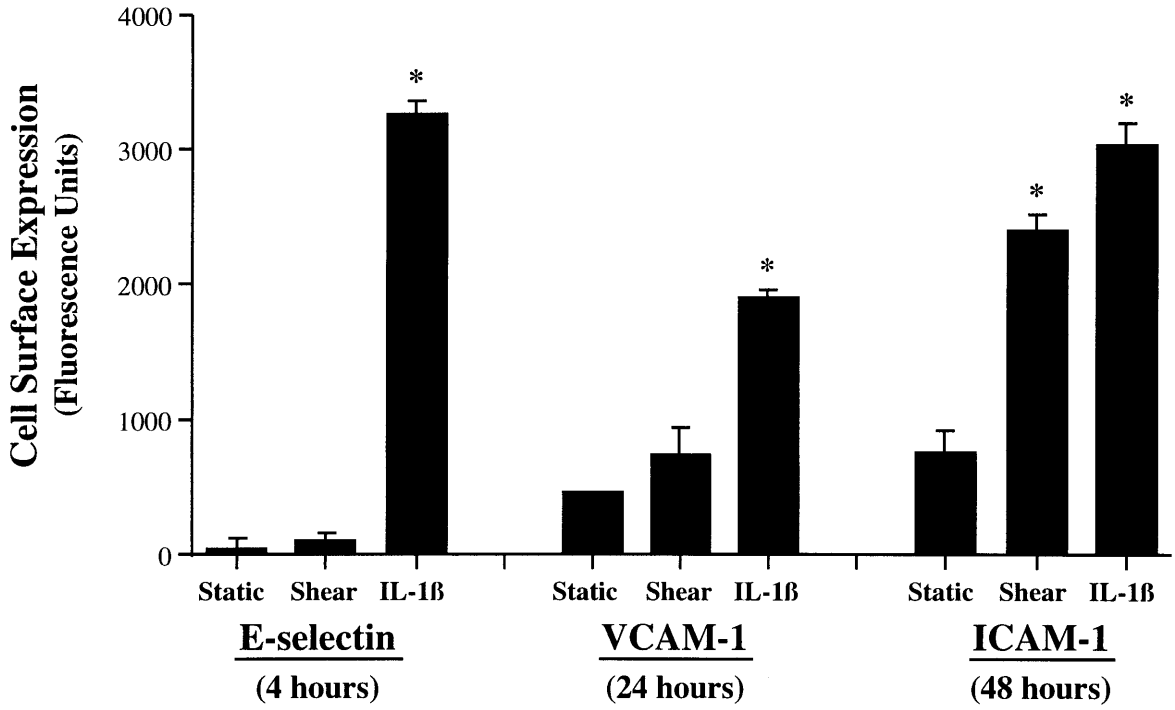

Figure 2.3. **Peak cell surface expression of endothelial-leukocyte adhesion molecules in HUVEC subjected to shear stress or IL-1ß.** HUVEC monolayers were maintained under static conditions, exposed to laminar shear stress (10 dynes/cm^2), or treated with a maximally effective concentration of IL-1ß (10 U/ml) for time periods corresponding to the peak cytokine-induced surface expression of E-selectin (4 hours), VCAM-1 (24 hours), or ICAM-1 (48 hours), respectively. Cell surface protein was measured using a fluorescence immunobinding assay, as described in Methods. n = 3-4 replicate coverslips for each controlled variable; data expressed as mean ± standard deviation, *$p < 0.01$ stimulus versus static (Student's t test).

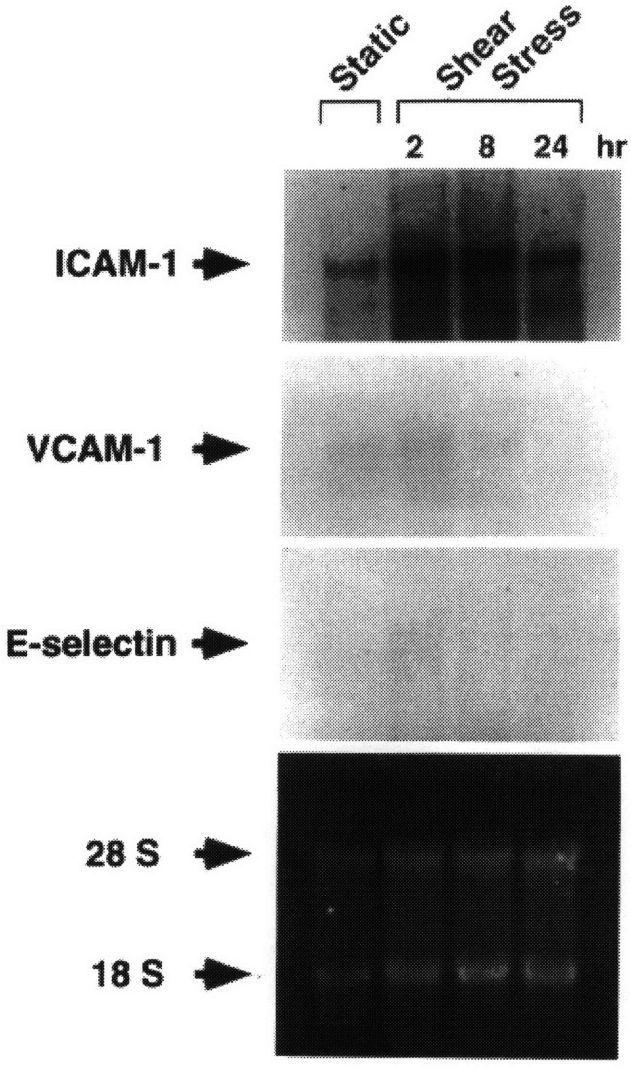

Figure 2.4. **Northern blot analysis of adhesion molecule induction by shear stress in HUVEC.** HUVEC monolayers were either maintained under static conditions or exposed to laminar shear stress (10 dynes/cm^2) for 2, 8, or 24 hours. Total cellular RNA was isolated for Northern blot analysis as described in Methods, and each lane was loaded with 15 μg aliquots (bottom panel, ethidium bromide staining of 18S and 28S ribosomal RNA). The membrane was sequentially hybridized with radiolabeled cDNA probes of ICAM-1, VCAM-1, and E-selectin.

to those seen in the same experiment with maximally IL-1ß activated (10 U/ml, 24 hours) HUVEC monolayers (**Figure 2.5**).

ICAM-1 is induced by shear stress at the level of transcription. The correlation of the selective shear stress inducibility of ICAM-1 with the presence of the SSRE in its promoter suggested that this regulatory element might be functional in the shear stress induction of ICAM-1. In order to investigate the potential role of the SSRE (located at position -644 bp in the ICAM-1 promoter) in the transcriptional regulation of ICAM-1, we utilized two ICAM-1 deletional promoter/reporter gene constructs, one which contains the SSRE (-716 to -12 bp) and one which lacks it (-617 to -12 bp), as depicted in **Figure 2.6**. Cultured BAEC were transfected with either of these constructs and subjected to laminar shear stress (10 dynes/cm^2, 3 hours) or maintained under static conditions. Normalization for both transfection efficiency and cell number was accomplished by co-transfecting with either CMV-CAT or CMV-ß-gal, both of which are constitutively expressed and non-shear-regulated. **Table 2.3** summarizes the results obtained from 5 separate experiments in which transfected endothelial monolayers on multiple coverslips were simultaneously exposed to the same fluid shear stress or static conditions. The promoter construct which contains the SSRE exhibited significant transcriptional activation by shear stress in 4 of 5 experiments ($p < 0.05$ versus static), whereas the construct lacking the SSRE displayed significant induction in only 1 experiment.

DISCUSSION

At the time they were performed, these studies provided the first evidence that physiologically relevant levels of laminar shear stress can differentially regulate the expression of endothelial-leukocyte adhesion molecules. This differential pattern of adhesion molecule expression elicited by laminar shear stress is in contrast to the coordinate activation profile typically observed in cultured HUVEC with cytokines such as TNFα, IL-1ß, or bacterial endotoxins [93-95], thus suggesting that distinct transduction pathways and/or transcriptional and post-transcriptional regulatory mechanisms are involved. In addition, both the lack of E-selectin upregulation by shear stress and the fact that conditioned media from shear stressed monolayers failed to induce adhesion molecule expression on static monolayers, strongly argue against the action of an endogenous cytokine (e.g., IL-1ß or IL-1α) as an autocrine mechanism of activation in this system.

The correlation of the shear stress-inducibility of ICAM-1 with the presence of the SSRE in its promoter region and, conversely, the non-inducibility of E-selectin and VCAM-1, suggested

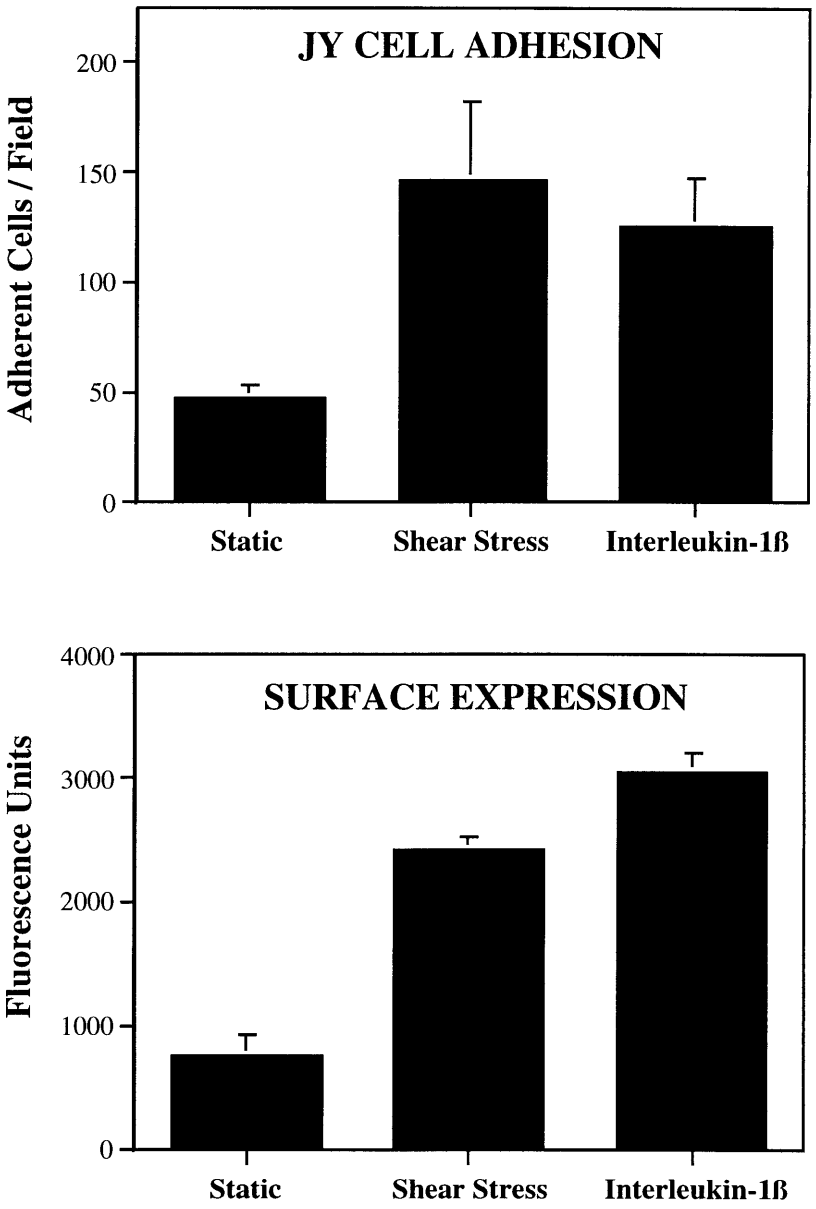

Figure 2.5. **ICAM-1 induction by shear stress in HUVEC is correlated with an increased adhesion of JY cells.** HUVEC monolayers were exposed to laminar shear stress (10 dynes/cm^2, 48 hours) or treated with IL-1ß (10 U/ml, 24 hours), and then were incubated in a standard adhesion assay with human JY cells, a lymphocytic cell line that expresses the ICAM-1 ligand, LFA-1 (CD11a/CD18), as described in Methods. Adherent JY cells (top panel) were counted in five randomly selected high power (100X) fields on each of two coverslips for each controlled variable. ICAM-1 cell surface expression (lower panel) was measured in parallel by a fluorescent immunobinding assay, as described in Methods. Data are presented as mean ± standard devation.

Figure 2.6. **ICAM-1 promoter/reporter gene constructs.** Deletional ICAM-1 promoter/luciferase constructs were made by cloning sequences from the ICAM-1 5' untranslated region into the luciferase reporter vector. The SSRE, located at position -644 bp in the ICAM-1 promoter, is present in the -716 bp construct, but absent in the -617 bp construct. A number of other putative transcriptional regulatory elements are also present in the ICAM-1 promoter, as shown.

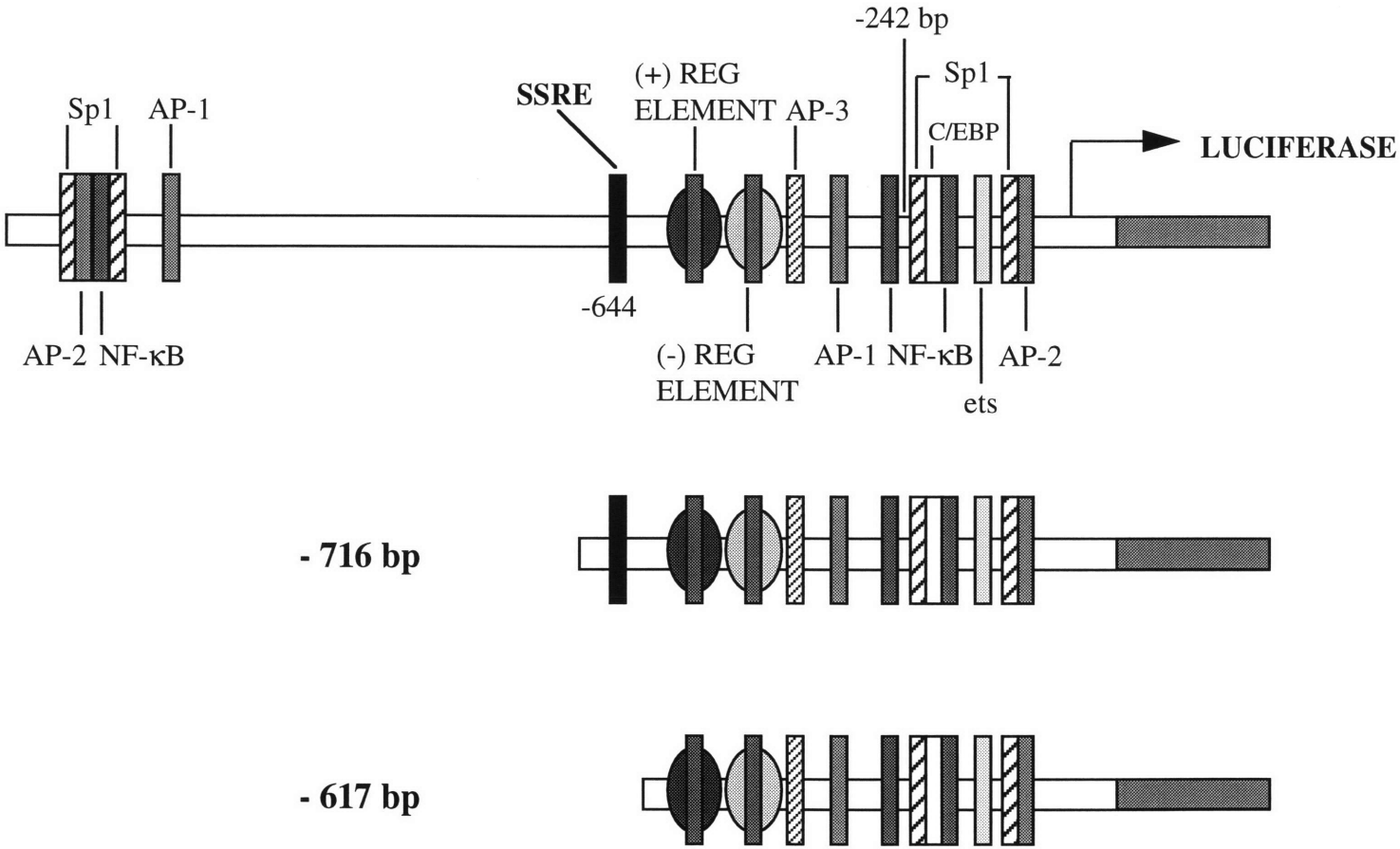

Table 2.3

Transcriptional Activation by Shear Stress is Enhanced with an ICAM-1 Deletional Promoter Construct Which Contains the SSRE

+SSRE Construct			-SSRE Construct		
Static	Shear Stress	SS/Static (*p)	Static	Shear Stress	SS/Static (*p)
Normalized with CMV-CAT:					
2.54±0.06	5.35±0.53	**2.11 (0.04)**	1.84±0.31	2.37±0.98	**1.29 (0.33)**
9.22±0.52	11.84±1.26	**1.28 (0.05)**	5.51±2.01	5.91±0.33	**1.07 (0.35)**
8.24±1.10	14.39±4.48	**1.75 (0.01)**	10.27±4.08	9.90±3.82	**0.96 (0.39)**
Normalized with CMV-ß-gal:					
.090±.017	.156±.009	**1.73 (0.01)**	.040±.003	.056±.005	**1.40 (0.01)**
.167±.017	.146±.008	**0.87 (0.13)**	.046±.008	.034±.009	**0.74 (0.07)**

** **p = 0.02**

Cultured BAEC were transfected with either the ICAM-1 deletional promoter construct containing the SSRE (+SSRE) or the deletional construct lacking the SSRE (-SSRE), and normalization was performed by co-transfecting with either CMV-CAT or CMV-ß-gal, as described in Methods. Transfected cells were then exposed to laminar shear stress (10 dynes/cm^2) for 3 hours, and the appropriate reporter gene assays were performed. Data are expressed as mean ± standard deviation; n = 2-6 samples in each experiment; Student's t-tests: * static versus shear stress for individual experiments, ** induction of +SSRE construct versus -SSRE construct for all experiments.

that this putative genetic regulatory element might be functional in the transcriptional upregulation of ICAM-1. Transfection experiments with ICAM-1 deletional promoter/reporter genes demonstrated that ICAM-1 was indeed upregulated by laminar shear stress at the level of transcription. Subsequent work in our laboratory has confirmed this finding by nuclear run-off analysis [96]. The ICAM-1 reporter gene experiments also revealed significantly greater shear stress induction of the construct which contained the SSRE, indicating that the SSRE may function to enhance the shear stress activation of ICAM-1. However, the fact that the reporter construct lacking the SSRE was still activated by shear stress, albeit in one experiment, indicates that the SSRE may not be necessary for shear stress induction of ICAM-1. Indeed, recent studies in our laboratory have demonstrated that another ICAM-1 deletional promoter construct which lacks the SSRE (-242 to -12 bp) was also shear stress responsive [97]. Thus, any functional shear stress response element(s) for ICAM-1 must be contained within the proximal 242 bp of its promoter. Interestingly, this is also the region most critical for TNFα induction of ICAM-1 in endothelial cells [98]. **Figure 2.6** illustrates the presence of several consensus sequences for known DNA-binding transcription factors within this region of the promoter, including Sp1, C/EBP, AP-2, ets, and NF-κB [98, 99]. Within this region, a 75 bp section containing the Sp1 and AP-2 sites is necessary for constitutive ICAM-1 expression [99], and the NF-κB site is required for TNF inducibility [98]. Identification of the functional shear stress responsive element(s) within this gene will require site-directed mutagenesis of these, and potentially other non-consensus, regulatory elements.

Since the initial publication of this work [100], several reports have generally confirmed and extended our findings. Tsuboi *et al.* demonstrated selective induction of ICAM-1 in HUVEC by shear stress at the levels of both cell surface protein and mRNA, with lack of VCAM-1 induction [101]. However, in contrast to our data, they found that the ICAM-1 upregulation was force-dependent (approximate range: 1 - 20 dynes/cm^2), in addition to being time-dependent (1 - 24 hours). It is quite probable that the method they utilized to measure cell surface protein, flow cytometry, is more sensitive than the fluorescence immunobinding assay we utilized, thus enabling them to detect the force-dependency. The Tsuboi report showed that the upregulation by shear stress was reversible, since induced surface protein levels (after 24 hours of flow) returned to baseline by 4 hours once the shear stress stimulus was terminated. In addition, experiments with different medium viscosities revealed that the ICAM-1 induction was shear stress- and not shear rate-dependent. Morigi *et al.* also reported selective upregulation of cell surface ICAM-1, as compared with E-selectin, together with increases in both firmly adherent and rolling leukocytes on

HUVEC monolayers exposed to laminar shear stress [102]. In the adhesion assay used in these experiments, endothelial monolayers which had been either maintained under static conditions or exposed to laminar shear stress (8 dynes/cm^2, 6 hours) were placed in a parallel plate flow chamber which was perfused with a fresh human leukocyte suspension at low flow velocity (0.6 - 3 dynes/cm^2) for less than 15 minutes, and endothelial-leukocyte interactions were analyzed with digitized microscopic images. With this system they further demonstrated that the increases in firmly adherent leukocytes could be completely blocked by treatment with an anti-ICAM-1 monoclonal antibody. Additionally, they showed that neither ICAM-1 nor E-selectin levels were affected by turbulent flow. Sampath *et al.* confirmed the specific ICAM-1 induction, though with different expression kinetics [103]. Peak mRNA levels were seen after 1 hour of shear stress exposure, then were downregulated below baseline at 6 hours. VCAM-1 and E-selectin transcript levels were depressed after both 1 and 6 hours of shear stress. It should be noted, however, that the HUVEC utilized in these studies exhibited relatively high basal levels of VCAM-1 and E-selectin, a finding which generally indicates cellular activation in this cell type [100, 104]. Their experimental conditions, therefore, may not be comparable to those in our studies. Taken together, these reports indicate that ICAM-1 is selectively and reversibly induced by laminar, but not turbulent, shear stress in a time- and force-dependent manner. This upregulation occurs at the levels of transcription, mRNA, and protein, and cell surface ICAM-1 specifically mediates leukocyte adhesion to the endothelial cells. In addition, recent preliminary data from Chappell *et al.* indicated that cell surface expression of both ICAM-1 and VCAM-1 were significantly induced in HUVEC by oscillatory flow (0 $\pm$ 5 dynes/cm^2, 24 hours), with concomitant increases in leukocyte adhesion, indicating that regular temporal variations in the shear stress stimulus may be important in cellular activation of adhesion molecule expression [105].

In contrast to HUVEC, cultured mouse lymph node endothelial cells constitutively express VCAM-1 under static conditions. Endothelial cells derived from this source demonstrated downregulation of VCAM-1 by laminar shear stress, both at the levels of protein and mRNA, which was time- and force-dependent as well as reversible when the cells were returned to static conditions [106, 107]. In addition, this downregulation was correlated with decreased lymphocyte adhesion which could be partially inhibited (70.6%) by treatment with an anti-VCAM-1 monoclonal antibody. Very recent studies with deletional VCAM-1 promoter/reporter gene constructs demonstrated that this regulation occurred, at least in part, at the level of transcription and appears to be mediated by two TRE response elements within the VCAM-1 promoter [108]. This finding is particularly intriguing since, as mentioned in Chapter 1, a non-consensus TRE site in the MCP-1 promoter mediates the upregulation of this gene in endothelial cells exposed to shear

stress. The ability of TRE sequences to both increase and decrease transcriptional activation may reflect differences in transcription factor binding between consensus and non-consensus response elements, as well as the importance of local promoter architecture in gene regulation.

The potential interaction of shear stress and biochemical stimuli in the regulation of endothelial adhesion molecule expression has also been investigated by other workers. Preliminary data has indicated that IL-1ß induction of VCAM-1 was significantly inhibited in HUVEC previously exposed to uniform laminar shear stress (5 dynes/cm^2, 24 hours) [109]. Also, upregulation of cell surface VCAM-1 by either oxidized LDL, or a combination of LPS and TNFα, was suppressed in human aortic endothelial cells pre-conditioned with only 4 hours of laminar shear stress (12 dynes/cm^2); these effects were potentially mediated by shear stress-induced NO production, since exposure of cells to nitro-L-arginine abolished the suppression [110]. ICAM-1 induction by IL-1ß, oxidized LDL, or LPS plus TNFα was not affected by shear stress pre-conditioning in any of these experiments.

In addition to regulating endothelial-leukocyte interactions by altering the expression of cell surface adhesion molecules, shear stress also modulates leukocyte adhesion by imparting a physical force opposing adhesive bonds formed between the two cell types. Gonzales *et al.* investigated the interrelationship of these dual effects by first exposing HUVEC monolayers to extended periods of laminar flow (on the order of hours), then perfusing leukocytes (U937 cells) over the monolayer under low shear stress conditions and assaying the number of leukocytes firmly adherent to the monolayer [111]. As documented previously by numerous reports, leukocyte adherence decreased as the cellular perfusate flow velocity increased, and this was true for all experimental conditions examined. Pre-conditioning with both low and medium level shear stresses (2 and 10 dynes/ cm^2, respectively) for 2 hours enhanced overall adhesion, whereas pre-conditioning with high shear stress (30 dynes/cm^2) had little effect. Surprisingly, the increased adhesion could be blocked with an anti-VCAM-1 antibody, and VCAM-1 surface protein was upregulated, albeit to a small extent (38%). In our laboratory, differential display analysis of mRNA transcripts in shear stressed endothelial cells has indicated that many genes, including VCAM-1, exhibit a brief upregulation immediately following onset of flow, with return to basal levels at longer time points (Dr. J. Topper, unpublished observations).

In vivo findings with acutely altered shear stress levels in experimental animal models have correlated well with *in vitro* data of adhesion molecule regulation. Average shear stresses within rabbit carotid arteries were increased (170%) in the right artery and decreased (73%) in the left artery by surgical manipulation, and subsequent alterations in ICAM-1 and VCAM-1 expression

and monocyte adhesion were analyzed [112]. Fluorescent en face staining revealed extensive ICAM-1 staining prior to shear stress alteration, and these levels were further upregulated with increased shear stress. Interestingly, staining was generally concentrated at the cell junctional regions. Experimental decreases in shear stress caused a reduction in ICAM-1 and loss of preferential junctional staining. VCAM-1 staining was modest under normal flow conditions, and was significantly induced by decreases in shear stress and, to a very minimal extent, by increases in shear stress. Monocyte adherence co-localized with some of the ICAM-1 and VCAM-1 positive endothelial cells. Thus, our demonstration that adhesion molecules are differentially regulated by shear stress *in vitro*, and in particular that ICAM-1 is selectively induced, appears to be relevant *in vivo*.

In the present study we have utilized a single shear stress regime, namely laminar flow, as a model system in which to study the response of endothelial cells to a defined biomechanical force. These experiments actually represent step functions in which endothelial cells were changed from static to shear stress conditions. The effective signal, responsible for initiation of gene regulation, may be a discrete alteration in shear stress magnitude above a minimum threshold. *In vivo*, the endothelium is exposed to complex shear stress patterns, due to the pulsatile flow of blood through a branched tubular network. Both the nonrandom distribution of atherosclerotic development and the correlation of endothelial cell shape with *in vivo* flow patterns strongly suggest that endothelium can distinguish between discrete hemodynamic variables [113]. Indeed, *in vitro* studies with shear stress regimes other than laminar flow have demonstrated that diverse shear stress parameters can differentially alter endothelial cell structure and function. For example, pulsatile shear stress, with its inherent temporal variations, has been shown to be more effective than steady flow in altering gene expression, in the case of c-*fos*, and less effective than steady flow, in the case of PDGF-A and -B [15]. When compared to laminar shear stress of comparable magnitude, turbulent flow, which has fluctuations in both its temporal and spatial components, is essentially indistinguishable from laminar shear stress in regulating the expression of certain genes, including PDGF-B, bFGF, endothelin-1, and thrombomodulin [13, 16, 39], but does not influence the expression of other laminar-induced genes, such as cyclooxygenase-2, manganese superoxide dismutase, and the endothelial cell nitric oxide synthase [96]. In the *in vitro* disturbed flow model, which mimics *in vivo* wall shear stress patterns at arterial bifurcations, the localized responses of the endothelial monolayer were found to vary with the shear stress gradient, rather than the absolute force [23]. Thus, we postulated that analysis of adhesion molecule expression within the disturbed flow field might provide more direct insights into the potential relevance of shear stress-induced endothelial changes in different pathophysiologic settings. In addition, more

detailed characterization of the nature of an effective shear stress stimulus might lead to a better understanding of the cellular transduction mechanisms that link these externally applied forces to genetic regulatory events [114]. These possibilities will be explored in greater detail in the Chapters 3 and 4.

In conclusion, we have demonstrated that adhesion molecule expression can be differentially regulated in vascular endothelium by a defined hemodynamic force, in contrast to the coordinate pattern of induction typically elicited by humoral stimuli, such as cytokines. These observations have important implications for the basic mechanisms of gene regulation in vascular endothelial cells. Furthermore, the selective upregulation of ICAM-1 by physiological levels of laminar shear stress *in vitro*, which has subsequently been confirmed by analogous experiments *in vivo*, indicates that the biomechanical regulation of this molecule may have significance in pathophysiologic settings such as inflammation and atherosclerosis.

Chapter 3

DIFFERENTIAL REGULATION OF ENDOTHELIAL-LEUKOCYTE ADHESION MOLECULES BY DISTURBED LAMINAR SHEAR STRESS

INTRODUCTION: DISTURBED LAMINAR SHEAR STRESS *IN VIVO*

The anatomically localized pattern of the earliest lesions of atherosclerosis strongly implicates hemodynamic forces in this disease process. This was first formally noted by Texon in 1957 who observed, in one hundred autopsied cases, that atherosclerotic lesions occurred most frequently in arterial geometries with similar flow patterns, including branch points, bifurcations, and curves [115]. By surgically altering vessel configurations to cause enhanced curves in animal models, several groups induced arterial lesions, further supporting the role of hemodynamics in disease development [116, 117]. Texon first proposed that these atherogenic sites share in common a low pressure profile. However, Caro *et al.* noted that such sites are exposed to low shear stress, and he proposed inhibited mass transport, secondary to the relatively thick boundary layers, as the mechanism of plaque initiation [118]. Over the past few decades, detailed flow studies of atherosclerotic loci have revealed that these anatomic locations are actually exposed to a unique flow pattern identified as disturbed laminar shear stress. This shear stress regime is characterized by regions of flow separation, reversal, reattachment, and perhaps most importantly, significant temporal and spatial gradients of shear stress.

In 1975 Friedman and coworkers developed the first two-dimensional numerical model of flow in the human aortic bifurcation [119]. This model identified the outer walls of the bifurcation as sites of low shear stress, with associated flow reversal and stagnation points. The model also indicated that pulsatile flow, as compared with steady flow, enhanced the temporal and spatial variations within the disturbed flow region. Recognizing that the flow environment was too complex to be modeled in greater detail by the computational techniques available at that time, they subsequently created a single physical cast of the aortic bifurcation of a 63 year old man [120, 121]. Flow patterns within this rigid model were visualized with laser Doppler anenometry and compared with histologic sections from the original vessel. These experiments confirmed a positive correlation between low shear regions and sites of atherosclerotic development. Building upon this study, Glagov and colleagues performed the first detailed study on a series of twelve human carotid artery bifurcations, incorporating steady and pulsatile flow visualization in rigid scale models, together with histologic analyses postmortem [122, 123]. They determined that intimal lesions were thickest along the outer wall of the carotid sinus and correlated with the presence of disturbed flow patterns. In a recent study, they extended this analysis to include flow models with compliant walls and found that compliancy resulted in lower mean shear stresses with smaller positive and negative peaks in shear stress values, indicating that the mechanical properties of the vessel wall can help minimize large variations in shear stress [124]. In addition, using a physical model of the abdominal aorta, they varied the outflow resistances of the celiac, superior

and inferior mesenteric, renal and iliac arteries to produce flow distributions consistent with rest, the postprandial state, and vigorous lower limb exercise [125-127]. While there was little difference between the rest and postprandial flow patterns, the exercise flow distribution markedly reduced or completely abolished the disturbed flow patterns, suggesting at least one mechanism for the proposed protective effects of exercise.

At the same time Glagov and coworkers were analyzing the human carotid bifurcations, Karino *et al.* developed a novel technique for isolating vessels in their native geometry and rendering them transparent [128]. Flow visualization studies identified sites of secondary flow, including recirculation and stagnation regions. The original studies focused on the human carotid and abdominal aorta bifurcations, but were rapidly extended to include other vascular sites, such as the aortic arch, cerebral arteries, and coronary arteries [129-132]. In all cases, intimal lesions were correlated with the presence of disturbed flow patterns. Using a model of a dog aorta, which included four major branching arteries, they also determined the critical Reynold's number for onset of flow reversal as compared with similar, though simpler, tube geometries [133]. Interestingly, critical Reynold's numbers were higher in the anatomic model than in the tubular model, indicating that *in vivo* geometries are well-suited for minimizing flow separation patterns.

The most extensive numerical models of *in vivo* disturbed flow patterns have been developed by Perktold and coworkers. Applying the finite element method, they have analyzed three dimensional, non-Newtonian, incompressible, pulsatile flow in models of both rigid and compliant human carotid and coronary arterial systems [134-137]. Their calculations confirmed previous predictions that the outer wall of the carotid sinus experiences low and oscillating shear stresses (mean = 0.4 dynes/cm^2; range = -19.2 to 12.2 dynes/cm^2) while the inner wall is exposed to unidirectional high shear stresses (mean = 19.7 dynes/cm^2; range = 11.6 to 41.8 dynes/cm^2) [138]. Comparisons of flow in rigid and compliant vessels predicted that flow separation and shear stress levels should be reduced in healthy compliant vessels and enhanced in diseased vessels, which tend to be more rigid, supporting earlier hypotheses that the normal vascular anatomy may help minimize detrimental flow patterns [139].

Perktold *et al.* also analyzed differences in flow patterns resulting from variations in carotid bifurcation geometries, as would be found in a normal population distribution. Using four models which differed slightly in the shape of the carotid sinus and/or the bifurcation angle, they demonstrated that these subtle geometrical differences had significant effects on the extension and location of the recirculation zone in the sinus, the duration of the flow separation during the cardiac cycle, and the overall shear stress level [140, 141]. Clinical experience has shown that in larger angle carotid bifurcations, lesions develop in the internal carotid artery, a short distance

downstream from the bifurcation; in smaller angle geometries, lesions generally develop at the terminal end of the common carotid artery and extend slightly into the internal carotid artery [142]. Perktold's numerical analyses identify these distinct loci as sites of flow separation in the corresponding numerical models. The scope of anatomic variability within the general population was more extensively documented by Friedman and colleagues, who analyzed 70 human aortic bifurcations postmortem for distributions of the flow divider offset (range = 0.04 to 8.1 mm), branch angle (range = 10.4 to 61.3 degrees), and angular asymmetry (range = 0.2 to 56.1 degrees) [143]. Since these parameters can influence the patterns of hemodynamic shear stress, the identification of significant deviations within the population suggests corresponding variability in the fluid mechanical environment *in vivo*. Thus, vessel geometry, as it relates to the development of disturbed flow patterns, may be an important complicating factor in atherogenesis. Emerging radiographic techniques may make it possible to detect such geometric risks. Ku *et al.* have measured detailed flow patterns by magnetic resonance imaging, moving toward a clinically achievable method of flow detection [144].

Other characteristics of the vasculature may also affect disturbed flow patterns *in vivo*. Using compliant physical and numerical models, Tarbell, Wang and colleagues demonstrated that the impedance phase angle -- the phase difference between pressure and flow pulses -- can affect peak shear stress levels and the onset of flow reversal [145, 146]. Vasoactive drugs may affect the impedance phase angle via complex modes of action on the arterial wall. Perhaps more significantly, the phase angle can be altered by hypertension, suggesting a mechanism by which a systemic risk factor may contribute to focal disease development.

A number of *in vivo* morphometric studies, both in native and surgically altered vessels, have demonstrated that endothelial cell structure is modified in regions of disturbed flow, with the cells displaying polygonal, non-oriented shapes, in contrast to the elongation and alignment of endothelial cells in regions of primarily unidirectional flow [7, 147-150]. These findings raise the question as to the potential role of hemodynamically induced endothelial alterations in atherosclerotic development. Previous studies in our laboratory with the *in vitro* disturbed flow system have confirmed the flow-specific cell shape changes and have also demonstrated that endothelial cell migration and proliferation are enhanced by disturbed flow as compared with uniform laminar shear stress [22-24]. In addition, as mentioned in Chapter 2, several endothelial expressed molecules implicated in atherogenesis are selectively upregulated at disease loci. Most notably, VCAM-1 is expressed on endothelial cells covering early aortic atherosclerotic lesions near branch points in a rabbit model, and ICAM-1 is significantly upregulated in both lesion-free and atherosclerotic human vessels on the outer wall of the carotid sinus -- the location of both

disturbed flow exposure and frequent disease development. Given the putative role that both endothelial adhesion molecules and disturbed flow play in atherogenesis, the studies reported here were undertaken to investigate the potential regulation of ICAM-1, E-selectin and VCAM-1 in cultured endothelial cells exposed to disturbed laminar shear stress. Comparison of these results with those obtained in the uniform laminar shear stress model should provide insight regarding the nature of an effective shear stress stimulus which is capable of altering endothelial gene expression.

METHODS

Cell Culture. Each primary HUVEC culture was established, as previously described, from either a segment from a single normal term umbilical cord or from multiple cord segments pooled together [89]. For experimental use, second passage cells were plated on tissue culture-treated polystyrene coated with 0.1% gelatin and grown to confluence in Medium 199 (with 25 mM HEPES) supplemented with 20% FBS, 2 mM glutamine, 100 U/ml penicillin, 100 µg/ml streptomycin, 50 µg/ml endothelial cell growth supplement, and 100 µg/ml heparin. In certain experiments, HUVEC monolayers were activated by treatment with recombinant human IL-1ß (Biogen, Cambridge, MA), as indicated.

Disturbed Laminar Shear Stress Apparatus. The basic cone-plate system was described under Methods in Chapter 2. In order to perform disturbed laminar shear stress experiments, a modified coverslip/ring geometry was utilized. Each tissue culture treated plastic coverslip was glued into a stainless steel ring which contained a protuberance, in the form of a rectangular bar, that disturbed the flow immediately downstream from the bar (**Figure 3.1**), as calculated by DePaola [22]. Further downstream, uniform laminar shear stress was re-established. The apparatus accommodated 8 rings, with each bar aligned in the radial direction. With this configuration, nearly concentric flow must be created so that the streamlines strike the bar at a perpendicular angle. Deviations of up to 2° from perpendicular were considered acceptable, which corresponded to $\tilde{R} \leq 0.0625$, as measured by Sdougos *et al.* [21]. In order to achieve physiologically relevant shear stress levels, given this constraint on $\tilde{R}$, it was necessary to increase the viscosity of the medium, which was accomplished by adding dextran to the medium (MW 510,000; 2.7 - 6% w/v; Sigma Chemical Company). The position of the reattachment point was approximated by:

$$L\ (mm) = (0.074)Re + 0.295 \qquad \text{for } 2 < Re < 7,$$

where Re, the local Reynolds number, was determined by:

$$Re = \frac{\omega r h^2}{\nu H}$$

and ω is angular velocity of the cone, r is radial location on the plate, h is bar height (0.4 mm), ν is kinematic viscosity of the medium, and H is the distance between the cone and plate at position r (DePaola, personal communication). For the experiments reported here, fluid mechanical parameters (cone angle, cone rotation, and medium viscosity) were adjusted such that endothelial monolayers in the uniform flow region were subjected to shear stresses of 5 - 12 dynes/cm^2 and the reattachment point was positioned 0.55 - 0.81 mm downstream from the bar.

Immunocytochemistry. For microscopic visualization of cell surface associated proteins, endothelial monolayers were fixed and stained as described under Methods in Chapter 2. The use of 2% paraformaldehyde as the primary fixative, without any secondary permeabilizing agent, was designed to detect cell surface expressed proteins. In certain experiments, permeabilization with 0.1% Nonidet P-40 (NP-40) for 1 minute was utilized to reveal total cellular proteins, as indicated.

RESULTS

HUVEC cultures derived from single umbilical cords exhibit a homogeneous pattern of cell surface ICAM-1, E-selectin, and VCAM-1. In general laboratory practice, HUVEC monolayers are derived from several umbilical cords, on the assumption that any genetic or environmental variations specific to one umbilical cord will be less significant in the pooled cultures. However, preliminary immunocytochemical staining of cytokine-induced HUVEC monolayers revealed heterogeneous expression of cell surface ICAM-1, E-selectin, and VCAM-1, (VCAM-1 shown in **Figure 3.2**). Such heterogeneous expression might complicate detection of a spatially distributed pattern of gene expression within the disturbed flow model, since the disturbed flow region is narrow (approximately 1.5 mm) and contains a relatively small number of cells. With the goal of obtaining a more homogeneous endothelial monolayer, we postulated that HUVEC cultures derived from an individual umbilical vein might exhibit more uniform cellular activation than pooled cultures. **Figure 3.2** demonstrates that single-cord-culture HUVEC monolayers do indeed display a homogeneous pattern of immunocytochemical staining for VCAM-1 when maximally induced by IL-1ß. Similar homogeneous staining was seen for ICAM-1 and E-selectin (data not shown). It is interesting to note that at time points corresponding to sub-maximal expression, the staining pattern is not

Figure 3.1. **The disturbed laminar shear stress model.** Disturbed laminar shear stress patterns were created within the cone and plate apparatus by positioning a bar (0.4 mm in height) in the flow field. Detailed characteristics of the downstream flow, including spatial variations in shear stress magnitudes and shear stress gradients, were determined previously by numerical analysis, as described in Methods.

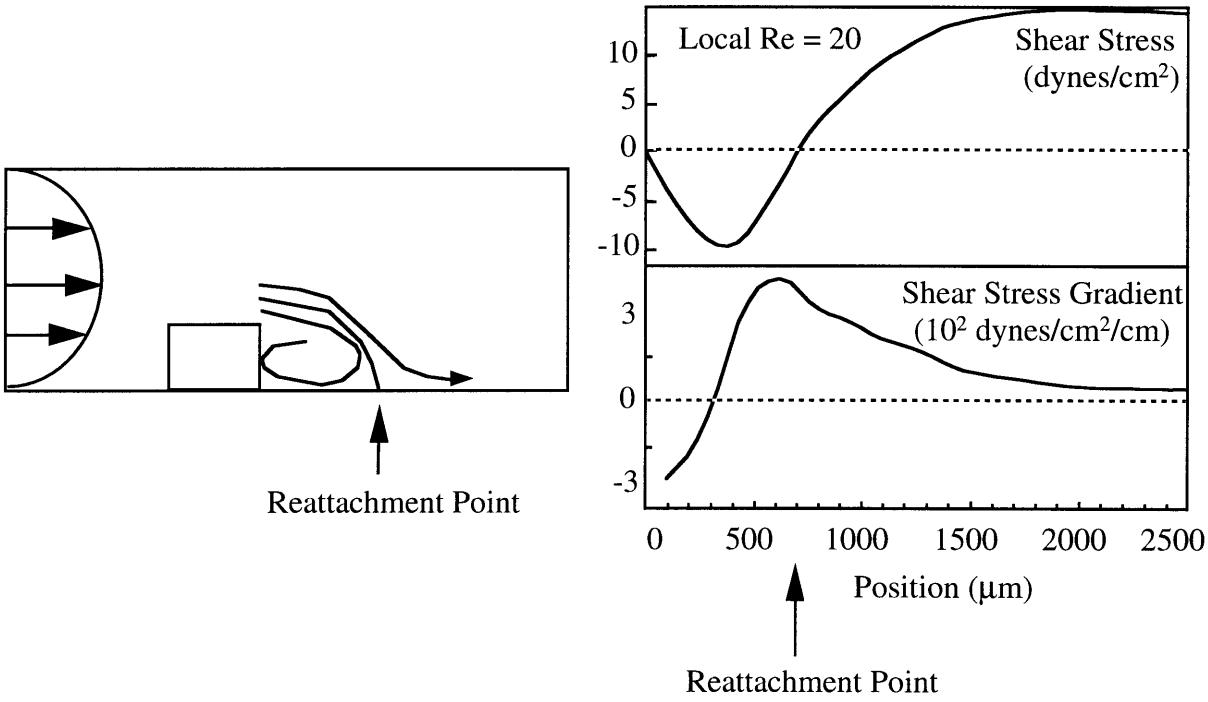

[Modified from Tardy *et al.*, 1994. Endothelial cell migration, division, and loss in regions of disturbed flow. *In* Proceedings of the Second World Congress of Biomechanics, Amsterdam.]

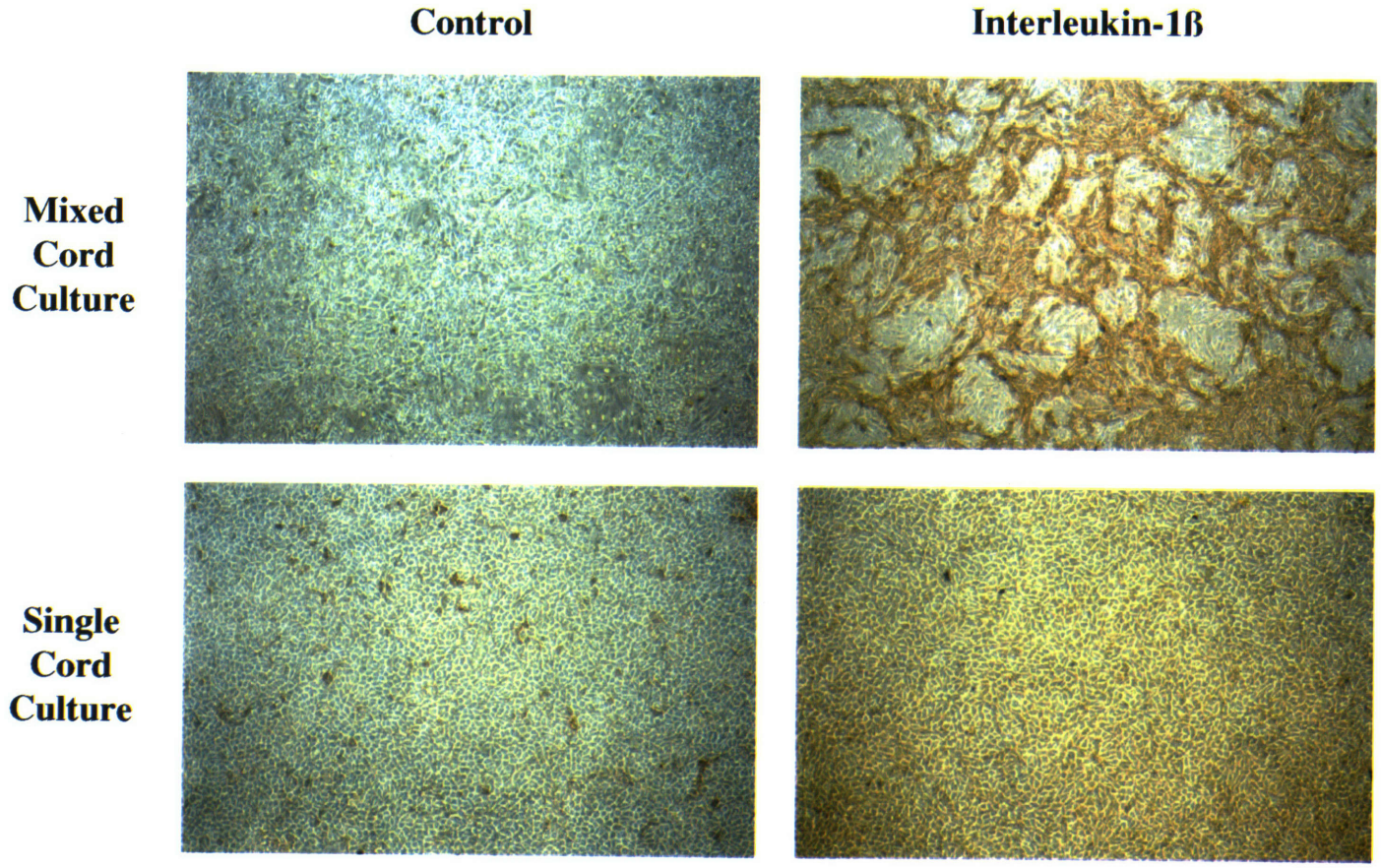

Figure 3.2. **Homogenous staining pattern of VCAM-1 protein in single cord HUVEC cultures.** HUVEC cultures were established either from a single normal term umbilical cord or from multiple cords pooled together. Confluent monolayers were maintained under static (no flow) conditions with or without IL-1ß (8 hours, 10 U/ml) and were then fixed with 2% paraformaldehyde and immunocytochemically stained using a VCAM-1 specific monoclonal antibody and visualized by phase contrast microscopy, as described in Methods. Original magnification = 12.5X.

homogeneous (see **Figure 3.8**, upper left panel). Based on this finding, all subsequent disturbed flow experiments were conducted with single cord HUVEC cultures.

Endothelial-leukocyte adhesion molecule expression by HUVEC in a disturbed flow model.

ICAM-1 is induced by both disturbed and uniform laminar shear stress. Immunocytochemical staining of HUVEC monolayers exposed to a disturbed flow field (τ = 12 dynes/cm^2 in the downstream uniform flow region) for 24 hours revealed increased cell surface ICAM-1 protein, detectable as a brown stain, on cells in both the disturbed and uniform flow regions, as compared with monolayers maintained under static conditions (**Figure 3.3**). While not all cells within the monolayer displayed enhanced staining, there appeared to be slightly more ICAM-1 expression on cells in the uniform flow region than in the disturbed flow region. However, previous studies with this model have demonstrated that monolayers subjected to extended periods of disturbed flow undergo reorganization due to enhanced migration away from the reattachment point. As a result, the disturbed flow region generally has a lower cell density than does the uniform laminar region, and such regional differences in cell density most likely account for the small spatial variation in ICAM-1 staining. In a series of 17 experiments, including ranges in both flow duration (4 - 48 hours) and shear stress levels (5 - 12 dynes/cm^2 in uniform flow region), time-dependent upregulation of ICAM-1 by both disturbed and uniform laminar shear stress was observed, but no significant differences in ICAM-1 induction were detectable in monolayers exposed to different shear stress levels (data not shown).

E-selectin and VCAM-1 are not upregulated in HUVEC by either disturbed or uniform laminar shear stress. In contrast to the induction of ICAM-1 within the disturbed flow model, no significant changes were observed in cell surface E-selectin or VCAM-1 expression in either the disturbed or uniform flow regions, as detected by immunocytochemistry, at any time point (4 - 48 hours) or shear stress level (5 - 12 dynes/cm^2 downstream) studied (see **Figures 3.4 and 3.5**). The data shown are representative of 21 experiments with E-selectin and 23 experiments with VCAM-1. Occasionally, a few isolated cells within the disturbed flow region exhibited increased VCAM-1 cell surface protein, indicated by the arrows in **Figure 3.5**. However, such staining was not apparent in all experiments.

Figure 3.3. **Induction of ICAM-1 protein within the disturbed flow field.** Confluent HUVEC cultures derived from a single umbilical cord were either maintained under static conditions or exposed to a disturbed flow field (12 dynes/cm^2 in the uniform flow region) for 24 hours. The monolayers were then fixed with 2% paraformaldehyde and immunocytochemically stained using an ICAM-1 specific monoclonal antibody and visualized by phase contrast microscopy, as described in Methods. Original magnification = 12.5X.

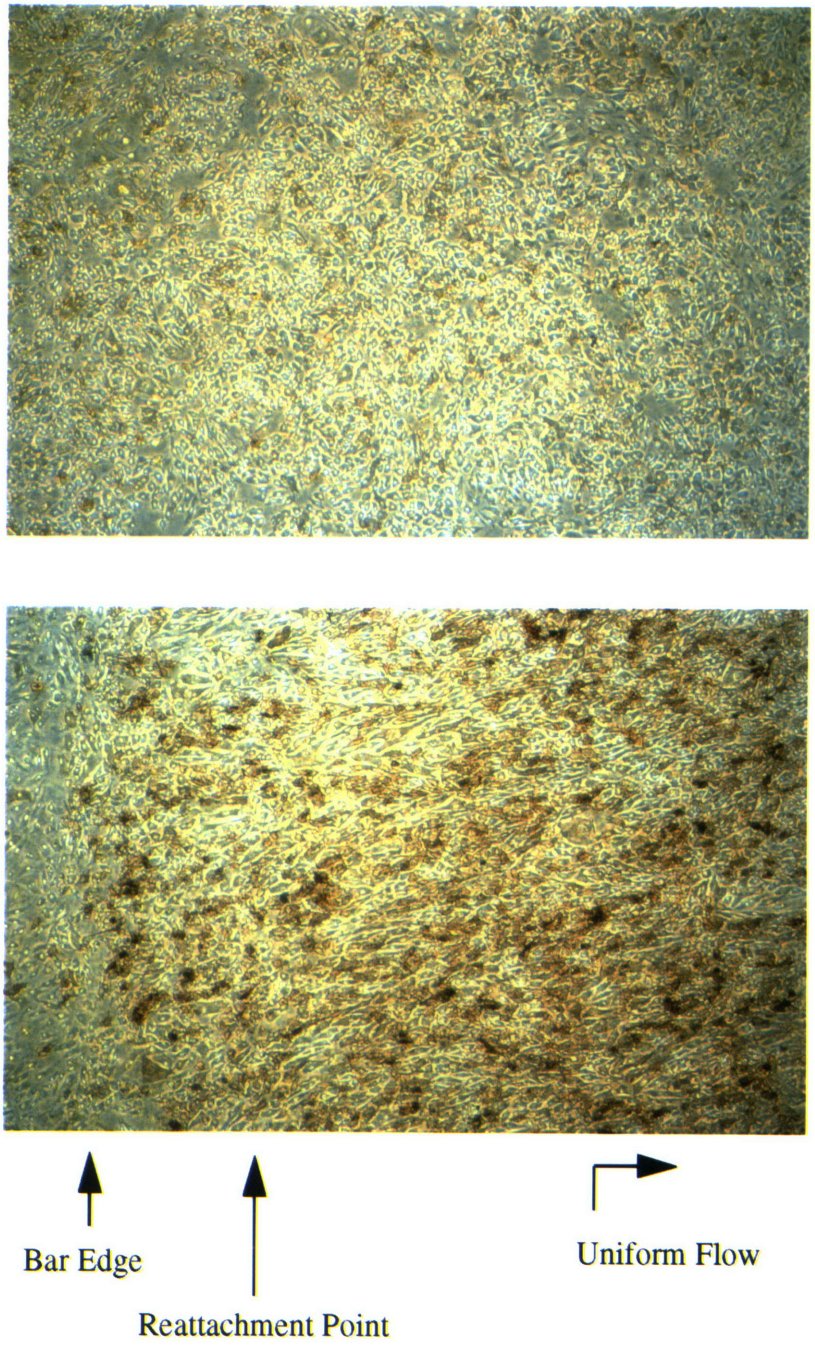

Figure 3.4. **E-selectin is not induced by exposure to the disturbed flow field.** Confluent HUVEC cultures derived from a single umbilical cord were either maintained under static conditions or exposed to a disturbed flow field (12 dynes/cm^2 in the uniform flow region) for 24 hours. The monolayers were then fixed with 2% paraformaldehyde and immunocytochemically stained using an E-selectin specific monoclonal antibody and visualized by phase contrast microscopy, as described in Methods. Original magnification = 12.5X.

Static

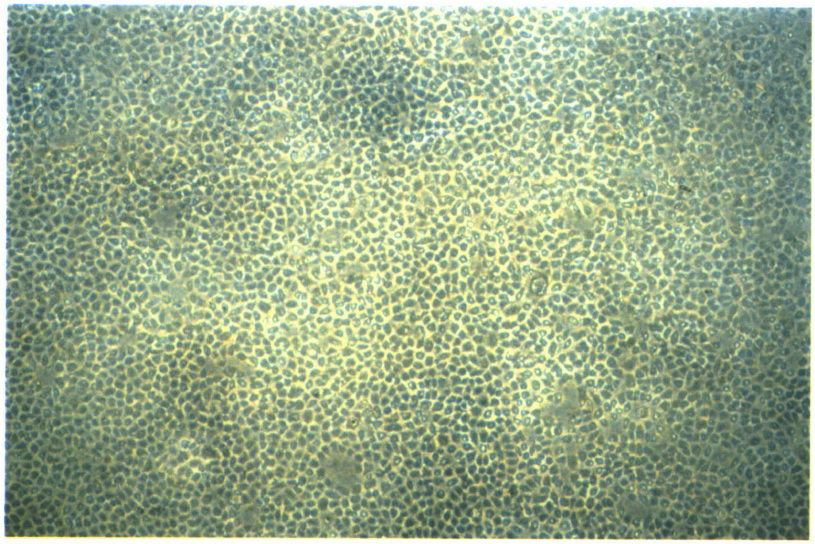

Disturbed Flow
(24 hr, 12 dynes/cm^2)

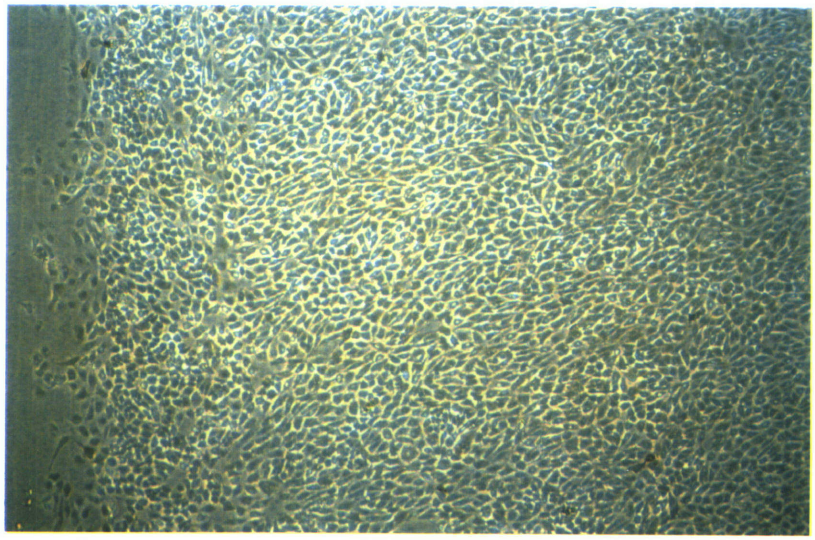

Figure 3.5. **VCAM-1 is not induced by exposure to the disturbed flow field.** Confluent HUVEC cultures derived from a single umbilical cord were either maintained under static conditions or exposed to a disturbed flow field (12 dynes/cm^2 in the uniform flow region) for 24 hours. The monolayers were then fixed with 2% paraformaldehyde and immunocytochemically stained using a VCAM-1 specific monoclonal antibody and visualized by phase contrast microscopy, as described in Methods. Arrows indicate individual cells within the disturbed flow region that were VCAM-1 positive. Original magnification = 12.5X.

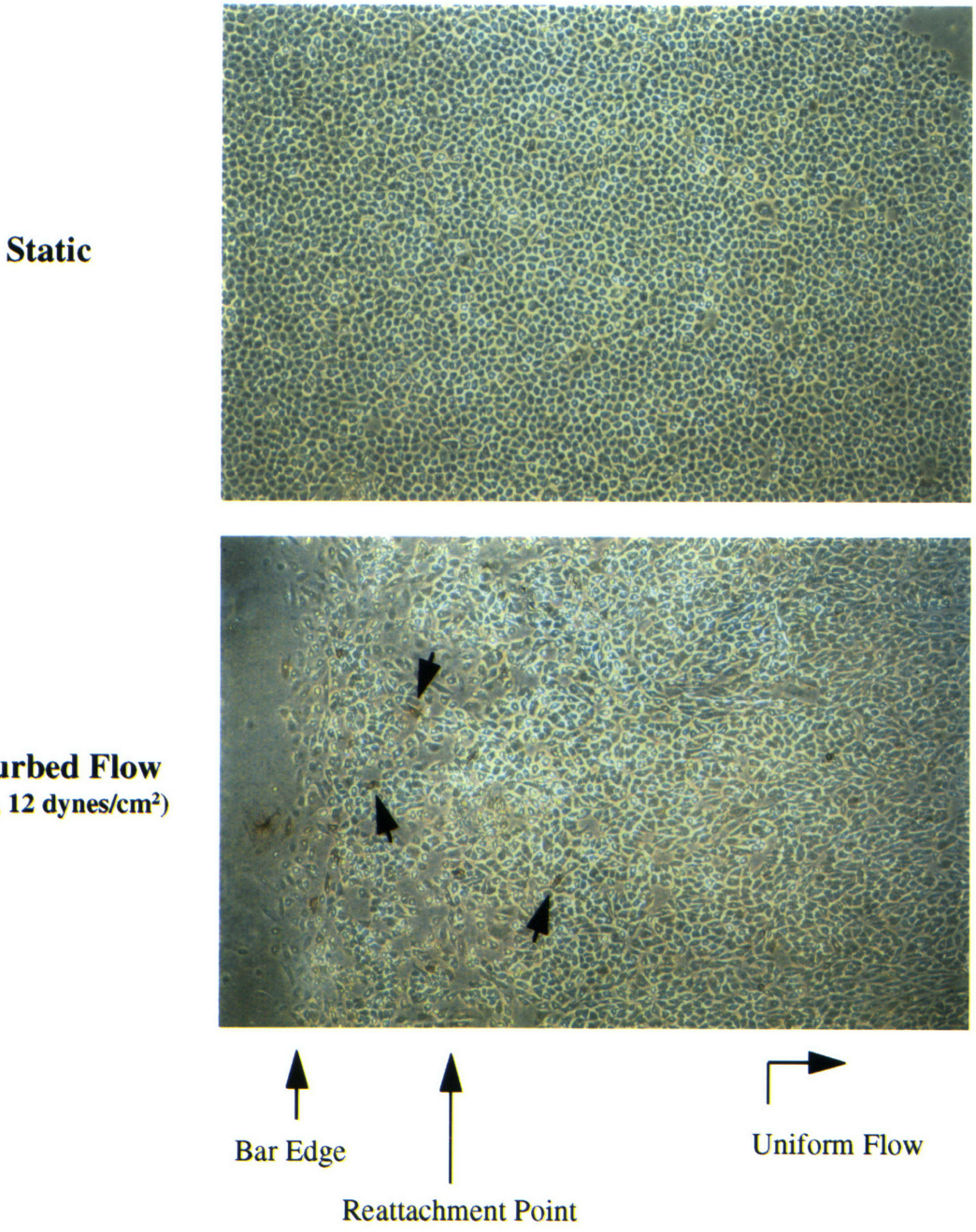

Influence of disturbed flow pre-conditioning on cytokine inducibility of adhesion molecules in HUVEC.

Cytokine induction of ICAM-1 and E-selectin is not affected by pre-conditioning with either disturbed or uniform laminar shear stress. In order to test whether endothelial cells exposed to the disturbed flow model were still responsive to other activating stimuli, such as cytokines, we subjected HUVEC monolayers to 24 hours of laminar shear stress at various levels followed by treatment under static conditions with IL-1ß over a range of concentrations for different time periods. For all experimental conditions, immunocytochemical staining of non-permeabilized monolayers revealed a homogeneous induction pattern of ICAM-1 and E-selectin in the uniform and disturbed flow regions, comparable to that observed in HUVEC that were not exposed to shear stress (see **Figures 3.6 and 3.7**). Data shown are representative of 2 experiments with ICAM-1 (5 and 12 dynes/cm^2 in uniform flow region; 10 U/ml IL-1ß; 4, 7, and 24 hours cytokine exposure) and 7 experiments with E-selectin (5, 12, or 19 dynes/cm^2 in uniform flow region; 0.33 - 10 U/ml IL-1ß; 0.5, 1, 1.5, 2, and 4 hours cytokine exposure).

Cytokine induction of VCAM-1 is inhibited by pre-conditioning with disturbed but not uniform laminar shear stress. Pre-conditioning of HUVEC monolayers with the disturbed flow model for 24 hours resulted in a diminished subsequent cytokine-induced expression of VCAM-1. This effect was non-uniform and appeared to be more pronounced in cells within the disturbed flow region, as compared with those in the uniform flow region (**Figure 3.8**). The inhibition of VCAM-1 protein induction by pre-conditioning for 24 hours with disturbed flow was detectable in each of 10 experiments spanning a range of IL-1ß concentrations (0.33 - 10 U/ml) as well as exposure durations (2 - 24 hours; data not shown). In particular, the heterogeneous staining pattern was most striking under conditions corresponding to sub-maximal levels of IL-1ß induction (4 hours exposure), as shown in **Figure 3.8**. In addition, the differential pattern of cytokine-induced VCAM-1 expression was similar in permeabilized and non-permeabilized endothelial monolayers (permeabilized monolayers shown in **Figure 3.8**).

DISCUSSION

Our previous data (presented in Chapter 2) demonstrated that a given shear stress regime, namely uniform laminar shear stress, could differentially regulate a class of endothelial expressed effector molecules. The current findings extend those results, demonstrating that disturbed laminar shear stress also differentially modulates endothelial adhesion molecule expression -- both as a direct stimulus, and indirectly by altering the responsiveness of the endothelial cell to a soluble stimulus such as IL-1ß. Of the three adhesion molecules studied, ICAM-1 is the only one that was

Figure 3.6. **Cytokine induction of ICAM-1 in a disturbed flow model.** Confluent HUVEC cultures derived from a single umbilical cord were first either maintained under static conditions or exposed to a disturbed flow field (12 dynes/cm^2 in the uniform flow region) for 24 hours, and were then stimulated with IL-1ß (7 hours, 10 U/ml) under static conditions. After fixation with 2% paraformaldehyde, the monolayers were immunocytochemically stained with an ICAM-1 specific monoclonal antibody and visualized by bright field microscopy, as described in Methods. Original magnification = 12.5X.

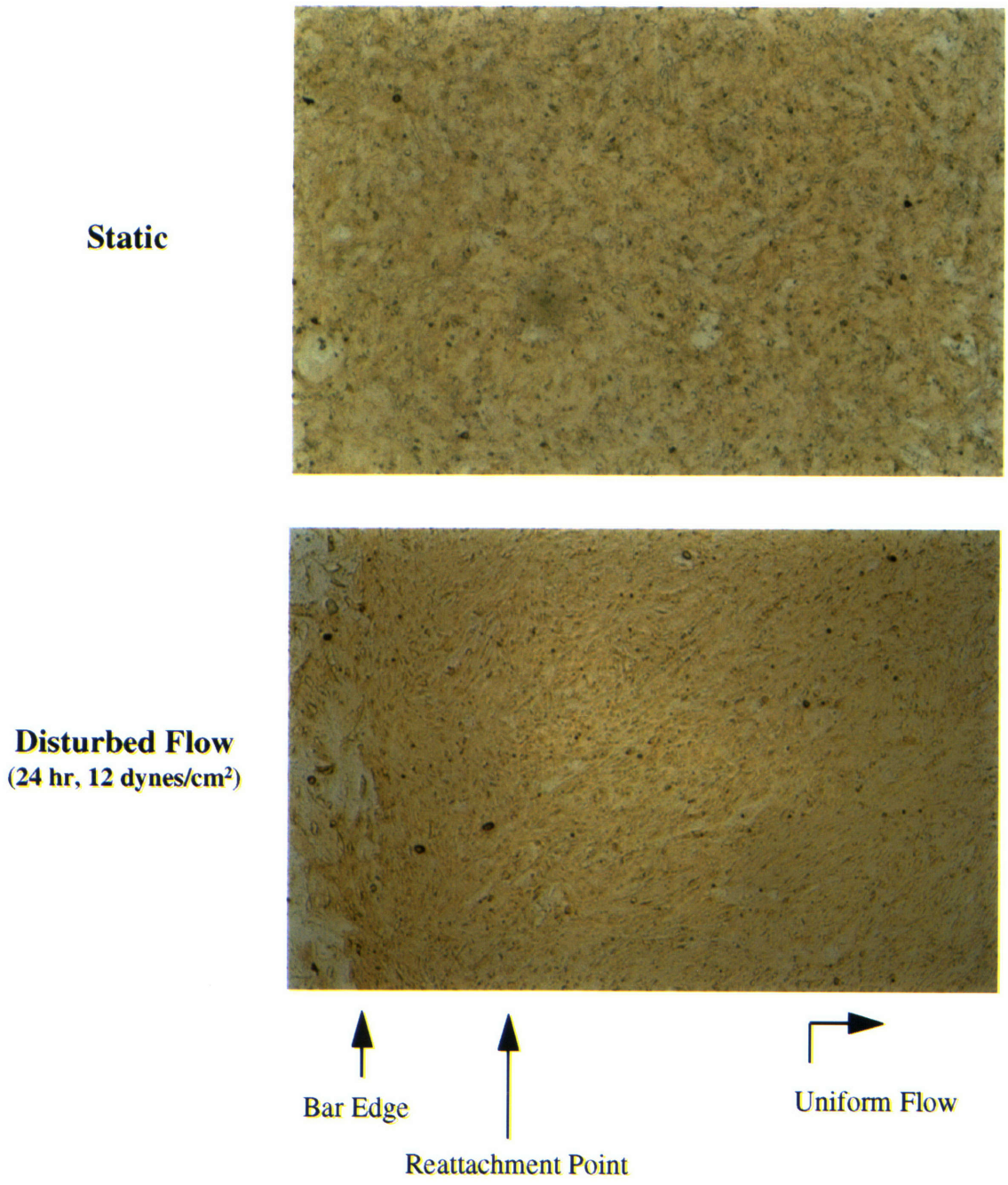

Figure 3.7. **Cytokine induction of E-selectin in a disturbed flow model.** Confluent HUVEC monolayers derived from a single umbilical cord were first either maintained under static conditions or exposed to a disturbed flow field (12 dynes/cm^2 in the uniform flow region) for 24 hours, and were then stimulated with IL-1ß (4 hours, 0.33 U/ml) under static conditions. After fixation with 2% paraformaldehyde, the monolayers were immunocytochemically stained with an E-selectin specific monoclonal antibody and visualized by phase contrast microscopy, as described in Methods. Original magnification = 12.5X.

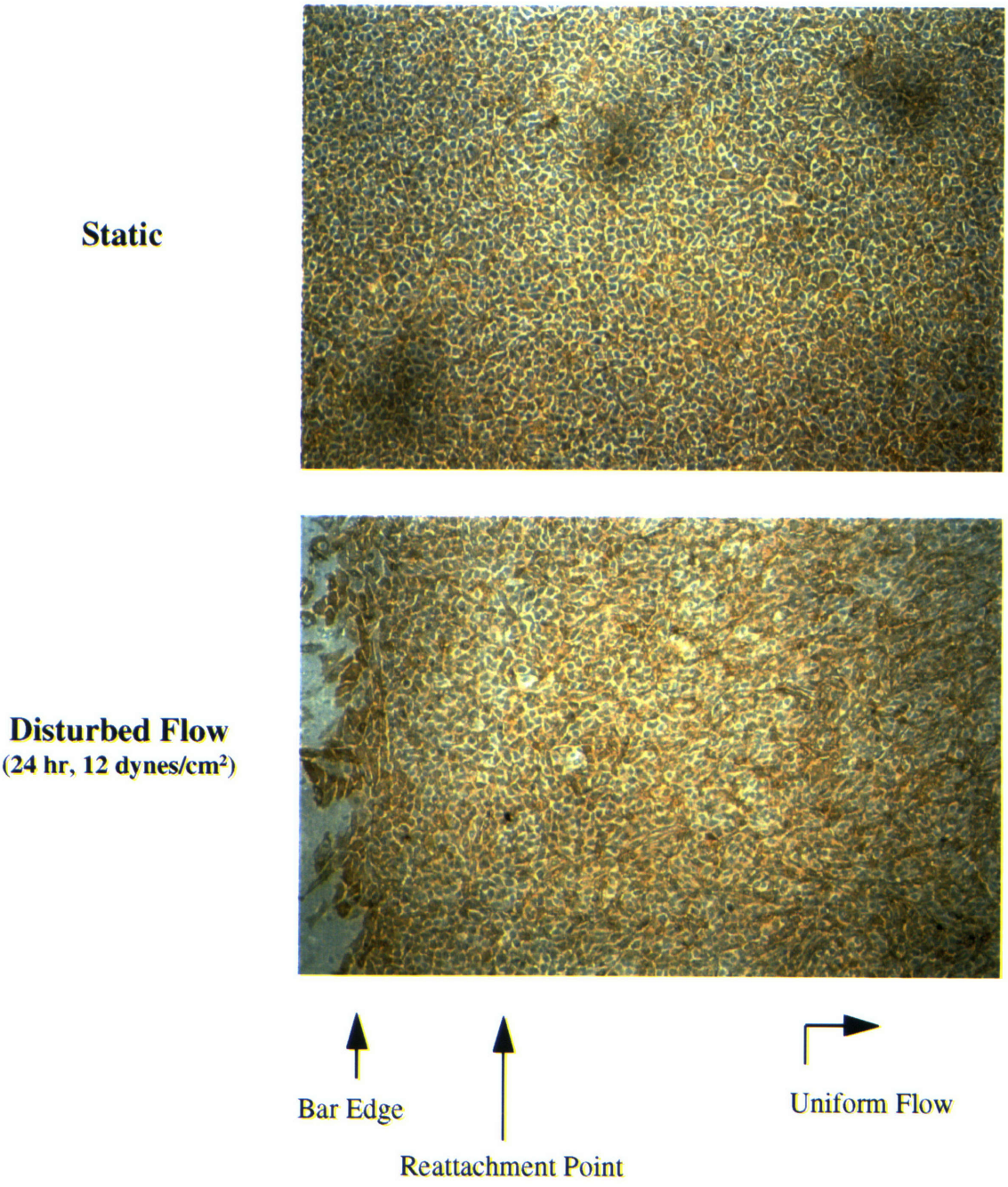

Figure 3.8. **Cytokine induction of VCAM-1 is inhibited by pre-conditioning with disturbed flow.** Confluent HUVEC monolayers derived from a single umbilical cord were first either maintained under static conditions or exposed to a disturbed flow field (12 dynes/cm^2 in the uniform flow region) for 24 hours, and were then stimulated with IL-1ß for 4 hours, at the concentrations indicated, under static conditions. After fixation with 2% paraformaldehyde, followed by permeabilization with 0.1% NP-40, the monolayers were immunocytochemically stained with a VCAM-1 specific monoclonal antibody and visualized by phase contrast microscopy, as described in Methods. Original magnification = 12.5X.

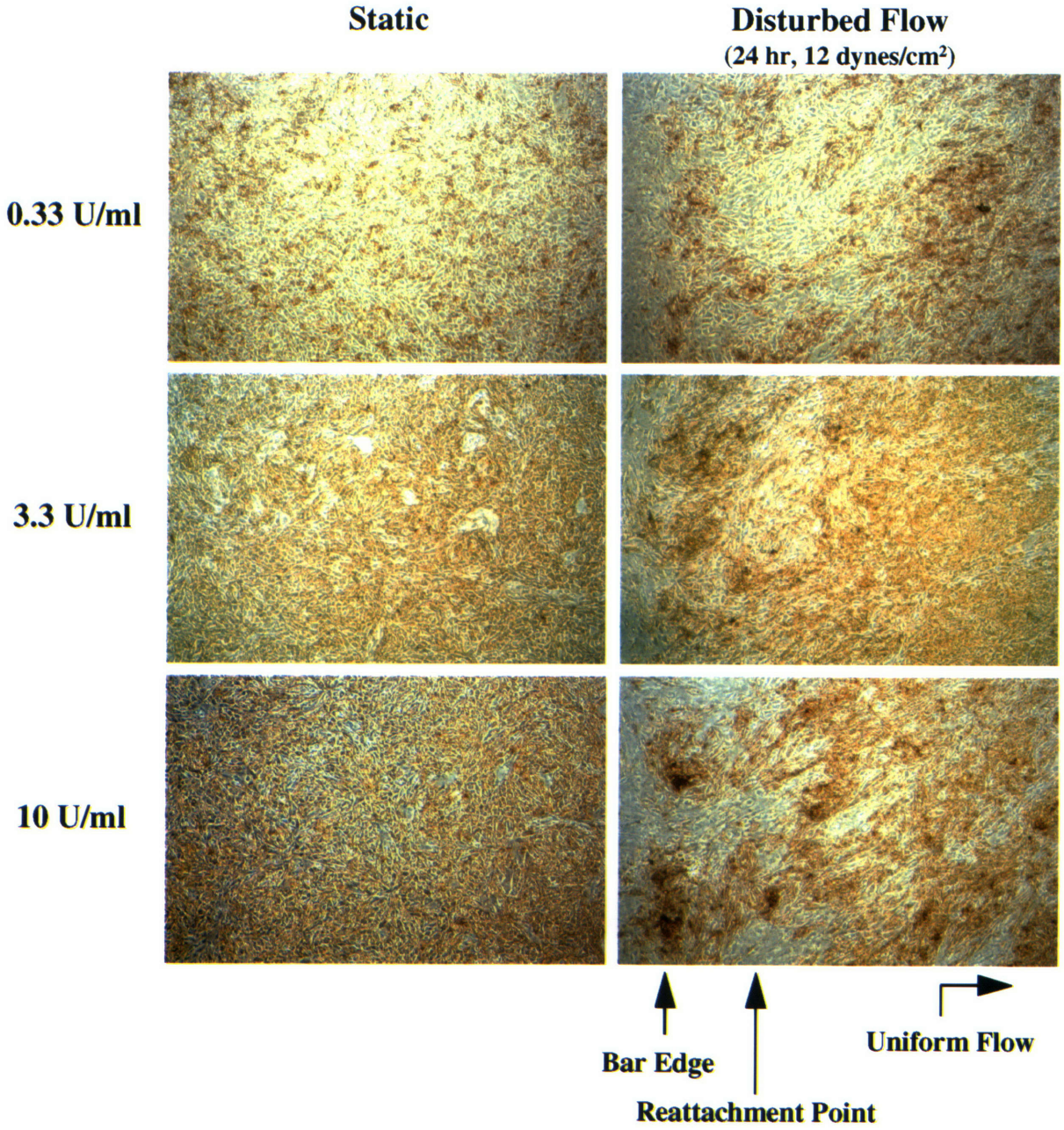

observed to be directly induced by both uniform and disturbed laminar shear stress in this model system. While VCAM-1 expression was not directly altered by exposure to disturbed flow, its subsequent activation by IL-1ß was inhibited by pre-conditioning with disturbed laminar shear stress for 24 hours. Neither uniform nor disturbed flow altered the expression of E-selectin or its capacity for cytokine inducibility. These profoundly different expression patterns of three endothelial adhesion molecules support our working hypothesis that the endothelial cell is capable of sensing its local environmental milieu and responding via coordinated expression of different genes. In addition, these data indicate that uniform and disturbed laminar shear stress act as distinct stimuli to the endothelium, indicating that the endothelial cell is capable of detecting subtle variations in biomechanical stresses.

To our knowledge, this report is the first documentation of homogeneous staining for endothelial adhesion molecules within single cord HUVEC cultures. Using flow cytometry, Bender *et al.* have previously demonstrated that single cord HUVEC cultures exhibit varying thresholds for cytokine activation of ICAM-1, E-selectin, and VCAM-1 [151]. Nuclear run-off experiments demonstrated that the varying phenotypes were a consequence of different levels of transcriptional activation between distinct cultures. However, the observed phenotypic differences did not appear to be due to variations in cell surface cytokine receptors, nor could they be attributed to differences in cell cycle phases between cultures. Thus, the heterogeneity among different HUVEC cultures could be due to genetic differences, manifested either as alterations in specific transcriptional activation pathways or as immunologic reactions between cells of distinct genetic origin. If the former were true, we would expect to find a non-responsive single cord culture, and one has not yet been identified in the 9 single cord HUVEC cultures utilized thus far. Immunologic reactions would presumably require the presence of contaminating lymphocytes within the HUVEC cultures, which if present at all, probably do not exist in high enough numbers to elicit the dispersed heterogeneous staining pattern.

Preliminary data from Varner *et al.* has shown that pre-conditioning of HUVEC with uniform laminar shear stress resulted in inhibition of IL-1ß induced VCAM-1 expression at the levels of both mRNA and protein [109, 152], whereas the data presented in this Chapter indicates no consistent inhibition of VCAM-1 protein by uniform laminar flow pre-conditioning. An identifiable distinction between the uniform laminar shear stress experiments in both laboratories and the uniform flow region within our disturbed flow model is the presence of dextran for viscosity modification in the disturbed flow culture medium. However, as mentioned in Chapter 2, the significance of this variable was ruled out by uniform laminar experiments without dextran, in which IL-1ß induced VCAM-1 cell surface expression was not altered by uniform laminar shear

stress pre-conditioning. It is possible that post-transcriptional and post-translational mechanisms may play significant roles in this setting, and it would be interesting to utilize in situ hybridization within the disturbed flow model to determine whether the inhibition of VCAM-1 activation by IL-1ß occurs at the level of mRNA.

In vivo, the endothelium must actually integrate both biochemical and biomechanical stimuli, and our disturbed flow pre-conditioning experiments, followed by cytokine activation, provide a simplified model of this complex *in vivo* environment. In this light, it is somewhat counter-intuitive that cytokine induction of VCAM-1 is inhibited by disturbed, but not uniform flow pre-conditioning, given the role that adhesion molecules, disturbed flow, and monocyte/macrophage-derived cytokines are thought to play in atherogenesis [2]. Also, elevated levels of both VCAM-1 and ICAM-1 have been detected in early atherosclerotic lesions at disturbed flow sites. However, while the *in vitro* disturbed laminar shear stress model was designed to mimic *in vivo* disturbed flow patterns, care must be taken in extrapolating the *in vitro* findings to *in vivo* settings. Not only are the cultured endothelial cells not able to interact with other cell types that would be present within the vessel wall, but they are exposed to an artificial culture medium, instead of the complete mixture of soluble and cellular constituents present within the blood. In addition, the entire biomechanical environment is not replicated in the *in vitro* system, since the endothelial monolayer is grown on a rigid substrate, as opposed to the elastic arterial wall. Also, as mentioned in Chapter 2, the *in vitro* experiments actually represent step functions in which the cells are rapidly changed from static to flow environments. All of the experiments reported here were conducted under steady flow conditions; additional information might be gained by utilizing an unsteady disturbed flow model, created with an eccentric rotating cone. While the resultant shear stress pattern is not identical to *in vivo* pulsatile flow, it does incorporate regular movement of the reattachment point forward and backward, which is a key element of pulsatile disturbed flow *in vivo*. Thus, the *in vitro* disturbed flow system is most appropriately viewed as a model in which to examine the relevant shear stress parameters -- most notably, spatial variations in both shear stress magnitudes and gradients -- that may regulate endothelial cell structure and function.

The data presented in this Chapter not only suggest that disturbed and uniform flow patterns can differentially regulate endothelial gene expression, but also emphasize the need for developing new analysis techniques for future disturbed flow studies. In particular, quantitative measurement of gene expression levels within both the disturbed and uniform flow regions will be important. Also, evaluation of end-point effector molecules such as ICAM-1, E-selectin, and VCAM-1 is undoubtedly complicated by the fact that cell surface adhesion molecule expression requires extended exposure to flow and probably involves regulatory mechanisms at a number of

different levels (e.g., transcriptional, post-transcriptional and post-translational). Thus, measurement of an earlier genetic regulatory event may allow for more direct correlation with shear stress parameters, both because fewer levels of regulation may come into play and because shorter exposure to the disturbed flow model will minimize the development of cell density variations due to migration and proliferation. Fluorescent image analysis of rapidly activated gene products, such as DNA-binding transcription factors may satisfy all of the above requirements. Specifically, measurement of the nuclear localization of these proteins will provide biologically relevant information, since the primary site of action of these proteins is in the nucleus. These experiments are the subject of Chapter 4.

Chapter 4

DIFFERENTIAL REGULATION OF TRANSCRIPTION FACTORS IN ENDOTHELIAL CELLS EXPOSED TO UNIFORM AND DISTURBED LAMINAR SHEAR STRESS

INTRODUCTION: THE ROLES OF NUCLEAR FACTOR-κB, EARLY GROWTH RESPONSE-1, C-JUN, AND C-FOS IN VASCULAR BIOLOGY

As mentioned in Chapter 1, following the identification of the functional "shear stress response element" (SSRE) within the promoter of the platelet-derived growth factor-B (PDGF-B) gene, several other "SSREs" have been described as requisite promoter elements for the shear stress induction of other endothelial genes, including monocyte chemotactic protein-1 (MCP-1), platelet-derived growth factor-A (PDGF-A), and tissue factor (TF). A key step in understanding the molecular mechanisms through which these various SSREs control gene expression is to identify the transcription factors which bind these response elements and activate transcription. In the case of the PDGF-B SSRE, data from our group has shown that this 6 bp motif (GAGACC) can be activated by the transcription factor nuclear factor-κB (NF-κB) [53]. Dimers of the transcription factor proteins c-Jun and c-Fos are necessary for MCP-1 gene induction by shear stress through a TRE (AP-1) site [54], while the nuclear proteins early growth response-1 (Egr-1) and Sp1 interact functionally with the SSREs in the promoters of the PDGF-A and TF genes, respectively [55, 56]. As such, each of these transcription factors appears to be an appropriate candidate for analysis within the disturbed laminar shear stress model. The expression patterns of each of these proteins *in vivo*, the mechanisms by which they activate transcription, as well as the data identifying their role in shear stress gene induction are reviewed below.

Nuclear Factor-κB

Nuclear factor-κB (NF-κB) is a transcription factor associated with rapid-response activation mechanisms that is composed of protein dimers of the Rel/NF-κB family. These dimers regulate transcriptional expression by binding κB response elements in the promoters of their target genes. The list of NF-κB activating stimuli is extensive and diverse, including biologic response modifiers such as cytokines, growth factors, viral products, oxidative stress, and cyclic strain [153, 154]. In addition, NF-κB has been implicated in the induction of downstream effector molecules involved in a variety of cellular processes such as growth, development, tumorigenesis, immunologic responses, inflammation and atherogenesis. Recent data has provided direct evidence that NF-κB is indeed upregulated in the vasculature during injury and may be involved in

the regulation of inflammatory molecules in that setting [155].

Members of the Rel/NF-κB protein family share in common the Rel homology domain (RHD), which is approximately 300 amino acids in length and is necessary for protein dimerization, nuclear translocation, and DNA binding [153]. The p50/p65 dimer is the predominantly expressed form of NF-κB, and the p65 subunit appears to contain the most transcriptionally active sites, presumably located outside the RHD. Although NF-κB may be transcriptionally induced to an extent, its activation is primarily regulated at a post-transcriptional level via interactions with members of a family of IκB inhibitor proteins [153, 156]. Under unstimulated conditions, constitutively expressed NF-κB is sequestered in the cytoplasmic compartment by binding to IκB [157]. IκB interacts with and masks the nuclear localization signal located in the RHD of NF-κB [158, 159]. Upon cellular activation, NF-κB is released from IκB by multi-step degradation of IκB, involving its phosphorylation, ubiquitination, and proteolysis within the proteasome [160-163]. NF-κB then translocates to the nucleus where it activates transcription by binding κB sites within the promoters of responsive genes. A critical cysteine residue within the DNA binding domain must be in its reduced state for functional interaction of NF-κB with its response element [164, 165]. Indeed, reduction/oxidation (redox) mechanisms appear to regulate NF-κB activation under a variety of stimuli [166-169].

Uniform laminar shear stress has been shown to induce nuclear localization of both p50 and p65 in endothelial cells as early as 10 minutes after the onset of flow [170]. In addition, electrophoretic mobility shift analysis demonstrated that binding of NF-κB to its consensus DNA sequence was stimulated within 30 minutes of exposure to shear stress [171]. Recent data indicated that NF-κB can also specifically bind the SSRE in the PDGF-B promoter and can induce transcriptional activation of PDGF-B/SSRE reporter gene constructs [53]. Thus, NF-κB may play a functional role in vascular disease via its regulation by hemodynamic forces, and investigation of its potential regulation by disturbed laminar shear stress would be valuable in this regard.

Early Growth Response-1

The early growth response-1 (Egr-1) gene encodes a protein with three zinc finger motifs

which mediate its DNA-binding and subsequent transcriptional activation of its target genes. Egr-1 is expressed in a wide variety of organ systems, including cells derived from renal, nervous, muscular, osteoblastic, immune, and vascular tissues [172-180]. In addition, Egr-1 gene expression is induced by a vast array of stimuli ranging from soluble cytokines (IL-1, TNF, IFN) [181] and vasoactive substances (angiotensin II, PDGF, thrombin) [182, 183] to physicochemical activators such as oxidative stress [178, 184-186], hypertonic stress [187], ischemia/reperfusion [172, 175], and cyclic stretch [177, 188, 189]. Once induced, Egr-1 in turn regulates the expression of target genes involved in proliferation [190, 191], differentiation [192, 193], immune responses [179, 194-197], and vascular activation [180, 198-202]. Recent data has implicated Egr-1 in the regulated expression of PDGF-B and other genes upregulated in mechanically injured endothelial cells *in vivo* [180]. Thus, Egr-1 appears to play important functional roles in a variety of biological settings.

Egr-1 expression is modulated by a number of other known transcription factors. Its promoter contains several putative regulatory elements, including two Sp1 sites, five serum response-like elements, two cAMP response-like elements, a tetra-decanoyl phorbol acetate (TPA)-responsive element, and an Egr-1 binding site through which Egr-1 regulates its own expression [203]. Thus, the ultimate transcriptional expression of this gene is due to the complex interplay of many DNA binding proteins.

Once it is transcribed, the activation state of the Egr-1 protein may be regulated through a variety of post-transcriptional mechanisms. For example, the phosphorylated form of this protein binds its DNA recognition sites more efficiently than the non-phosphorylated form [204]. At least one stimulus, granulocyte-macrophage colony-stimulating factor, has been shown to upregulate Egr-1 expression by significantly increasing the protein half life within the cell [205]. Also, a number of studies have demonstrated that Egr-1 binding to its DNA recognition sequences can be regulated by the intercellular redox state [178, 184-186].

DNA binding sites for Egr-1 are frequently found together with response elements for Sp1, another zinc finger transcription factor, since both proteins recognize specific GC-rich DNA sequences (Egr-1 consensus sequence: GCGGGGGCG; Sp1 consensus sequence: GGCGGG) [174, 176, 206]. In such settings, binding of Egr-1 and Sp1 is generally mutually exclusive, with occupancy dependent on the concentrations and binding affinities of both transcription factors [207]. In most cases Sp1 constitutively occupies the site and mediates basal promoter activity, often as a repressor [198, 200]. Induced Egr-1 then displaces Sp1 and enhances transcriptional activity. However, in a few instances Egr-1 binding can result in repression, while Sp1 interaction activates transcription [208-212], indicating that transcriptional regulation by Egr-1 may be quite

complex. Interestingly, Egr-1 can also bind response elements specifically recognized by the Wilms' tumor transcription factor (WT1), with similar mechanisms of competitive occupancy [213-217]. However, it is unclear the extent to which WT1 is expressed in endothelial cells. In addition, two co-repressors of Egr-1 have recently been identified, NAB1 and NAB2, which can downregulate Egr-1 activity by binding an inhibitory domain in the Egr-1 protein [218, 219]. The diverse regulatory functions of Egr-1 are undoubtedly due, at least in part, to this interplay of Egr-1 with Sp1, WT1, NAB1 and NAB2, as well as with other proteins which are expressed in a cell-specific manner and function within the context of the local promoter architecture.

Sp1 recently has been shown to be the functional shear stress response element mediating the induction of tissue factor by uniform laminar shear stress [56]. Interestingly, the mechanism of activation is not via increased binding of Sp1 to its target sequence, but rather appears to involve the enhanced phosphorylation of Sp1 by exposure to shear stress. Since Sp1 appears to be both constitutively expressed and primarily resident in the nucleus, it would not be an appropriate gene product for analysis of nuclear localization in the disturbed flow model. However, recent data from our laboratory has demonstrated that Egr-1 functions as a shear stress response element in the upregulation of PDGF-A by uniform laminar shear stress [55]. The PDGF-A promoter contains overlapping Sp1 and Egr-1 sites, and DNA footprinting has revealed that constitutively expressed Sp1 occupies the region and is subsequently displaced by increasing levels of Egr-1. Gel retardation assays also show that nuclear extracts from shear stressed endothelial cells exhibit enhanced binding to the Egr-1 consensus sequence. Additionally, both Northern blot analysis and transfection experiments with an Egr-1/luciferase reporter construct display dramatic upregulation of Egr-1 at the level of transcription and steady state message [55, 220]. Taken together, these data identify Egr-1 as an excellent candidate gene to investigate in the disturbed flow model.

c-Jun/c-Fos

The c-*jun* and c-*fos* immediate-early genes encode proteins that interact via a leucine zipper structure to form homodimers (c-Jun/c-Jun) and heterodimers (c-Jun/c-Fos) called activator protein-1 (AP-1). AP-1 regulates transcriptional activity by binding a consensus DNA sequence termed either AP-1 or tetra-decanoyl phorbol acetate-responsive element (TPA response element, TRE). Like NF-κB and Egr-1, c-*jun* and c-*fos* are ubiquitously expressed *in vivo*, but their expression patterns have been studied even more extensively than NF-κB and Egr-1, since identifying reagents have been available for a longer period of time. Within the vasculature, c-*jun* or c-*fos* may be induced by soluble growth factors, vasoactive substances, angiogenic factors,

cytokines and coagulation factors [183, 221-230], as well as by the biomechanical forces of pressure, strain, and shear stress [154, 171, 177, 188, 231-236]. As immediate-early genes, c-*jun* and c-*fos* also are rapidly and transiently upregulated by various stresses including hypoxia, ischemia/reperfusion, and oxidative and osmotic stresses [175, 182, 187, 237-241]. The clinical relevance of c-*jun* and c-*fos* expression in vascular disease have been directly demonstrated in several vascular balloon injury models. Immediately following vessel damage, c-*jun* and c-*fos* mRNAs were upregulated at levels proportional to the extent of injury, but this induction was limited in the presence of an angiotensin converting enzyme inhibitor, a factor known to decrease intimal hyperplasia after balloon injury [242-244]. In addition, elevated levels of c-*fos* were detected in saphenous veins utilized as coronary artery bypass grafts [245]. Findings such as these have provided impetus for further studies characterizing the molecular mechanisms underlying c-*fos* and c-*jun* regulation.

AP-1 activity can be regulated at the level of transcription of the c-*jun* and c-*fos* genes, as well as by various post-translational mechanisms of protein activation. Transcriptional induction of c-*jun* is primarily modulated through a positive feedback loop involving a non-consensus TRE site located within the c-*jun* promoter. Both AP-1 and a related transcription factor, ATF2, can bind this site. c-*fos* transcriptional activation is more complex, being mediated by either a cAMP response element, a serum response element, or a sis-inducible enhancer, depending on the stimulus [246].

Activation of the transcribed AP-1 protein dimer has been shown to be regulated by at least two mechanisms: phosphorylation and reduction/oxidation (redox). Two protein residues in c-Jun, serine-266 and cysteine-252, appear to be involved in the respective phosphorylation and redox regulation of AP-1 binding. The physiological importance of these two regulatory domains is emphasized by the fact that v-Jun, the oncogenic counterpart of c-Jun, is mutated at both sites [247]. Several domains within c-Jun may be phosphorylated by a complex network of kinases collectively termed the mitogen-activated protein kinase (MAPK) cascade [248]. The c-Jun N-terminal kinases (JNKs) are MAPKs that may act directly on c-Jun and are in turn phosphorylated by a MEK (MAPK kinase). The MEK is activated by a MEKK (MAPK kinase kinase) [249]. c-Fos may be phosphorylated by a specific MAPK as well [250]. Phosphorylation generally occurs on AP-1 dimers constitutively bound to the cognate DNA sequence, indicating that only the transactivation potential of the protein is affected, not the DNA binding affinity [251-253]. In contrast, redox regulation of AP-1 directly influences its DNA binding. Reduction of conserved cysteine residues by either chemical reducing agents or Ref-1, a nuclear redox molecule, enhances DNA binding of AP-1. Conversely, oxidation or chemical modification of the cysteine residues

decreases DNA binding [169, 254, 255]. However, the redox regulation of AP-1 is quite complex and not yet fully understood, since both oxidant and antioxidant stimuli have been reported to induce AP-1 activation [256]. In addition, recent data indicates that JNK can be activated by antioxidants, suggesting that phosphorylation and redox mechanisms may function synergistically or antagonistically in regulating AP-1 function [256].

Both c-*jun* and c-*fos* mRNA levels have been demonstrated to be upregulated in endothelial cells subjected to either pulsatile or steady laminar shear stress, with c-*fos* displaying a more dramatic induction, especially after the pulsatile flow stimulus [235]. In addition, nuclear localized c-Fos protein, as detected by image analysis of the fluorescently stained protein, was significantly increased after a 1 hour exposure to high levels of uniform laminar shear stress (25 dynes/cm^2), whereas low level shear stress (4 dynes/cm^2) resulted in a more modest induction without preferential nuclear localization [257]. However, the method for identifying the nuclear space was not reported in these experiments. In the same studies, induction of c-Fos protein could be detected in HeLa cells after only 1 minute of shear stress [236]. Exposure of endothelial cells to uniform laminar shear stress induced a biphasic pattern of DNA binding by AP-1, with peak activity at 20 minutes and 2 hours [171]. More recent data has shown that a divergent TRE sequence in the promoter of the MCP-1 gene is required for the shear stress induction of this gene [54]. Subsequent studies have identified the Ras/MEKK/JNK pathway as the primary signaling mechanism in the shear stress induction of TRE/luciferase reporter gene constructs [258]. Given this substantial body of data regarding AP-1 activation by uniform laminar shear stress, it would be interesting to examine the expression patterns of c-Jun and c-Fos in endothelial cells exposed to disturbed laminar shear stress.

In summary, the transcription factors, NF-κB, Egr-1, and c-Jun/c-Fos, each display a different general pattern of activation:

- NF-κB: Degradation of IκB leading to rapid nuclear translocation of the active dimeric protein complex (e.g., p50/p65).
- Egr-1: Rapid transcriptional induction of Egr-1 protein, followed by competitive binding (versus Sp1) to GC-rich DNA sites.
- c-Jun/c-Fos: Rapid transcriptional induction, dimerization of proteins, and subsequent phosphorylation.

In addition, each of these transactivating proteins is ubiquitously expressed *in vivo* and has been implicated in the response of endothelial genes to biomechanical forces. Thus, it will be interesting to investigate the potential differential regulation of each transcription factor within the disturbed laminar shear stress model. The amount of nuclear localized protein, total cellular protein, and cell to cell variability within the endothelial monolayer will be analyzed.

METHODS

Cell Culture. Each primary HUVEC culture was derived from a single normal term umbilical cord by the method described previously [89]. For experimental use, second passage cells were plated on tissue culture-treated polystyrene (Costar Corporation, Cambridge, MA; Lectro Engineering Co., St. Louis, MO) coated with 0.1% gelatin (Difco Laboratories Inc., Detroit, MI) and grown to confluence in Medium 199 (with 25 mM HEPES; Gibco BRL, Gaithersburg, MD) supplemented with 20% fetal bovine serum (FBS; Gibco BRL), 2 mM glutamine, 100 U/ml penicillin, 100 μg/ml streptomycin, 50 μg/ml endothelial cell growth supplement (ECGS; Collaborative Research Inc., Bedford, MA), and 100 μg/ml heparin (Sigma Chemical Company, St. Louis, MO). The cells were then cultured in Medium 199 supplemented with 5% FBS, 2 mM glutamine, 100 U/ml penicillin, and 100 μg/ml streptomycin (no ECGS or heparin) for at least 16 hours prior to, as well as during, the exposure to shear stress. To alter the viscosity of the culture medium, dextran (MW 510,000; 6% w/v; Sigma Chemical Company) was added to the medium contained within the cone-plate apparatus and to static coverslips in parallel.

Shear Stress Apparatus. The *in vitro* disturbed flow system was described in Methods in Chapter 3. For the experiments reported here, fluid mechanical parameters (cone angle, cone rotation, medium viscosity) were adjusted such that endothelial monolayers were subjected to shear stress of 12 dynes/cm^2 in the downstream uniform laminar flow region. In addition, the reattachment point was positioned 0.55 mm downstream from the bar.

Immunofluorescence. Immediately upon removal from the cone-plate apparatus, the cells were fixed in 2% paraformaldehyde at 4°C for 20 minutes. The coverslips were then removed from the rings and the cells were permeabilized in Nonidet P-40 (0.1% in PBS, 1 minute; Sigma Chemical Company), pre-incubated in a blocking solution of 10% goat serum, 3% bovine serum albumin, and 0.1% glycine (in PBS, 30 minutes), and then incubated overnight (15-18 hours) with rabbit polyclonal antibodies specific for human transcription factors (Egr-1, NF-κB [p65], c-Jun, c-Fos; 1 μg/ml in PBS plus 2% bovine serum; Santa Cruz Biotechnology, Santa Cruz, CA). Next the cells were successively incubated in biotinylated goat anti-rabbit IgG (15 μg/ml in PBS plus

2% bovine serum, 45 minutes; Vector Laboratories, Inc., Burlingame, CA), Texas Red Avidin D (15 μg/ml in PBS, 45 minutes; Vector Laboratories, Inc.), and 4',6-diamidino-2-phenylindole, dihydrochloride (DAPI; 10 μM in deionized water, 2 minutes; Molecular Probes, Eugene, OR), a DNA-intercalating fluorescent dye. All incubations were performed at room temperature (25°C). The conditions of this staining protocol had been optimized in pilot studies in which fixation with methanol or shorter incubations with the primary antibodies had resulted in little or no fluorescent signal. Before mounting on glass microscope slides, the coverslips were allowed to completely air dry overnight, since any residual liquid on the coverslips would immiscibly separate from the water-insoluble mounting medium (Vectashield, Vector Laboratories, Inc.). This anti-fade mounting medium diminishes bleaching of fluorophores by scavenging free radicals. Since the medium does not harden, fingernail polish was used to fix the coverslips to the microscope slides.

Image Analysis System. Fluorescent images were acquired and analyzed with the Oncor Image software package (Oncor, Inc., Gaithersburg, MD) together with acquisition hardware mounted on a Nikon Microphot-FXA upright microscope (Nikon Corporation, Tokyo, Japan) (**Figure 4.1**). Stained endothelial monolayers were imaged through a 20X Plan Apo objective (Nikon Corporation), fluorescently illuminated through a computer-controlled filter wheel and shutter (Ludl Electronic Products Ltd, Hawthorne, NY), and images were digitized via a 12-bit cooled CCD SenSys camera (Photometrics, Tucson, AZ). The position of the imaged endothelial cells in relation to the disturbed flow field was determined with the aid of an XYZ motorized microscope stage (Ludl Electronic Products Ltd). All acquisition and analysis was processed by a Power Macintosh 8500/120 configured with 64 MB RAM and a Radius ThunderColor graphics interface card (Radius, Inc., Sunnyvale, CA).

RESULTS

NF-κB

Exposure of endothelial cells to disturbed laminar shear stress increases total cellular content of NF-κB (p65). HUVEC monolayers which had been subjected to disturbed laminar shear stress for 30 minutes exhibited significant increases in the p65 subunit of NF-κB, detected by immunofluorescence microscopy, as compared with static endothelial monolayers. Exposure of HUVEC to uniform laminar shear stress also enhanced p65 expression, but to a lesser extent than did disturbed flow (**Figure 4.2**). Quantitation of total cellular p65 protein was accomplished by computerized analysis of digitized images of the endothelial monolayers (280 μM in each

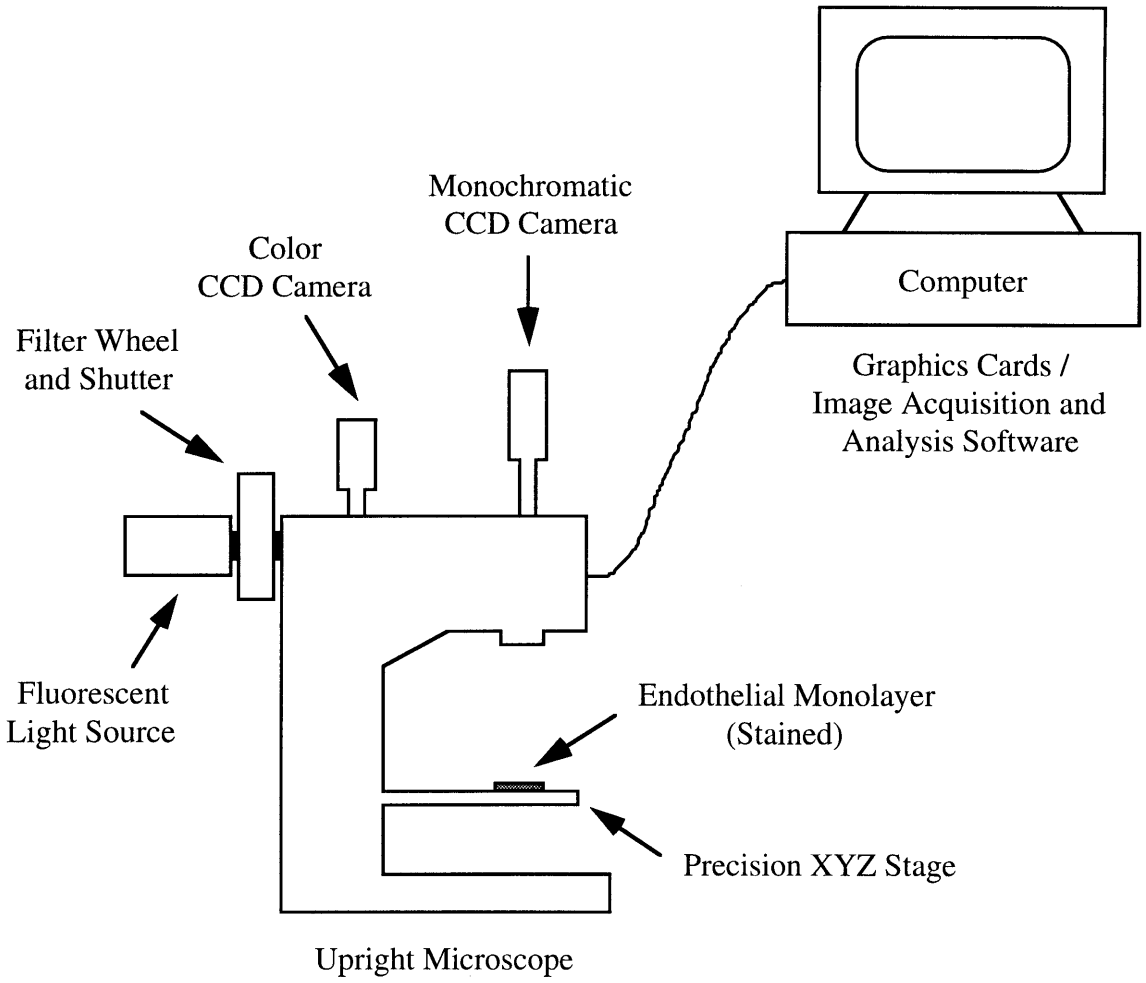

Figure 4.1. **Image analysis system.** Fluorescent images of stained endothelial monolayers were acquired and analyzed with the Macintosh-based Oncor Image software package together with acquisition hardware mounted on a Microphot-FXA upright microscope, as described in Methods.

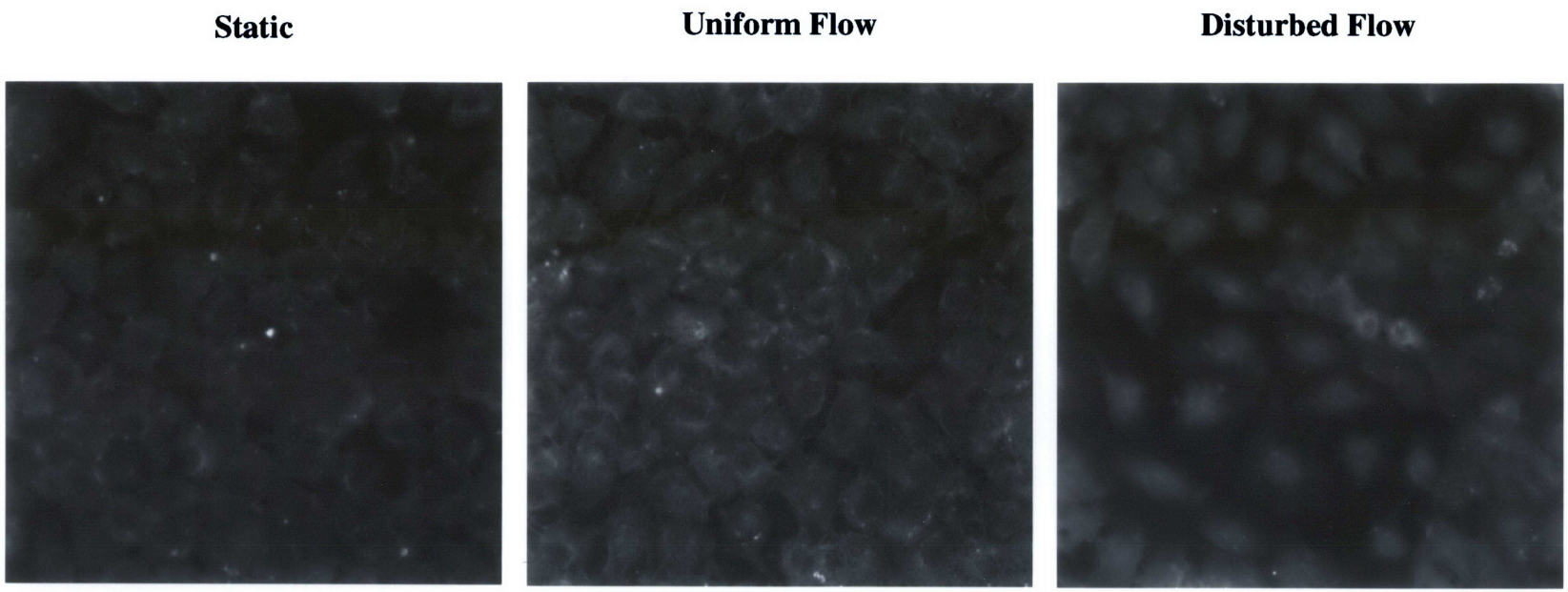

Figure 4.2. **Induction of NF-κB (p65) in a disturbed flow model.** HUVEC monolayers were maintained under static conditions or exposed to a disturbed flow model (30 minutes) in which cells were subjected to uniform or disturbed laminar shear stress on different regions of the same coverslip. After fixation and permeabilization in 2% paraformaldehyde and 0.1% NP-40, the monolayers were immunocytochemically stained with a polyclonal antibody specific for human p65, as described under Methods, and fluorescent images were digitized with a cooled CCD camera. Original magnification = 250X.

dimension, containing approximately 70 cells per image). Up to 3 rows of 10 images each were acquired on each coverslip, positioned relative to the bar on each shear stressed coverslip (as shown in **Figure 4.3**), and randomly positioned on each static coverslip. Two static and two shear stressed coverslips were analyzed for each experiment. For this analysis, images of endothelial monolayers that were less than 95% confluent were excluded (within an image, pixels having values below background fluorescence levels were considered devoid of cells and counted as non-confluent areas). The average fluorescence (greyscale value from 0 to 4095) of each image was determined and plotted as a function of position on the coverslip (**Figure 4.4**). The reattachment point in the disturbed flow field (near the region of maximal shear stress gradient) was at the junction between the second and third image field downstream from the bar (0.55 mm), and uniform flow was re-established by the seventh image field (1.68 mm). There was a small, though statistically significant increase in total cellular p65 protein content in cells in the disturbed flow region as compared with those in the uniform flow region and, overall, the shear stressed monolayers exhibited more p65 protein than did the static monolayers.

Disturbed laminar shear stress enhances nuclear localization of NF-κB (p65). Since NF-κB can perform its function as a DNA-binding protein only when in the nuclear compartment of the cell, and since much of the shear stress-induced p65 protein appeared to reside in the nucleus, we developed an image analysis algorithm to quantitate the amount of nuclear localized protein. For each image field, two fluorescent images were acquired: a Texas Red image, indicating the amount and cellular localization of p65, and a DAPI image, delineating the nuclear space. A mask of the nuclear space was created from the DAPI image and superimposed on the Texas Red image. Thus, the resulting masked image displayed protein contained primarily within the nucleus (**Figure 4.5**). The average fluorescence of the nuclear area was determined for each masked image and plotted as a function of position in the flow field (**Figure 4.6**). These data indicate that nuclear localization of p65 was significantly enhanced by exposure to disturbed flow, as compared with both uniform flow and static conditions. Nuclear localization in cells within the uniform flow region was only slightly greater than that in static cells, and this difference was not statistically significant.

Endothelial cells within the disturbed flow region exhibit greater population diversity of nuclear NF-κB (p65) content. Not all cells within a given image appeared to stain equally for nuclear p65, suggesting that there might be significant variability in cellular responsiveness within the population, even in cells exposed to the same conditions. In order to quantitatively analyze this, we determined the average fluorescence for each individual nucleus in images of endothelial

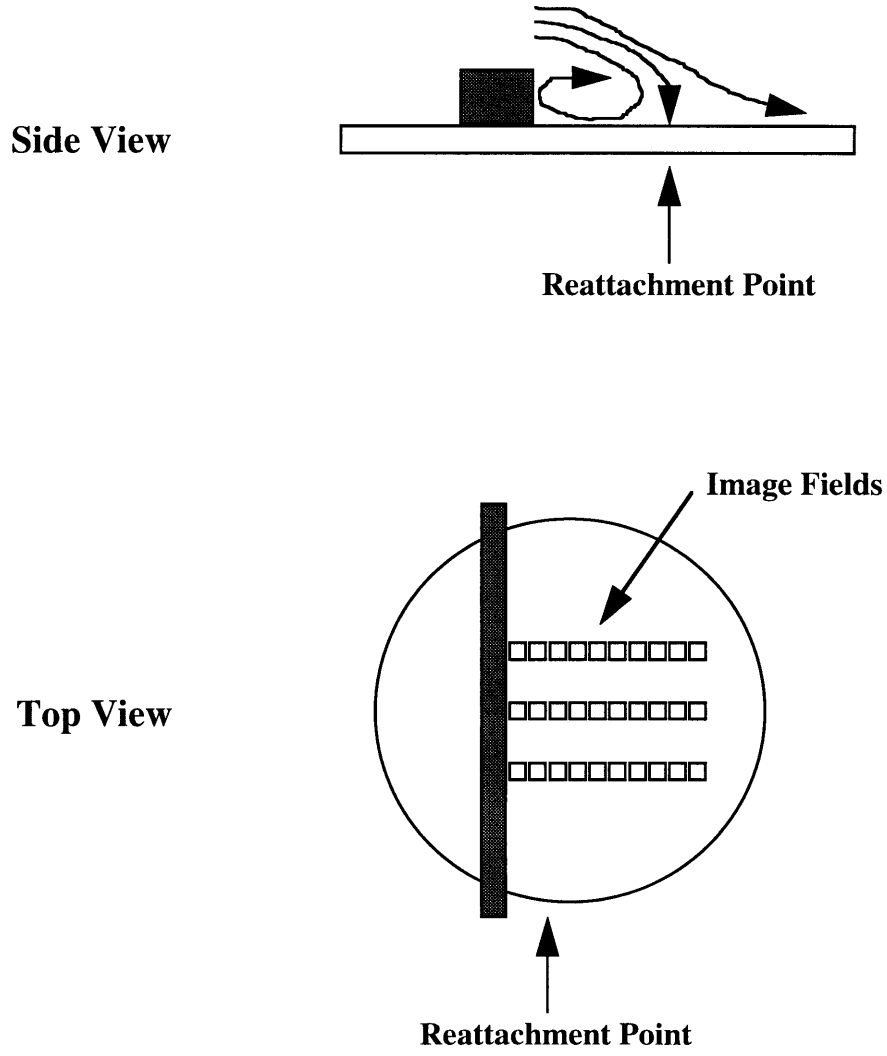

Figure 4.3 **Acquisition of microscopic images in the disturbed flow model.** Endothelial monolayers grown on 12 mm diameter coverslips were exposed to disturbed laminar shear stress which developed immediately downstream of the bar (0.4 mm in height), as previously described. After fixation and staining, microscopic images (280 μM in each dimension) were acquired at multiple positions relative to the bar, as described in Methods.

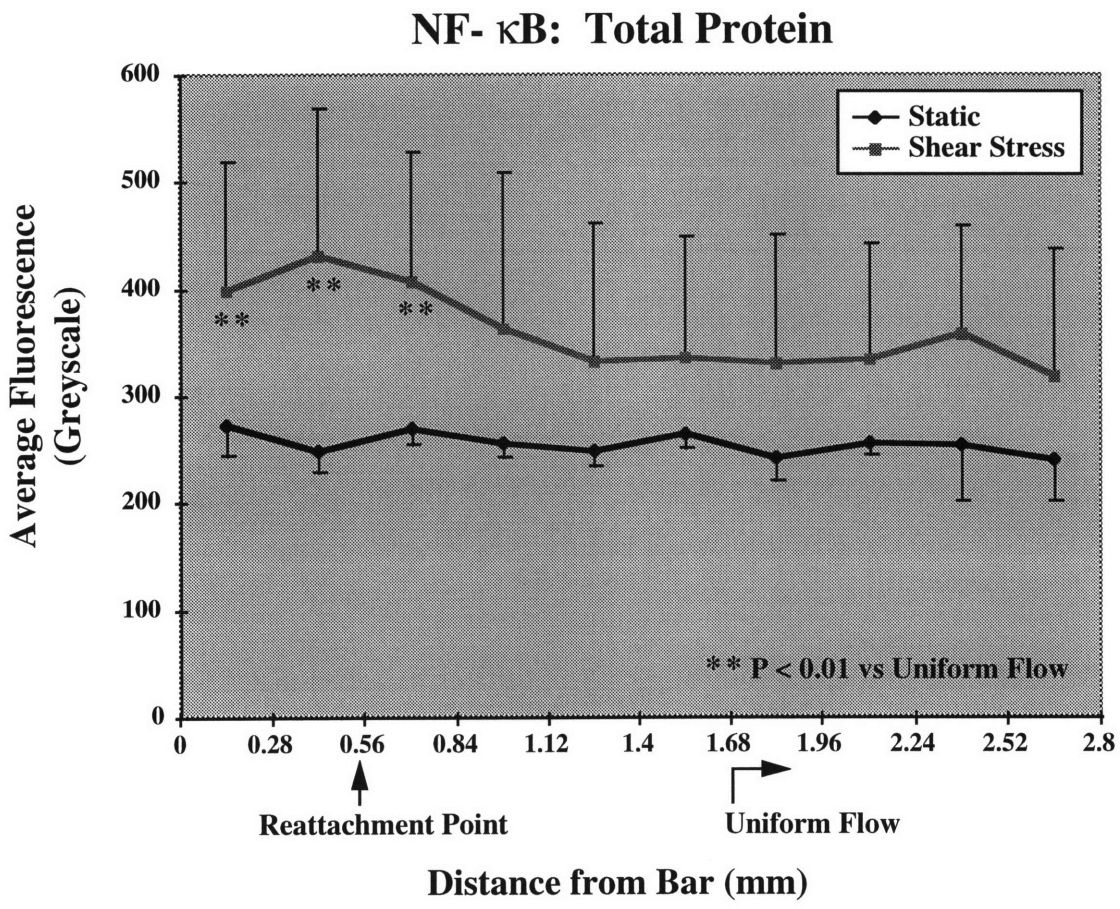

Figure 4.4. **Induction of total cellular NF-κB (p65) in a disturbed flow model.** HUVEC monolayers were maintained under static conditions or exposed to the disturbed flow model for 30 minutes. Total cellular p65 protein was quantitated from digitized images of monolayers which had been fluorescently stained for p65, as described in Methods. Images of monolayers that were less than 95% confluent were excluded. Data are presented as mean fluorescence per image ± standard deviation (n = 2-5 images for static conditions and 6 images for shear stress).

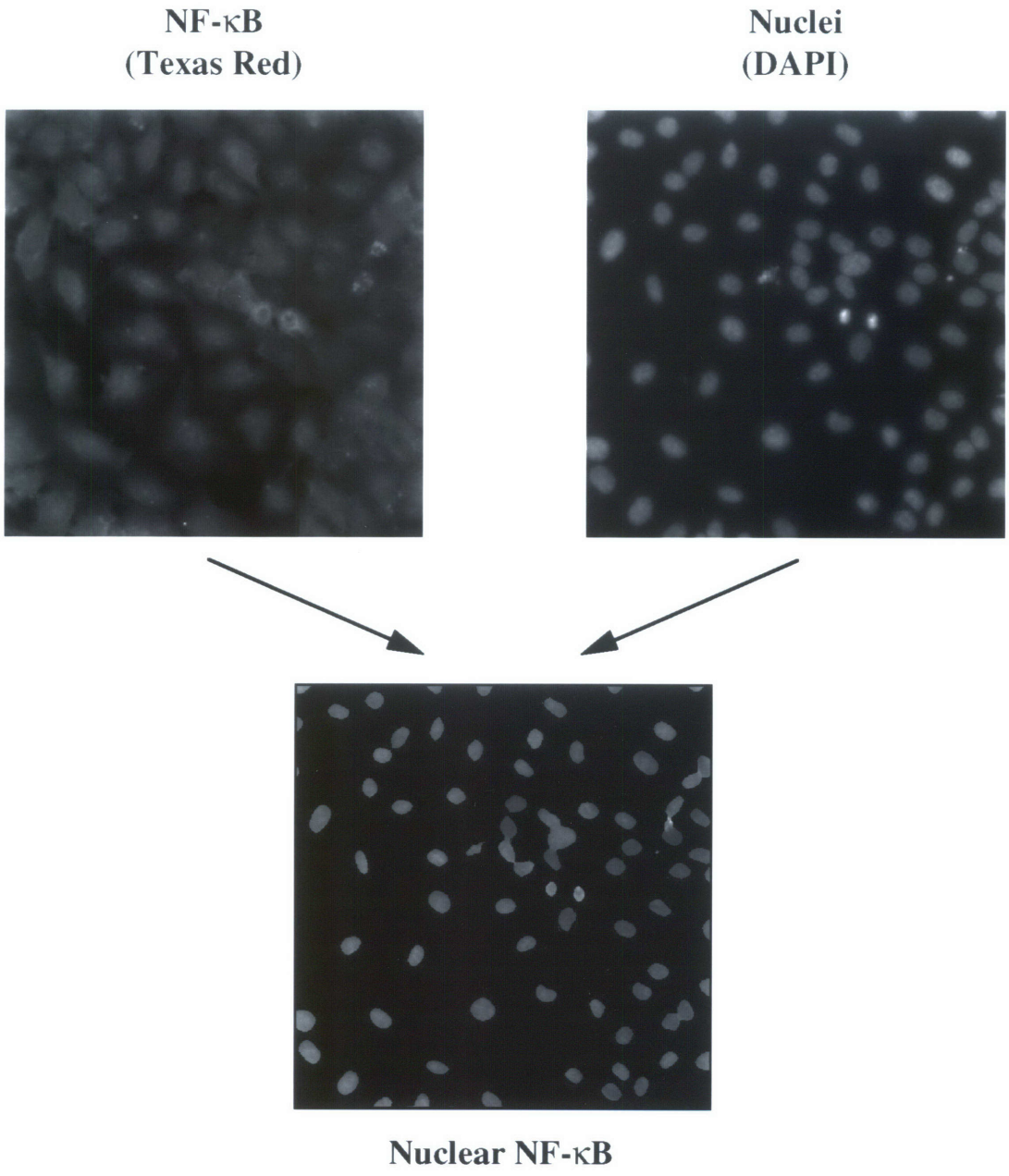

Figure 4.5. **Analysis of nuclear localization of NF-κB (p65) protein.** **HUVEC** monolayers were stained for NF-κB using a Texas Red fluorophore and counter-stained with the nuclear marker, DAPI, as described under Methods. For each image field, a fluorescent image of each dye was digitized with a cooled CCD camera, and a nuclear mask was created from the DAPI image and superimposed on the Texas Red image. Average nuclear fluorescence was then determined from the resultant masked image.

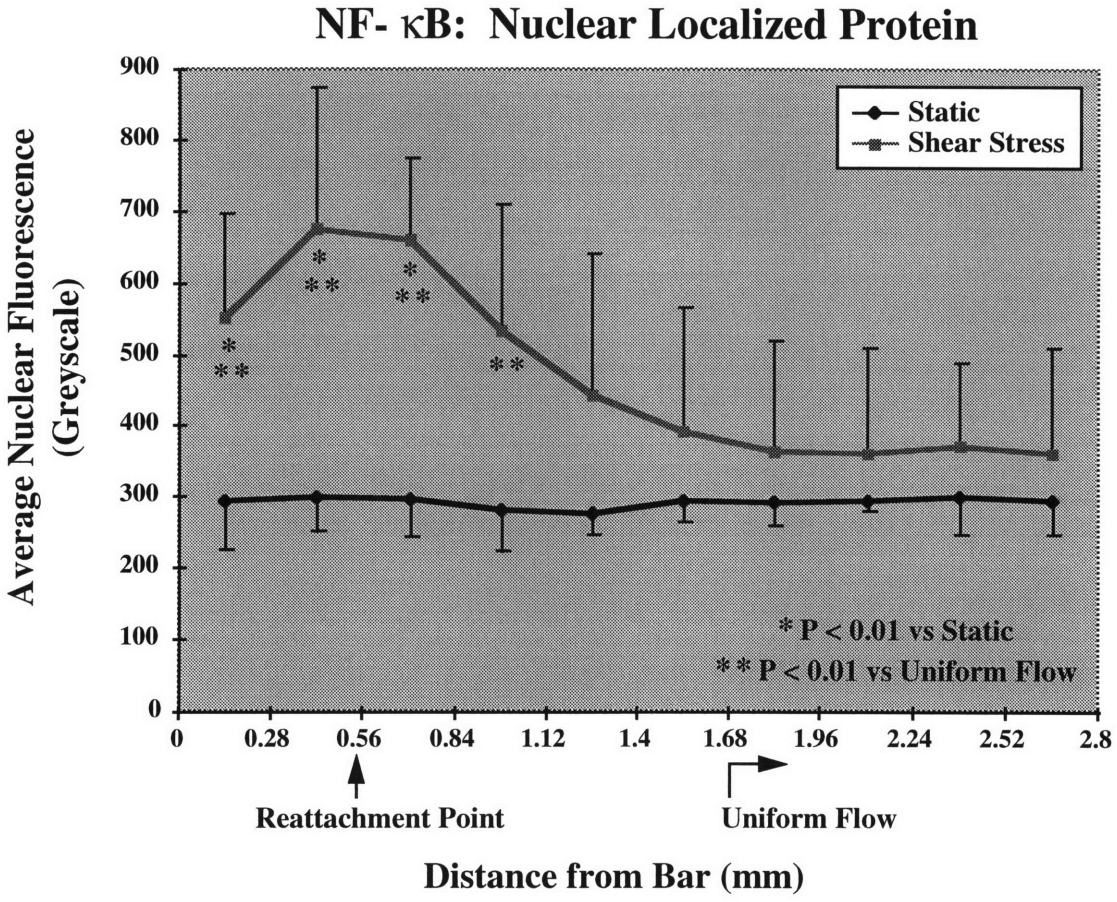

Figure 4.6. **Induction of nuclear localized NF-κB (p65) protein in a disturbed flow model.** HUVEC monolayers were maintained under static conditions or exposed to the disturbed flow model for 30 minutes. The amount of nuclear localized p65 protein was determined from digitized images of endothelial cells, as described in Methods. Data are presented as mean nuclear fluorescence per image ± standard deviation (n = 5 images for static conditions and 6 images for shear stress).

cells from the disturbed flow region (specifically, images at the second and third positions downstream from the bar), the uniform flow region (images at the ninth and tenth positions), and static coverslips. The results, displayed as histograms in **Figure 4.7**, indicate that the cells did indeed exhibit a population distribution of nuclear p65, and these data confirm that the mean nuclear fluorescence was greater in cells exposed to uniform and disturbed flow, as compared with static conditions. In addition, the population diversity was greatest in endothelial cells in the disturbed flow region, with static cells displaying the smallest variance.

Egr-1

HUVEC exposed to flow for 30 minutes in the disturbed laminar shear stress model displayed enhanced immunofluorescent staining of total Egr-1 protein, as compared with static monolayers, with the most significant increases occurring in the disturbed flow region (**Figures 4.8** and **4.9A**). Quantitation of nuclear localization, as described above, revealed striking elevations of nuclear Egr-1 protein in cells in the disturbed flow region which were significantly greater than in cells in the uniform flow region or maintained under static conditions. (**Figure 4.9B**). Population analysis indicated that there was a greater population diversity of nuclear Egr-1 protein within the endothelial monolayers, as compared with NF-κB (**Figures 4.10** and **4.7**) but, like NF-κB, the population distribution of nuclear Egr-1 was greatest in cells subjected to disturbed flow and least in static cells.

c-Jun

HUVEC maintained under static conditions displayed substantial basal levels of c-Jun protein, even in reduced serum conditions, and much of this protein appeared to be in the nuclear compartment (**Figure 4.11**). After exposure to 30 minutes of either disturbed or uniform flow, total cellular c-Jun protein was dramatically elevated, particularly by disturbed flow (**Figure 4.12A**). Nuclear localized c-Jun levels were also increased by both disturbed and uniform flow, but the induction of nuclear protein was not as striking as the upregulation of total protein, probably owing to the high basal levels of nuclear staining under static conditions (**Figure 4.12B**). Endothelial monolayers also exhibited an extensive population distribution of nuclear localized c-Jun protein (**Figure 4.13**), which was further broadened by exposure to uniform and, especially, disturbed flow.

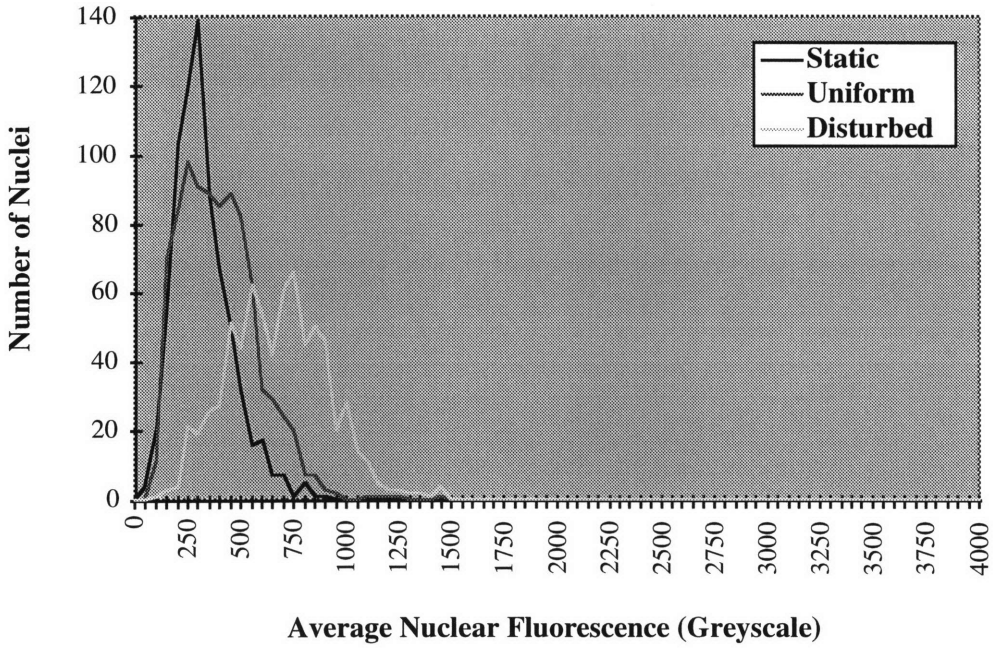

Figure 4.7. **Population distribution of nuclear localized NF-κB (p65) in HUVEC exposed to a disturbed flow model.** Endothelial monolayers were either maintained under static conditions or exposed to the disturbed flow model, which incorporates separate regions of uniform and disturbed laminar shear stress on the same coverslip. The NF-κB (p65) content of individual nuclei was determined from digitized images of the endothelial cells, as described in Methods, and the frequencies of average nuclear fluorescence are presented.

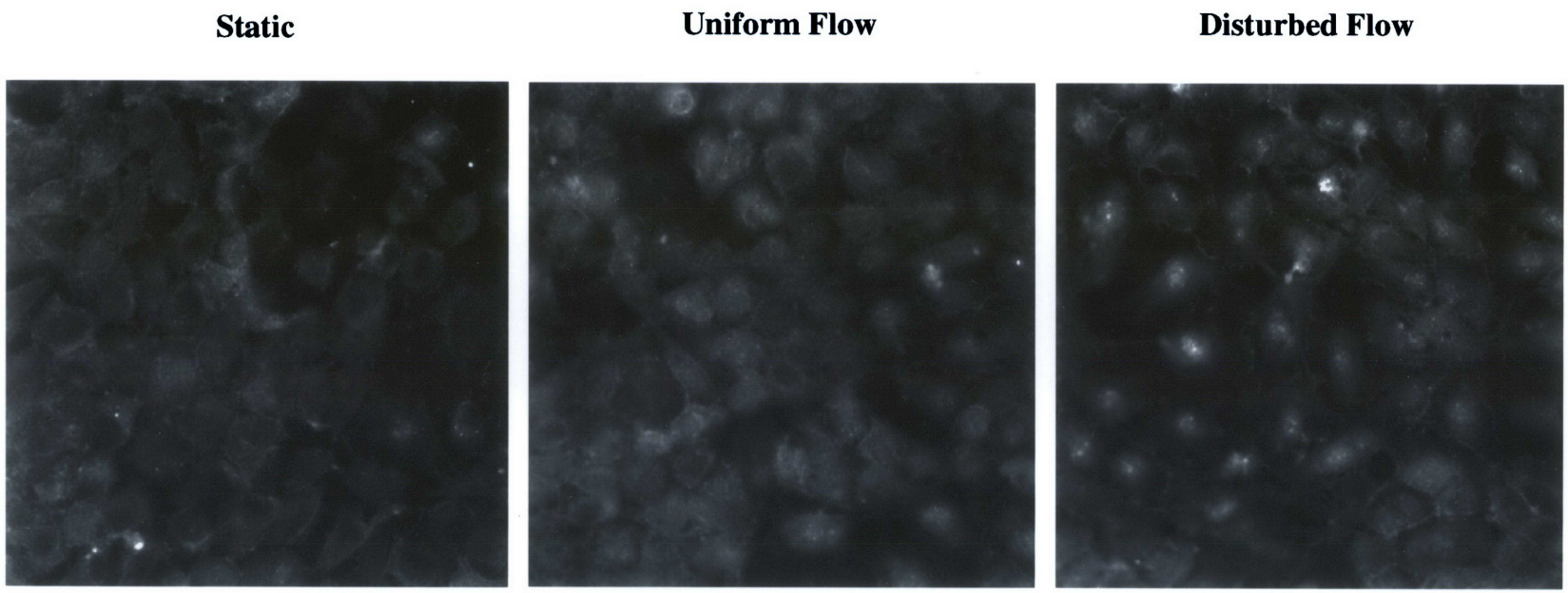

Figure 4.8. **Induction of Egr-1 in a disturbed flow model.** HUVEC monolayers were maintained under static conditions or exposed to a disturbed flow model (30 minutes) in which cells were subjected to uniform or disturbed laminar shear stress on different regions of the same coverslip. After fixation and permeabilization in 2% paraformaldehyde and 0.1% NP-40, the monolayers were immunocytochemically stained with a polyclonal antibody specific for human Egr-1, as described under Methods, and fluorescent images were digitized with a cooled CCD camera. Original magnification = 250X.

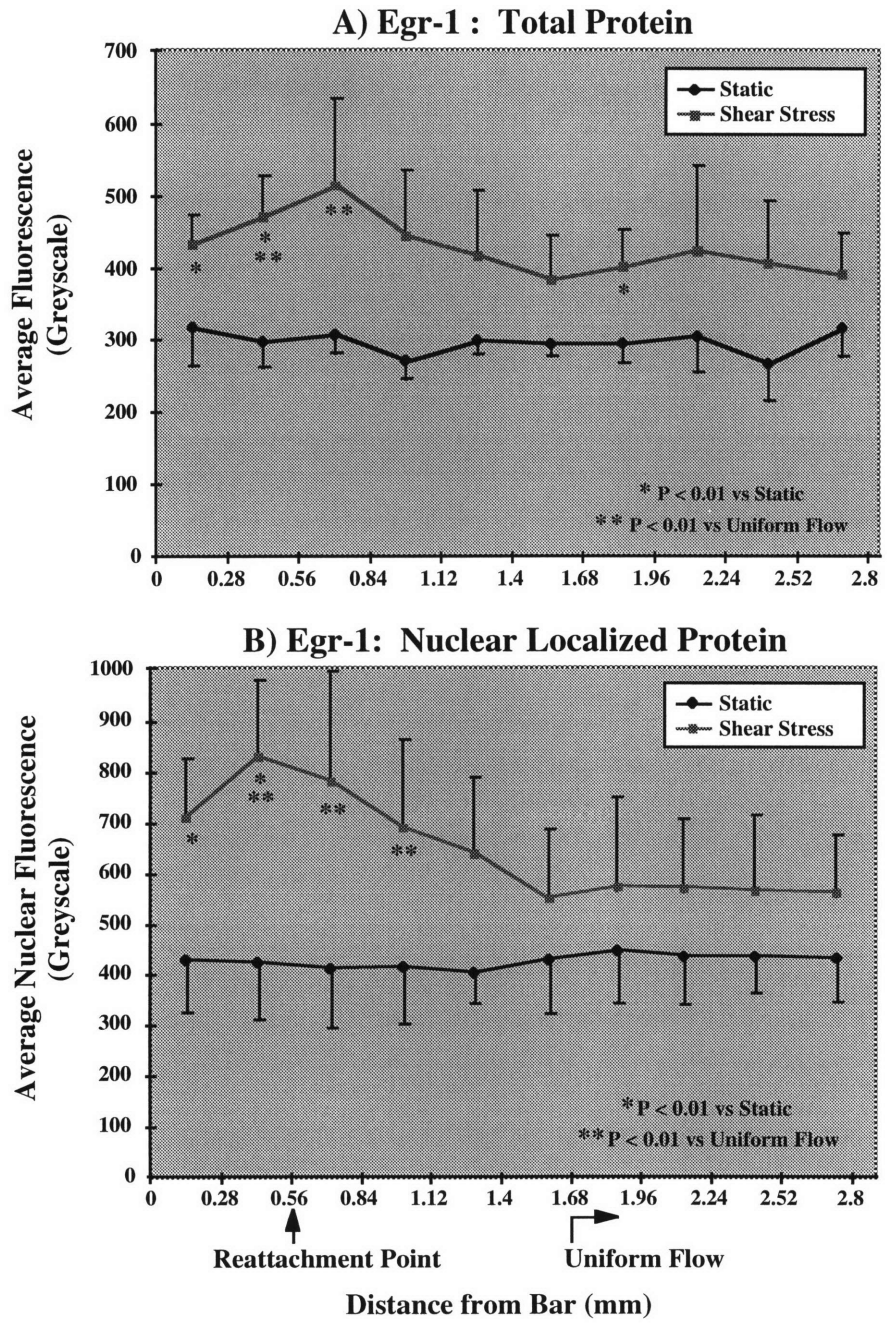

Figure 4.9. **Induction of total cellular and nuclear localized Egr-1 protein in a disturbed flow model.** HUVEC monolayers were maintained under static conditions or exposed to the disturbed flow model for 30 minutes. The amount of total cellular and nuclear localized Egr-1 protein was determined from digitized images of endothelial cells which had been fluorescently stained for Egr-1, as described in Methods. For total protein analysis, images of monolayers that were less than 95% confluent were excluded. Data are presented as mean total or nuclear fluorescence per image ± standard deviation (A: n = 2-5 images for static conditions and 6 images for shear stress; B: n = 6 images for static and shear stress).

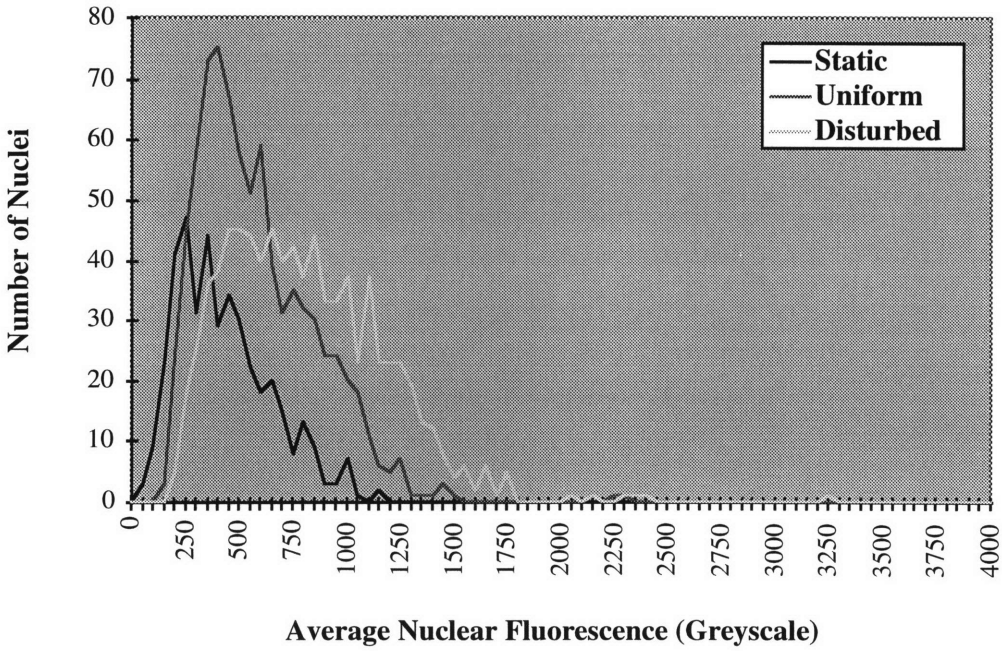

Figure 4.10. **Population distribution of nuclear localized Egr-1 in HUVEC exposed to a disturbed flow model.** Endothelial monolayers were either maintained under static conditions or exposed to the disturbed flow model, which incorporates separate regions of uniform and disturbed laminar shear stress on the same coverslip. The Egr-1 content of individual nuclei was determined from digitized images of the endothelial cells, as described in Methods, and the frequencies of average nuclear fluorescence are presented.

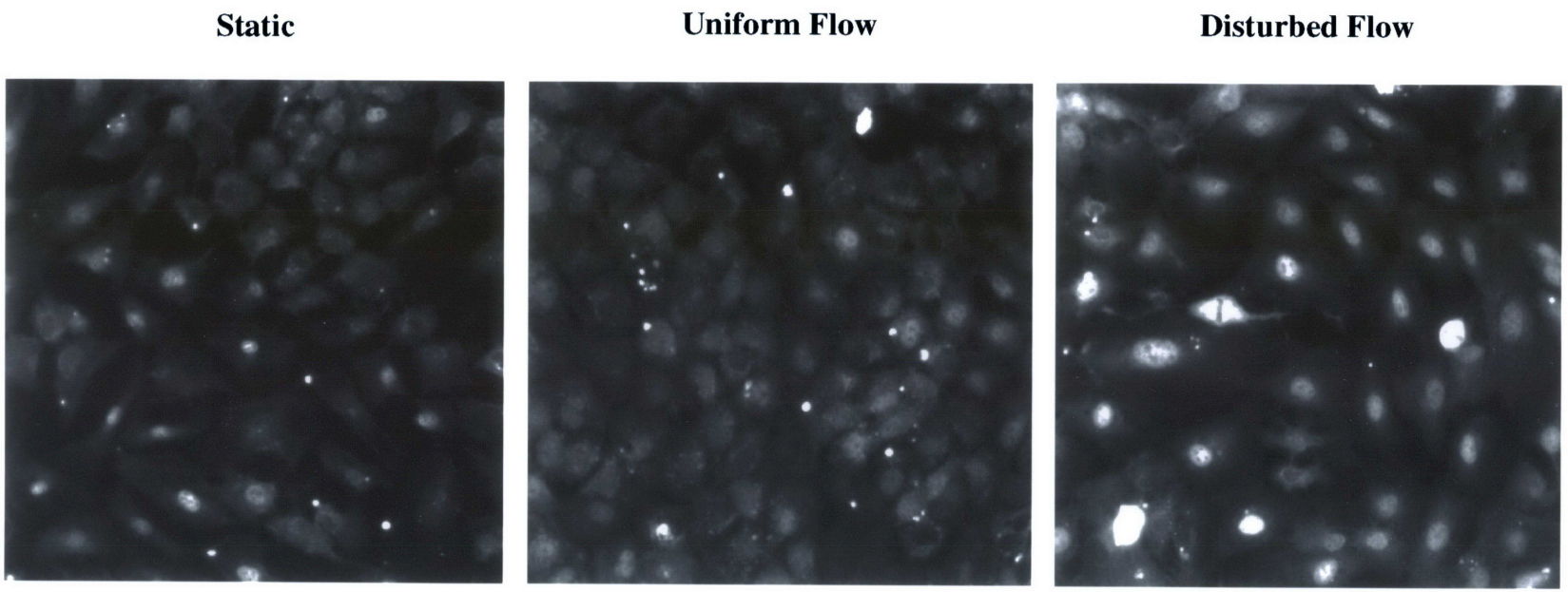

Figure 4.11. **Induction of c-Jun in a disturbed flow model.** HUVEC monolayers were maintained under static conditions or exposed to a disturbed flow model (30 minutes) in which cells were subjected to uniform or disturbed laminar shear stress on different regions of the same coverslip. After fixation and permeabilization in 2% paraformaldehyde and 0.1% NP-40, the monolayers were immunocytochemically stained with a polyclonal antibody specific for human c-Jun, as described under Methods, and fluorescent images were digitized with a cooled CCD camera. Original magnification = 250X.

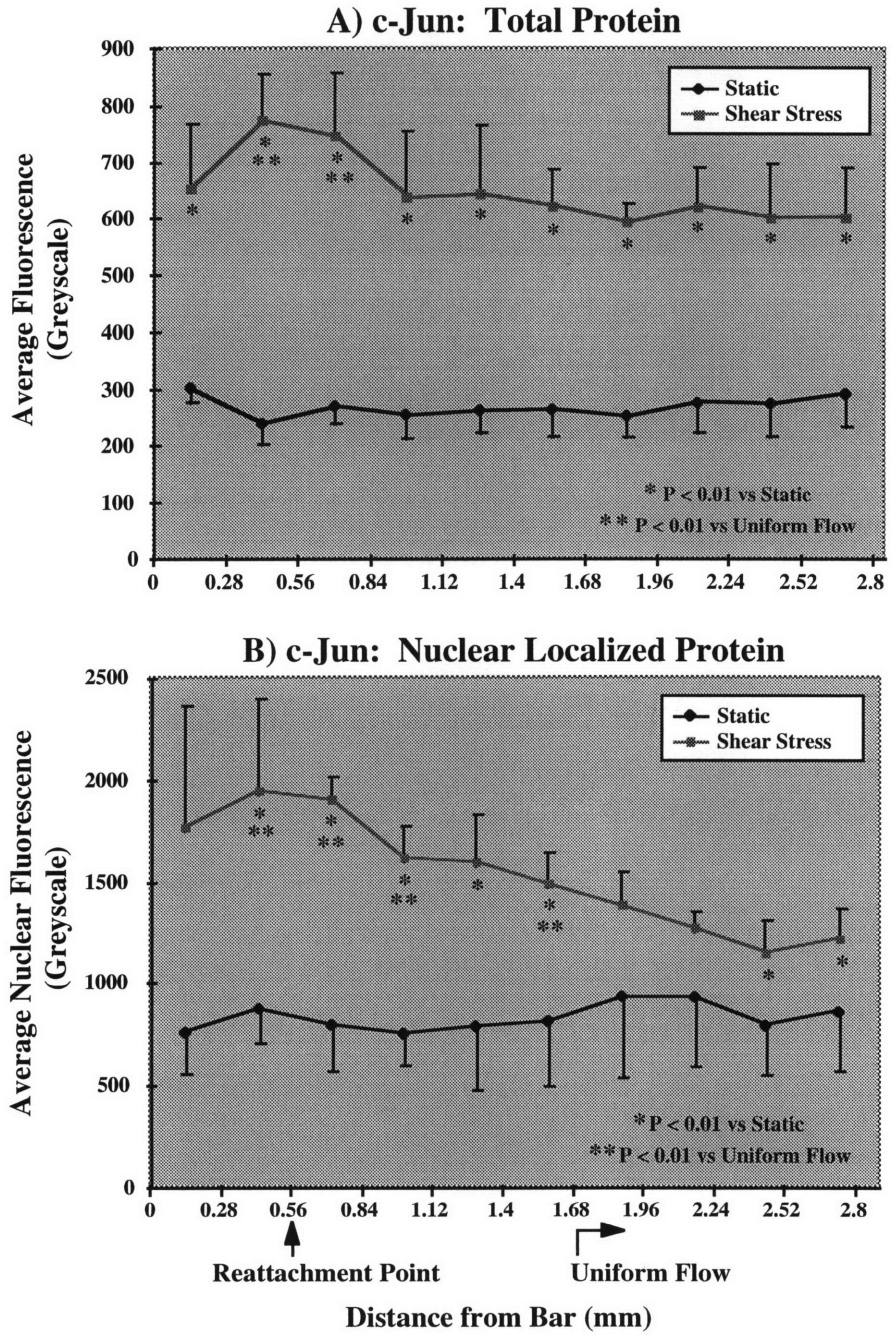

Figure 4.12. **Induction of total cellular and nuclear localized c-Jun protein in a disturbed flow model.** HUVEC monolayers were maintained under static conditions or exposed to the disturbed flow model for 30 minutes. The amount of total cellular and nuclear localized c-Jun protein was determined from digitized images of endothelial cells which had been fluorescently stained for c-Jun, as described in Methods. For total protein analysis, images of monolayers that were less than 95% confluent were excluded. Data are presented as mean total or nuclear fluorescence per image ± standard deviation (A: n = 3-5 images for static conditions and 6 images for shear stress; B: n = 5 images for static and 6 images for shear stress).

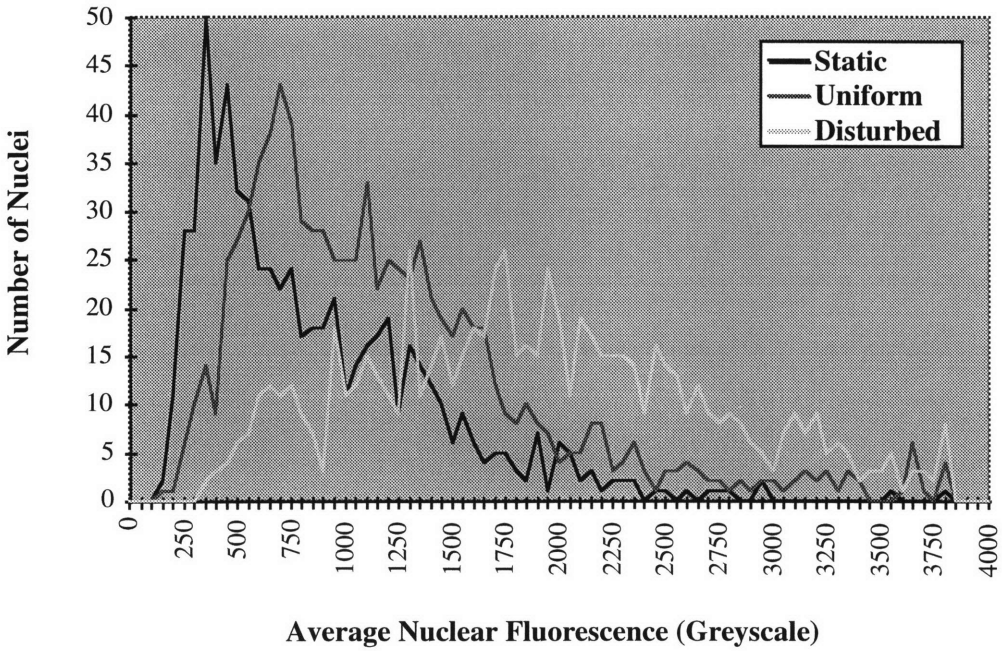

Figure 4.13. **Population distribution of nuclear localized c-Jun in HUVEC exposed to a disturbed flow model.** Endothelial monolayers were either maintained under static conditions or exposed to the disturbed flow model, which incorporates separate regions of uniform and disturbed laminar shear stress on the same coverslip. The c-Jun content of individual nuclei was determined from digitized images of the endothelial cells, as described in Methods, and the frequencies of average nuclear fluorescence are presented.

c-Fos

Like NF-κB and Egr-1, c-Fos protein levels were quite low in static HUVEC cultures grown in reduced serum conditions (**Figure 4.14**). Exposure of the cells to either disturbed or uniform flow for 30 minutes significantly upregulated total cellular c-Fos protein, slightly more so by disturbed flow than uniform flow (**Figure 4.15A**). Nuclear localization of c-Fos was more dramatically induced by disturbed flow than by uniform flow (**Figure 4.15B**), and the population distribution of nuclear c-Fos was larger in cells in the disturbed flow region and, to a lesser extent, in the uniform flow region, as compared with static cells (**Figure 4.16**).

DISCUSSION

These studies provide the first evidence that a nuclear genetic regulatory event can be differentially altered by disturbed laminar shear stress as compared with uniform laminar shear stress. Previous experiments by DePaola, using the same disturbed flow system, indicated that long-term exposure (on the order of hours to days) to disturbed flow led to enhanced proliferation and migration, with resulting spatial variations in cell density [23]. Data shown in Chapter 3 demonstrated that differential regulation of adhesion molecules by uniform and disturbed flow, if existent, was subtle, probably owing to the combination of transcriptional, post-transcriptional and post-translational regulatory mechanisms. Therefore, it seemed efficacious to focus on transcription factor regulation within the disturbed flow model, both because these proteins were rapidly activated by shear stress and because nuclear localized protein, in particular, provided a biologically relevant marker that could be quantitated irrespective of cell density. The current data indicate that total cellular content of the transcription factors, NF-κB, Egr-1, c-Jun and c-Fos, was increased by exposure to disturbed laminar shear stress for 30 minutes, as compared with both uniform flow and static conditions, and suggest that most of the induced protein was localized to the nucleus. In addition, the cell to cell variability, in terms of the amount of nuclear localized protein, was greatest in cells subjected to disturbed flow.

In our *in vitro* disturbed flow model, both the shear stress magnitudes and shear stress gradients vary in the disturbed flow region, whereas these variables remain constant in the uniform flow region. Similar distinctions exist *in vivo*, with the disturbed flow sites, occurring at bifurcations and arterial curvatures, characterized by significant shear stress variations, and the relatively atherosclerotic lesion-protected regions experiencing primarily unidirectional laminar shear stress. However, disturbed flow *in vivo* is actually accentuated by the pulsatile blood flow, which moves the reattachment point forward and backward along the arterial wall with each cardiac

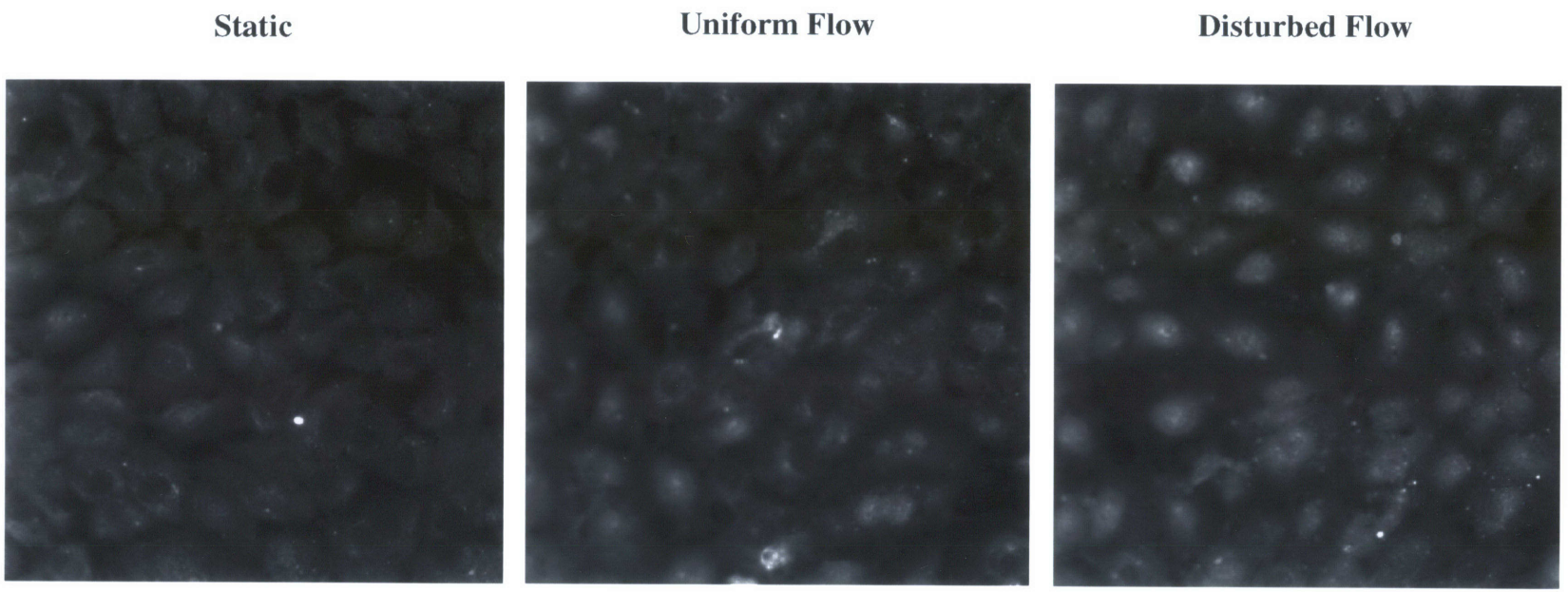

Figure 4.14. Induction of c-Fos in a disturbed flow model. HUVEC monolayers were maintained under static conditions or exposed to a disturbed flow model (30 minutes) in which cells were subjected to uniform or disturbed laminar shear stress on different regions of the same coverslip. After fixation and permeabilization in 2% paraformaldehyde and 0.1% NP-40, the monolayers were immunocytochemically stained with a polyclonal antibody specific for human c-Fos, as described under Methods, and fluorescent images were digitized with a cooled CCD camera. Original magnification = 250X.

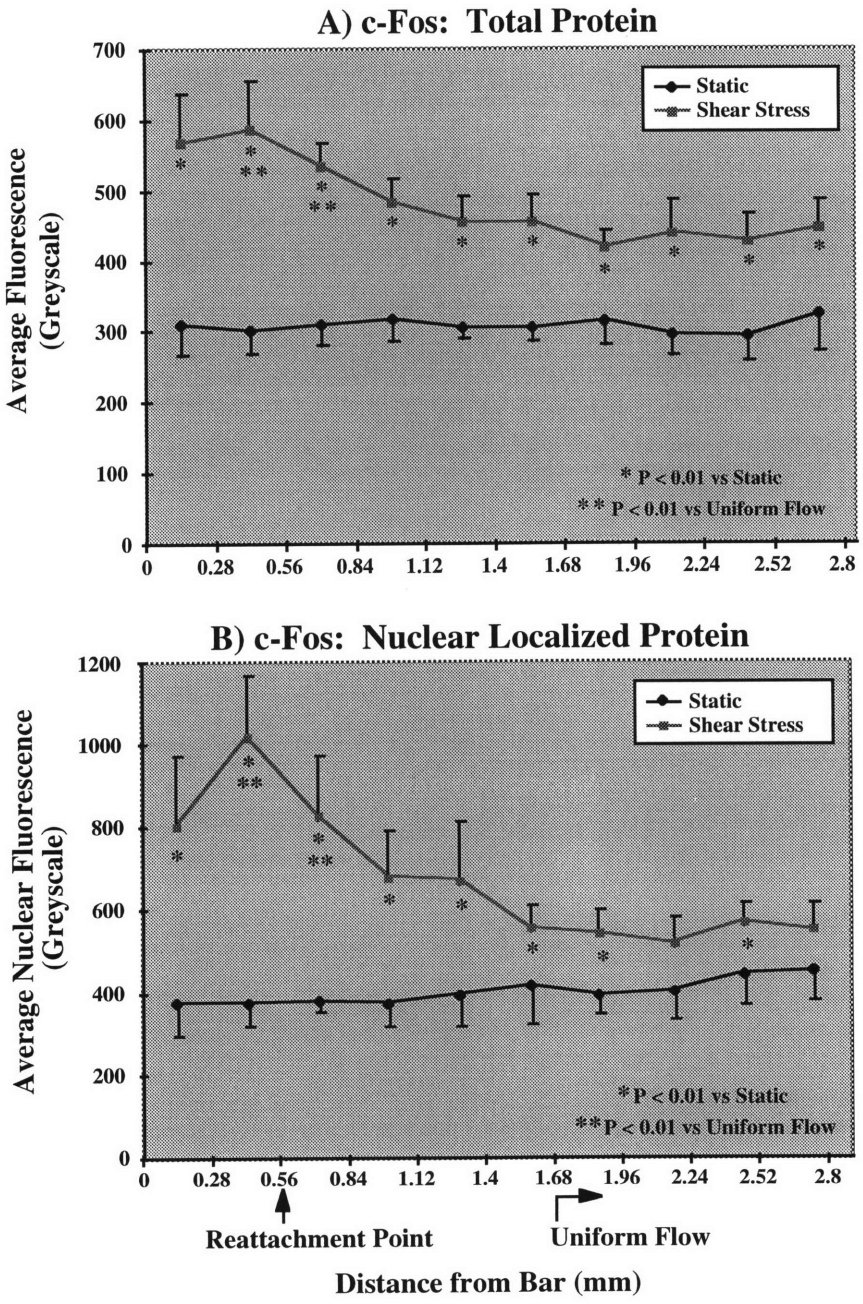

Figure 4.15. **Induction of total cellular and nuclear localized c-Fos protein in a disturbed flow model.** HUVEC monolayers were maintained under static conditions or exposed to the disturbed flow model for 30 minutes. The amount of total cellular and nuclear localized c-Fos protein was determined from digitized images of endothelial cells which had been fluorescently stained for c-Fos, as described in Methods. For total protein analysis, images of monolayers that were less than 95% confluent were excluded. Data are presented as mean total or nuclear fluorescence per image ± standard deviation (A: n = 5-6 images for static conditions and 6 images for shear stress; B: n = 6 images for static and shear stress).

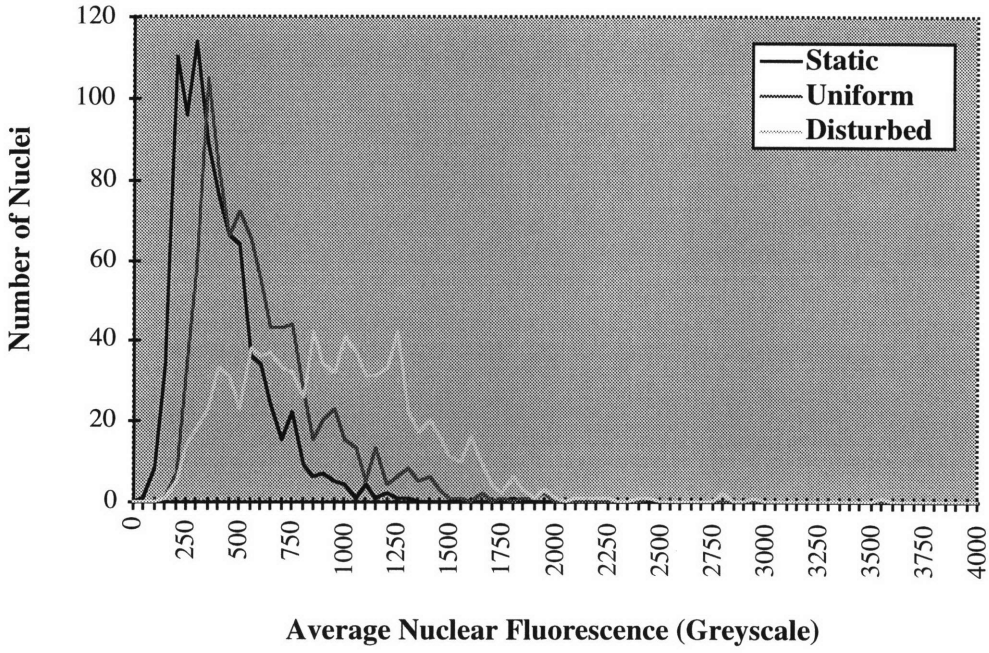

Figure 4.16. **Population distribution of nuclear localized c-Fos in HUVEC exposed to a disturbed flow model.** Endothelial monolayers were either maintained under static conditions or exposed to the disturbed flow model, which incorporates separate regions of uniform and disturbed laminar shear stress on the same coverslip. The c-Fos content of individual nuclei was determined from digitized images of the endothelial cells, as described in Methods, and the frequencies of average nuclear fluorescence are presented.

cycle and creates time-dependent fluctuations in the spatial shear stress patterns. In such an environment, an endothelial cell at the vessel wall may be exposed to relatively high, forward flow at one instant, low or zero flow the next instant (at the reattachment point), and finally reverse flow. Thus, both the temporal and the spatial components of fluid shear stress gradients may be important in regulating endothelial cell biology. The steady disturbed flow model utilized in these experiments isolates the spatial variables from the temporal, and permits determination of endothelial cell responses to spatial distributions of shear stress magnitudes and gradients, which are obviously intimately linked. The studies presented here indicate that endothelial cells can indeed sense differences in the spatial pattern of shear stress and can alter their gene regulation accordingly. Unsteady disturbed flow patterns, which incorporate regular movement of the reattachment point, may also be created within the cone and plate system by utilizing an asymmetric cone. Future studies with this model may provide insights regarding the importance of temporal shear stress fluctuations in the regulation of endothelial gene expression.

Because of the experimental configuration of the disturbed flow model -- in particular, the small size of the disturbed flow region (less than 2 mm in width) -- the application of many standard analysis techniques was precluded (e.g., Northern blot analysis, transiently transfected promoter/reporter genes, flow cytometry). Thus, it was necessary to devise a novel examination technique in order to investigate nuclear regulatory processes in the disturbed flow field. The image acquisition and analysis algorithms developed for this purpose enabled detailed investigation on several levels. First, this technique made feasible the correlation of spatially distributed cellular responses with shear stress variations that occurred over very small dimensions. Second, it was possible to visualize the intracellular location of transcription factors, as well as to measure the total amount of protein present. It must be recognized, however, that the nuclear localization algorithm employed here may include some cytoplasmic transcription factor in the measure of nuclear protein content (*i.e.*, cytoplasmic protein located immediately above or below the nucleus, as illustrated in **Figure 4.17**). However, studies by Davies and coworkers with transmission electron microscopy indicate that, under static conditions, the nuclei of cultured endothelial cells in confluent monolayers occupy approximately 85% to 90% of the region of the endothelial cell that is investigated in our nuclear localization algorithm [259, 260]. Using atomic force microscopy, Davies *et al.* have also measured the total thickness of endothelial cells under both static and shear stress conditions and have determined that exposure of cells to 24 hours of laminar shear stress elicits a decrease in cell height, at the nuclear bulge, of approximately 25% or less [261, 262]. While they have not measured morphological variations resulting from much shorter shear stress exposures, it seems appropriate to assume that no significant alterations will occur in the

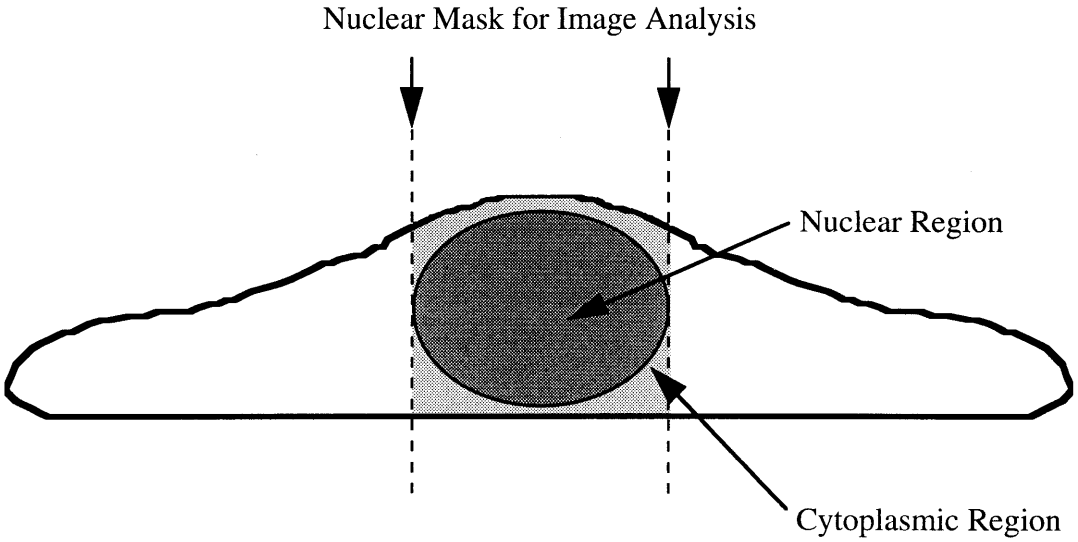

Figure 4.17. **Cross-section of an endothelial cell.** The nuclear localization algorithm employed in these studies may include some cytoplasmic protein in the measure of nuclear protein content. However, data from transmission electron micrographs and atomic force microscopy indicate that the cytoplasmic region, illustrated above, comprises a small fraction of the total nuclear region, as discussed in the text.

intracellular dimensions after 30 minutes of shear stress, as compared with static conditions. Based on these data, we estimate that the cytoplasmic space occupies at most 15% of the intracellular region included in our nuclear localization algorithm. However, much less than 15% of the measured transcription factor protein may actually reside in the cytoplasm, since it is well-documented that activated NF-κB, Egr-1, c-Jun, and c-Fos translocate efficiently from the cytoplasm into the nucleus via defined molecular mechanisms. As such, the image analysis technique for nuclear localization appears to provide a reasonable measure of the amount of transcription factor in the nucleus under the experimental conditions employed in the current studies. Finally, image analysis permitted population distribution studies on a cell by cell basis. These data suggest that cells in the disturbed flow region display a non-uniform response to the flow stimulus, in terms of nuclear localized NF-κB, Egr-1, c-Jun, and c-Fos, as compared with cells in the uniform flow region as well as those maintained under static conditions. Since these experiments were conducted with endothelial cultures derived from single umbilical cords, genetic variability cannot be considered a contributing factor in the heterogeneous response observed.

Given that NF-κB, Egr-1, c-Jun, and c-Fos are each regulated through distinct activation mechanisms, it is particularly intriguing that all four transcription factors exhibit enhanced induction and nuclear localization in endothelial cells exposed to disturbed laminar shear stress. This may reflect the fact that Egr-1, c-Jun, and c-Fos, each being immediate-early genes, are coordinately activated by a diverse array of stimuli, and NF-κB displays similarly rapid activation via nuclear translocation mechanisms. However, it will be important to identify other transcription factors and/or soluble cytoplasmic proteins which do not exhibit enhanced activation in disturbed flow. Potential candidates include IκB, which must be degraded in the process of NF-κB activation, and Sp1 which, as mentioned earlier, mediates the shear stress activation of the tissue factor gene through modification of it phosphorylation state, rather than through increased expression or changes in intracellular location.

It is interesting to note that one common feature amongst NF-κB, Egr-1, c-Jun, and c-Fos is their sensitivity to regulation via the redox state of the cell. Reduction of cysteine residues in the DNA binding domains of p65, p50, c-Jun, and c-Fos, results in stimulation of DNA binding, and conversely, oxidation of these sites inhibits binding [165, 169, 263]. The nuclear redox enzyme, Ref-1, is capable of reducing these cysteine residues, and over-expression of Ref-1 has been shown to stimulate DNA binding of NF-κB, Egr-1, and AP-1 [169, 185]. More recent data has

demonstrated that oxidative stress can induce Egr-1, c-*jun*, and c-*fos* transcript levels *in vitro* [186, 240, 264]. Most strikingly, preliminary data from Hsieh *et al.* has demonstrated that the levels of intracellular reactive oxygen species (ROS) are increased in HUVEC subjected to uniform laminar shear stress, in a force-dependent manner, and the enhanced ROS mediate the induction of c-*fos* by shear stress [51]. Thus, shear stress may also regulate the expression of NF-κB, Egr-1, and c-Jun by altering the intracellular redox state. Differential regulation of these transcription factors by disturbed flow, as compared to uniform flow, could involve variations in the redox state of cells exposed the two flow regimes, and such potential differences could be investigated in future experiments using redox sensitive fluorescent dyes [186]. Recent data from out laboratory has demonstrated that the intracellular antioxidant enzyme, manganese superoxide dismutase, is selectively induced by laminar but not turbulent shear stress, suggesting that the intracellular redox state may indeed be differentially regulated by subtle differences in shear stress parameters [96].

While the differential regulation of immediate-early transcription factors by disturbed shear stress is readily detectable, the modulation of target genes that are functional at the intercellular level is undoubtedly more complex. In particular, as shown in Chapter 3, cell surface expression of ICAM-1, VCAM-1 and E-selectin -- genes which contain a variety of NF-κB, Egr-1 and AP-1 sites in their promoter regions -- is not differentially regulated by disturbed flow versus uniform flow. These findings emphasize the potential importance of the interplay of multiple transcription factors within the local physical environment of a given promoter, as well as post-transcriptional and post-translational regulatory mechanisms that ultimately determine the regulation of gene expression. In this regard, transcription factor analysis, rather than protein product analysis, provides a more direct index of the modulatory effects of shear stress on endothelial gene expression.

In conclusion, with the aid of specialized image analysis techniques, we have demonstrated that uniform and disturbed laminar shear stress can differentially regulate the induction and, more strikingly, the nuclear localization of the transcription factors, NF-κB, Egr-1, c-Jun, and c-Fos in endothelial cells. These findings provide insights regarding the shear stress parameters which regulate endothelial gene expression and the nature of a potential shear stress "mechanosensor(s)". Furthermore, the enhanced activation of these transcription factors by disturbed flow may have important implications for the role of hemodynamically-induced alterations in endothelial gene expression in the focal development of atherosclerotic lesions.

Chapter 5

CONCLUSIONS AND FUTURE DIRECTIONS

The findings presented in this thesis suggest that the spectrum of biomechanical forces encountered in the circulatory system may represent important stimuli that are relevant to both the physiology and pathology of vascular endothelium. In particular, the present data demonstrate that a single fluid shear stress regime can differentially regulate a class of biologically relevant endothelial genes, the endothelial-leukocyte adhesion molecules. In addition, these and previous experiments in our laboratory indicate that endothelial cells can distinguish between different laminar shear stress regimes, namely disturbed and uniform flow, at the levels of cellular proliferation and migration, cytokine-inducibility of adhesion molecules and even nuclear localization of transcription factors. Thus, endothelial biology may be selectively regulated by hemodynamic shear stress, both in terms of the specific endothelial genes that are regulated, and the discrete shear stress parameters which modulate the expression of an individual gene. More recent work in our laboratory, utilizing the differential display technique, has identified distinct patterns of gene regulation by both uniform laminar and turbulent shear stress [96]. Future work in this field will be aided by the development of additional analysis techniques which permit the simultaneous analysis of multiple variables (e.g., different genes, shear stress parameters, time scales, and potential interactions between biomechanical and biochemical stimuli).

Since a primary distinction between uniform and disturbed laminar shear stress is the existence of significant shear stress gradients, such gradients may comprise important force parameters that are detectable by mechanosensors within an endothelial cell. Future experiments will be needed to test this hypothesis, and may require the development of new models as well as analysis techniques. In addition, the relative importance of both spatial and temporal gradients in shear stress must be explored. Previous experiments by numerous groups with turbulent and pulsatile flow regimes indicate that the temporal attributes of the flow stimulus can significantly affect endothelial structure and function [12, 13, 32, 34, 102, 235, 265]. Also, on-going experiments by Frangos and colleagues with various ramp, step, and impulse flow models have demonstrated that the kinetics of the flow onset may be important in endothelial gene regulation, even at extremely short time points [266]. Thus, further characterization of the temporal and spatial shear stress parameters which alter endothelial gene expression, as well as the spectrum of genes which are regulated, should provide insights regarding the mechanisms through which endothelial cells sense their biomechanical environment.

Work in several laboratories is currently aimed at identifying putative cellular mechanosensors by tracing the signal transduction pathways involved in gene regulation by fluid shear stress. Specific endothelial cell components and organelles, including the cytoskeleton, stretch activated ion channels, plasma membrane coupled G-proteins, and calveolae, have been

proposed either as the specific intracellular sites of mechanotransduction or as the transducers themselves. Alternatively, such signaling might be mediated through cellular structures which remain unidentified as yet. Conceivably, energy transfer from the moving fluid could be imparted to the cell via conformational alterations in specific cell surface proteins, changing from one energy state to another, with resultant activation of the protein as well as downstream signaling mechanisms. Most of these models, however, assign the task of mechanotransduction to a single structure, and it is difficult to envision one mechanosensor mediating the diverse array of endothelial cell responses to shear stress. In this regard, reductionist experimental approaches may not be the most suitable avenues of investigation. Instead, integrated network analyses may be more appropriate, and future work may need to incorporate concepts from systems engineering in the analysis of cellular signal transduction. In certain time scales (acute, intermediate, or chronic responses), one type of mechanosensor may predominate, while under other conditions, other mechanisms may be important.

The knowledge gained from characterization of important shear stress parameters which regulate endothelial gene regulation *in vitro*, and even future identification of putative shear stress mechanosensing mechanisms, must ultimately be tested in *in vivo* models and investigated in human disease processes. Transgenic mouse models should provide powerful tools for analyzing the roles of certain genes and hemodynamic parameters in disease development. In other animal models, alterations in shear stress magnitudes and spatial gradients have been studied by introducing anatomic modifications, and the effects of the temporal shear stress components may be investigated in future experiments with the use of artificial pump devices to either remove the pulsatile component of the blood flow or create experimental flow patterns. Most importantly, experiments in such models incorporate all of the variables of the complex *in vivo* environment which can not be fully replicated *in vitro*, and provide a bridge to understanding how hemodynamics can directly affect human health and disease. Knowledge of the underlying mechanisms through which cells and tissues sense and respond to their biomechanical environment will hopefully lead to the identification of interventional and even preventative measures for the treatment of human vascular diseases.

While the studies presented in this thesis have focused on the specific effects of fluid shear stress on endothelial cells, it is important to recognize that most biological tissues are regularly exposed to many types of physical forces which can profoundly alter their structure and function at the cellular level. For example, compression forces exerted upon bone tissue cause changes in its structure and mass and even elicit microscopic fluid fluxes within the lacunar-canalicular system [267]. The musculature resists externally applied forces by actually generating its own counter-

forces, and unstressed muscles will eventually atrophy. In addition, physical forces may play significant roles in organismal development, even before distinct tissues have formed. In each case, a thorough understanding of the biological system must include identification of the significant force parameters which influence the tissue, how those forces are detected by the cells within the tissue, and how such stresses ultimately lead to alterations in gene expression. In this light, the rapidly growing interest in the topic of shear stress regulation of endothelial biology presumably represents just one aspect of a larger field of investigation, and the insights gained from this specialty may be transferable to studies of other biological systems.

REFERENCES

1. Frangos, J.A., editor. 1993. Physical Forces and the Mammalian Cell. Academic Press: San Diego.
2. Gimbrone, M.A., Jr. 1995. Vascular Endothelium in Health and Disease. *In* Molecular Cardiovascular Medicine. E. Haber, editor. Scientific American Medicine: New York. 49-61.
3. Fry, D.L. 1968. Acute vascular endothelial changes associated with increased blood velocity gradients. *Circ Res* 22:165-197.
4. Langille, B.L. and S.L. Adamson. 1981. Relationship between blood flow direction and endothelial cell orientation at arterial branch sites in rabbits and mice. *Circ Res* 48:481-488.
5. Nerem, R.M., M.J. Levesque, and J.F. Cornhill. 1981. Vascular endothelial morphology as an indicator of the pattern of blood flow. *J Biomech Eng* 103:172-176.
6. Langille, B.L., M.A. Reidy, and R.L. Kline. 1986. Injury and repair of endothelium at sites of flow disturbances near abdominal aortic coarctations in rabbits. *Arteriosclerosis* 6(2):146-54.
7. Levesque, M.J., D. Liepsch, S. Moravec, and R.M. Nerem. 1986. Correlation of endothelial cell shape and wall shear stress in a stenosed dog aorta. *Arteriosclerosis* 6(2):220-9.
8. Kim, D.W., A.I. Gotlieb, and B.L. Langille. 1989. *In vivo* modulation of endothelial F-actin microfilaments by experimental alterations in shear stress. *Arteriosclerosis* 9(4):439-45.
9. Tohda, K., H. Masuda, K. Kawamura, and T. Shozawa. 1992. Difference in dilatation between endothelium-preserved and -desquamated segments in the flow-loaded rat common carotid artery. *Arterioscler Thromb* 12(4):519-28.
10. Markle, R.A. and T.M. Hollis. 1981. Influence of locally altered *in vivo* shear stress on aortic histamine-forming capacity and aortic albumin uptake. *Blood Vessels* 18(1-2):45-57.
11. Skarlatos, S.I. and T.M. Hollis. 1987. Cultured bovine aortic endothelial cells show increased histamine metabolism when exposed to oscillatory shear stress. *Atherosclerosis* 64(1):55-61.
12. Frangos, J.A., S.G. Eskin, L.V. McIntire, and C.L. Ives. 1985. Flow effects on prostacyclin production by cultured human endothelial cells. *Science* 227(4693):1477-9.
13. Malek, A. and S. Izumo. 1992. Physiological fluid shear stress causes downregulation of endothelin-1 mRNA in bovine aortic endothelium. *Am J Physiol* 263(2 Pt 1):C389-96.
14. Nishida, K., D.G. Harrison, J.P. Navas, A.A. Fisher, S.P. Dockery, M. Uematsu, R.M. Nerem, R.W. Alexander, and T.J. Murphy. 1992. Molecular cloning and characterization of the constitutive bovine aortic endothelial cell nitric oxide synthase. *J Clin Invest* 90(5):2092-6.
15. Hsieh, H.J., N.Q. Li, and J.A. Frangos. 1991. Shear stress increases endothelial platelet-derived growth factor mRNA levels. *Am J Physiol* 260(2 Pt 2):H642-6.
16. Malek, A.M., G.H. Gibbons, V.J. Dzau, and S. Izumo. 1993. Fluid shear stress differentially modulates expression of genes encoding basic fibroblast growth factor and platelet-derived growth factor B chain in vascular endothelium. *J Clin Invest* 92(4):2013-21.
17. Ohno, M., J.P. Cooke, V.J. Dzau, and G.H. Gibbons. 1995. Fluid shear stress induces endothelial transforming growth factor ß-1 transcription and production. Modulation by

potassium channel blockade. *J Clin Invest* 95(3):1363-9.

18. Giddens, D.P., C.K. Zarins, and S. Glagov. 1993. The role of fluid mechanics in the localization and detection of atherosclerosis. *J Biomech Eng* 115(4B):588-94.
19. Dewey, C.F., Jr, S.R. Bussolari, M.A. Gimbrone, Jr, and P.F. Davies. 1981. The dynamic response of vascular endothelial cells to fluid shear stress. *J Biomech Eng* 103(3):177-85.
20. Eskin, S.G., C.L. Ives, L.V. McIntire, and L.T. Navarro. 1984. Response of cultured endothelial cells to steady flow. *Microvasc Res* 28(1):87-94.
21. Sdougos, H.P., S.R. Bussolari, and C.F. Dewey, Jr. 1984. Secondary flow and turbulence in a cone-and-plate device. *J Fluid Mech* 138:379-404.
22. DePaola, N. 1991. Focal and Regional Responses of Endothelium to Disturbed Flow *In Vitro*. Ph.D. Thesis, Massachusetts Institute of Technology.
23. DePaola, N., M.A. Gimbrone, Jr., P.F. Davies, and C.F. Dewey, Jr. 1992. Vascular endothelium responds to fluid shear stress gradients [published erratum appears in *Arterioscler Thromb* 1993 Mar;13(3):465]. *Arterioscler Thromb* 12(11):1254-7.
24. Tardy, Y., N. Resnick, T. Nagel, M.A. Gimbrone, Jr., and C.F. Dewey, Jr. 1997. Shear stress gradients remodel endothelial monolayers *in vitro* via a cell proliferation-migration-loss cycle. *Arterioscler Thromb Vasc Biol*, in press.
25. Remuzzi, A., C.F. Dewey, Jr, P.F. Davies, and M.A. Gimbrone, Jr. 1984. Orientation of endothelial cells in shear fields *in vitro*. *Biorheology* 21(4):617-30.
26. Levesque, M.J. and R.M. Nerem. 1985. The elongation and orientation of cultured endothelial cells in response to shear stress. *J Biomech Eng* 107(4):341-7.
27. Koslow, A.R., R.R. Stromberg, L.I. Friedman, R.J. Lutz, S.L. Hilbert, and P. Schuster. 1986. A flow system for the study of shear forces upon cultured endothelial cells. *J Biomech Eng* 108(4):338-41.
28. Viggers, R.F., A.R. Wechezak, and L.R. Sauvage. 1986. An apparatus to study the response of cultured endothelium to shear stress. *J Biomech Eng* 108(4):332-7.
29. Dewey, C.F., Jr. 1984. Effects of fluid flow on living vascular cells. *J Biomech Eng* 106(1):31-5.
30. Wechezak, A.R., R.F. Viggers, and L.R. Sauvage. 1985. Fibronectin and F-actin redistribution in cultured endothelial cells exposed to shear stress. *Lab Invest* 53(6):639-47.
31. Sato, M., M.J. Levesque, and R.M. Nerem. 1987. Micropipette aspiration of cultured bovine aortic endothelial cells exposed to shear stress. *Arteriosclerosis* 7(3):276-86.
32. Davies, P.F., A. Remuzzi, E.J. Gordon, C.F. Dewey, Jr, and M.A. Gimbrone, Jr. 1986. Turbulent fluid shear stress induces vascular endothelial cell turnover *in vitro*. *Proc Natl Acad Sci U S A* 83(7):2114-7.
33. Ando, J., H. Nomura, and A. Kamiya. 1987. The effect of fluid shear stress on the migration and proliferation of cultured endothelial cells. *Microvasc Res* 33(1):62-70.
34. Levesque, M.J., R.M. Nerem, and E.A. Sprague. 1990. Vascular endothelial cell proliferation in culture and the influence of flow. *Biomaterials* 11(9):702-7.
35. Davies, P.F., C.F. Dewey, Jr, S.R. Bussolari, E.J. Gordon, and M.A. Gimbrone, Jr. 1984. Influence of hemodynamic forces on vascular endothelial function. *In vitro* studies of shear stress and pinocytosis in bovine aortic cells. *J Clin Invest* 73(4):1121-9.

36. Grabowski, E.F., E.A. Jaffe, and B.B. Weksler. 1985. Prostacyclin production by cultured endothelial cell monolayers exposed to step increases in shear stress. *J Lab Clin Med* 105(1):36-43.

37. Diamond, S.L., S.G. Eskin, and L.V. McIntire. 1989. Fluid flow stimulates tissue plasminogen activator secretion by cultured human endothelial cells. *Science* 243(4897):1483-5.

38. Diamond, S.L., J.B. Sharefkin, C. Dieffenbach, S.K. Frasier, L.V. McIntire, and S.G. Eskin. 1990. Tissue plasminogen activator messenger RNA levels increase in cultured human endothelial cells exposed to laminar shear stress. *J Cell Physiol* 143(2):364-71.

39. Malek, A.M., R. Jackman, R.D. Rosenberg, and S. Izumo. 1994. Endothelial expression of thrombomodulin is reversibly regulated by fluid shear stress. *Circ Res* 74(5):852-60.

40. Takada, Y., F. Shinkai, S. Kondo, S. Yamamoto, H. Tsuboi, R. Korenaga, and J. Ando. 1994. Fluid shear stress increases the expression of thrombomodulin by cultured human endothelial cells. *Biochem Biophys Res Commun* 205(2):1345-52.

41. Yoshizumi, M., H. Kurihara, T. Sugiyama, F. Takaku, M. Yanagisawa, T. Masaki, and Y. Yazaki. 1989. Hemodynamic shear stress stimulates endothelin production by cultured endothelial cells. *Biochem Biophys Res Commun* 161(2):859-64.

42. Sharefkin, J.B., S.L. Diamond, S.G. Eskin, L.V. McIntire, and C.W. Dieffenbach. 1991. Fluid flow decreases preproendothelin mRNA levels and suppresses endothelin-1 peptide release in cultured human endothelial cells. *J Vasc Surg* 14(1):1-9.

43. Sterpetti, A.V., A. Cucina, A.R. Morena, D.S. Di, L.S. DAngelo, A. Cavalarro, and S. Stipa. 1993. Shear stress increases the release of interleukin-1 and interleukin-6 by aortic endothelial cells. *Surgery* 114(5):911-4.

44. Morita, T., M. Yoshizumi, H. Kurihara, K. Maemura, R. Nagai, and Y. Yazaki. 1993. Shear stress increases heparin-binding epidermal growth factor-like growth factor mRNA levels in human vascular endothelial cells. *Biochem Biophys ResCommun* 197(1):256-62.

45. Ando, J., T. Komatsuda, and A. Kamiya. 1988. Cytoplasmic calcium response to fluid shear stress in cultured vascular endothelial cells. *In Vitro Cell Dev Biol* 24(9):871-7.

46. Nollert, M.U., E.R. Hall, S.G. Eskin, and L.V. McIntire. 1989. The effect of shear stress on the uptake and metabolism of arachidonic acid by human endothelial cells. *Biochim Biophys Acta* 1005(1):72-8.

47. Nollert, M.U., S.G. Eskin, and L.V. McIntire. 1990. Shear stress increases inositol trisphosphate levels in human endothelial cells. *Biochem Biophys Res Commun* 170(1):281-7.

48. Ohno, M., G.H. Gibbons, V.J. Dzau, and J.P. Cooke. 1993. Shear stress elevates endothelial cGMP. Role of a potassium channel and G protein coupling. *Circulation* 88(1):193-7.

49. Gudi, S.R.P., C.B. Clark, and J.A. Frangos. 1996. Fluid flow rapidly activates G proteins in human endothelial cells. *Circ Res* 79:834-839.

50. Tseng, H., T.E. Peterson, and B.C. Berk. 1995. Fluid shear stress stimulates mitogen-activated protein kinase in endothelial cells. *Circ Res* 77(5):869-78.

51. Hsieh, H.-J., C.-C. Cheng, and S.-T. Wu. 1997. Increase of reactive oxygen species (ROS) in endothelial cells by shear flow and involvement of ROS in shear-induced c-*fos* expression. *Microcirculation* 4(1):A167.

52. Resnick, N., T. Collins, W. Atkinson, D.T. Bonthron, C.F. Dewey, Jr, and M.A. Gimbrone, Jr. 1993. Platelet-derived growth factor B chain promoter contains a cis-acting fluid shear-stress-responsive element [published erratum appears in *Proc Natl Acad Sci U S A* 1993 Aug 15;90(16):7908]. *Proc Natl Acad Sci U S A* 90(10):4591-5.

53. Khachigian, L.M., N. Resnick, M.A. Gimbrone, Jr., and T. Collins. 1995. Nuclear factor-κB interacts functionally with the platelet-derived growth factor B-chain shear-stress response element in vascular endothelial cells exposed to fluid shear stress. *J Clin Invest* 96(2):1169-75.

54. Shyy, J.Y., M.C. Lin, J. Han, Y. Lu, M. Petrime, and S. Chien. 1995. The cis-acting phorbol ester "12-O-tetradecanoylphorbol 13-acetate"-responsive element is involved in shear stress-induced monocyte chemotactic protein 1 gene expression. *Proc Natl Acad Sci U S A* 92(17):8069-73.

55. Khachigian, L.M., K.R. Anderson, N.J. Halnon, M.A. Gimbrone, Jr., N. Resnick, and T. Collins. 1997. Egr-1 is activated in endothelial cells exposed to fluid shear stress and interacts with a novel shear-stress response element in the PDGF A-chain promoter. *Arterioscler Thromb Vasc Biol*, in press.

56. Lin, M.-C., F. Almus-Jacobs, H.-H. Chen, G.C.N. Parry, N. Mackman, J.Y.-J. Shyy, and S. Chien. 1997. Shear stress induction of the tissue factor gene. *J Clin Invest* 99:737-744.

57. Collins, T., M.A. Read, A.S. Neish, M.Z. Whitley, D. Thanos, and T. Maniatis. 1995. Transcriptional regulation of endothelial cell adhesion molecules: NF-κB and cytokine-inducible enhancers. *FASEB J* 9(10):899-909.

58. Springer, T.A. 1994. Traffic signals for lymphocyte recirculation and leukocyte emigration: The multistep paradigm. *Cell* 76:301-314.

59. Albelda, S.M. 1993. Biology of disease; role of integrins and other cell adhesion molecules in tumor progression and metastasis. *Lab Invest* 68(1):4-17.

60. Hammer, D.A. and S.M. Apte. 1992. Simulation of cell rolling and adhesion on surfaces in shear flow: general results and analysis of selectin-mediated neutrophil adhesion. *Biophys J* 63(1):35-57.

61. Hammer, D.A., L.A. Tempelman, and S.M. Apte. 1993. Statistics of cell adhesion under hydrodynamic flow: simulation and experiment. *Blood Cells* 19(2):261-75; discussion 275-7.

62. Goetz, D.J., M.E. el-Sabban, B.U. Pauli, and D.A. Hammer. 1994. Dynamics of neutrophil rolling over stimulated endothelium *in vitro*. *Biophys J* 66(6):2202-9.

63. Alon, R., D.A. Hammer, and T.A. Springer. 1995. Lifetime of the P-selectin-carbohydrate bond and its response to tensile force in hydrodynamic flow [published erratum appears in *Nature* 1995 Sep 7;376(6544):86]. *Nature* 374(6522):539-42.

64. Luscinskas, F.W. 1997. The Endothelium in Leukocyte Recruitment, in Adhesion Molecules in Allergic Disease. B.S. Bochner, Editor. Marcel Dekker, Inc.: New York. p. 25-41.

65. Carlos, T.M. and J.M. Harlan. 1994. Leukocyte-endothelial adhesion molecules. *Blood* 84(7):2068-2101.

66. Cotran, R.S., V. Kumar, and S.L. Robbins. 1989. Robbins Pathologic Basis of Disease, 4th edition. Philadelphia: W. B. Saunders Company.

67. Staunton, D.E., V.J. Merluzzi, R. Rothlein, R. Barton, S.D. Marlin, and T.A. Springer. 1989. A cell adhesion molecule, ICAM-1, is the major surface receptor for rhinoviruses. *Cell* 56(5):849-53.

68. Greve, J.M., G. Davis, A.M. Meyer, C.P. Forte, S.C. Yost, C.W. Marlor, M.E. Kamarck, and A. McClelland. 1989. The major human rhinovirus receptor is ICAM-1. *Cell* 56(5):839-47.

69. Berendt, A.R., D.L. Simmons, J. Tansey, C.I. Newbold, and K. Marsh. 1989. Intercellular adhesion molecule-1 is an endothelial cell adhesion receptor for Plasmodium falciparum. *Nature* 341(6237):57-9.

70. Ockenhouse, C.F., T. Tegoshi, Y. Maeno, C. Benjamin, M. Ho, K.E. Kan, Y. Thway, K. Win, M. Aikawa, and R.R. Lobb. 1992. Human vascular endothelial cell adhesion receptors for Plasmodium falciparum-infected erythrocytes: roles for endothelial leukocyte adhesion molecule 1 and vascular cell adhesion molecule 1. *J Exp Med* 176(4):1183-9.

71. Rice, G.E. and M.P. Bevilacqua. 1989. An inducible endothelial cell surface glycoprotein mediates melanoma adhesion. *Science* 246(4935):1303-6.

72. Billaud, M., A. Calendar, M.-M. Seigneurin, and G.M. Lenoir. 1987. LFA-1, LFA-3, and ICAM-1 expression in Burkitt's lymphoma. *Lancet* ii:1327-1328.

73. Stauder, R., R. Greil, T.F. Schultz, J. Thaler, C. Gattringer, T. Radaskiewicz, M.P. Dierich, and H. Huber. 1989. Expression of leukocyte function-associated antigen-1 and 7F7-antigen, an adhesion molecule related to intercellular adhesion molecule-1 (ICAM-1) in non-Hodgkin lymphomas and leukaemias: Possible influence on growth pattern and leukaemic behaviour. *Clin Exp Immunol* 77:234-238.

74. Natali, P., M.R. Nicorta, R. Cavaliere, A. Bigotti, G. Romano, M. Temponi, and S. Ferrone. 1990. Differential expression of intercellular adhesion molecule 1 in primary and metastatic melanoma lesions. *Cancer Res* 50:1271-1278.

75. Johnson, J.P., B.G. Stade, B. Holzmann, W. Schwable, and G. Riethmuller. 1989. *De novo* expression of intercellular-adhesion molecule 1 in melanoma correlates with increased risk of metastasis. *Proc Natl Acad Sci U S A* 86:641-644.

76. van de Stolpe, A. and P.T. van der Saag. 1996. Intercellular adhesion molecule-1. *J Mol Med* 74(1):13-33.

77. Marazuela, M., A.A. Postigo, A. Acevedo, F. Diaz-Gonzalez, F. Sanchez-Madrid, and M.O. de Landazuri. 1994. Adhesion molecules from the LFA-1/ICAM-1,3 and VLA-4/VCAM-1 pathways on T lymphocytes and vascular endothelium in Graves' and Hashimoto's thyroid glands. *Eur J Immunol* 24(10):2483-90.

78. Stoll, G., S. Jander, S. Jung, J. Archelos, T. Tamatani, M. Mayasaka, K.V. Toyka, and H. H.-P. 1993. Macrophages and endothelial cells express intercellular adhesion molecule-1 in immune-mediated demyelination but not in Wallerian degeneration of the rat peripheral nervous system. *Lab Invest* 68(6):637-644.

79. Yoshida, M., W.F. Westlin, N. Wang, D.E. Ingber, A. Rosenzweig, N. Resnick, and M.A. Gimbrone, Jr. 1996. Leukocyte adhesion to vascular endothelium induces E-selectin linkage to the actin cytoskeleton. *J Cell Bio* 133(2):445-55.

80. Gerrity, R.G., H.K. Naito, M. Richardson, and C.J. Schwartz. 1979. Dietary induced atherogenesis in swine. *Am J Pathol* 95:775-785.

81. Joris, T., J.J. Nunnari, F.J. Krolikowski, and G. Majno. 1983. Studies on the pathogenesis of atherosclerosis. I. Adhesion and emigration of mononuclear cells in the aorta of

hypercholesterolemic rats. *Am J Pathol* 113:341-358.

82. Faggiotto, A., R. Ross, and L. Harker. 1984. Studies of hypercholesterolemia in the nonhuman primates. I. Changes that lead to fatty streak formation. *Arteriosclerosis* 4:323-340.

83. Gimbrone, M.A., Jr., N. Kume, and M.I. Cybulsky. 1993. Vascular endothelial dysfunction and the pathogenesis of atherosclerosis. *Atheroscler Rev* 25:1-9.

84. Cybulsky, M.I. and M.A. Gimbrone, Jr. 1991. Endothelial expression of a mononuclear leukocyte adhesion molecule during atherogenesis. *Science* 251(4995):788-91.

85. Endres, M., U. Laufs, H. Merz, and M. Kaps. 1997. Focal expression of intercellular adhesion molecule-1 in the human carotid bifurcation. *Stroke* 28(1):77-82.

86. O'Brien, K.D., T.O. McDonald, A. Chait, M.D. Allen, and C.E. Alpers. 1996. Neovascular expression of E-selectin, intercellular adhesion molecule-1, and vascular cell adhesion molecule-1 in human atherosclerosis and their relation to intimal leukocyte content. *Circulation* 93(4):672-82.

87. Johnson-Tidey, R.R., J.L. McGregor, P.R. Taylor, and R.N. Poston. 1994. Increase in the adhesion molecule P-selectin in endothelium overlying atherosclerotic plaques. Coexpression with intercellular adhesion molecule-1. *Am J Pathol* 144(5):952-61.

88. Gimbrone, M.A., Jr., T. Nagel, and J.N. Topper. 1997. Biomechanical activation: An emerging paradigm in endothelial adhesion biology. *J Clin Invest* 99(8):1809-1813.

89. Gimbrone, M.A., Jr. 1976. Culture of vascular endothelium. *In* Progress in Hemostasis and Thrombosis. T. Spaet, editor. Vol 3. Grune and Stratton, Inc.: New York. 1-28.

90. Rothlein, R. and T.A. Springer. 1986. The requirement for lymphocyte function-associated antigen 1 in homotypic leukocyte adhesion stimulated by phorbol ester. *J Exp Med* 163:1132-1149.

91. Sambrook, J., E.F. Fritsch, and T. Maniatis. 1989. Molecular Cloning: A Laboratory Manual. Cold Spring Harbor Laboratories: Plainview, NY.

92. Ling, S.C., H.B. Atabek, D.L. Fry, D.J. Patel, and J.S. Janicki. 1968. Application of heated-film velocity and shear probes to hemodynamic studies. *Circ Res* 23:789-801.

93. Bevilacqua, M.P. and R.M. Nelson. 1993. Selectins. *J Clin Invest* 91(2):379-87.

94. Pober, J.S., M.A. Gimbrone, Jr., L.A. Lapierre, D.L. Mendrick, W. Fiers, R. Rothlein, and T.A. Springer. 1986. Overlapping patterns of activation of human endothelial cells by interleukin 1, tumor necrosis factor and immune interferon. *J. Immunol.* 137:1893-1896.

95. Osborn, L., C. Hession, R. Tizard, C. Vassallo, S. Luhowskyj, G. Chi-Rosso, and R. Lobb. 1989. Direct expression cloning of vascular cell adhesion molecule 1, a cytokine-induced endothelial protein that binds to lymphocytes. *Cell* 59(6):1203-11.

96. Topper, J.N., J. Cai, D. Falb, and M.A. Gimbrone, Jr. 1996. Identification of vascular endothelial genes differentially responsive to fluid mechanical stimuli: cyclooxygenase-1, manganese superoxide dismutase, and endothelial cell nitric oxide synthase are selectively up-regulated by steady laminar shear stress. *Proc Natl Acad Sci U S A* 93:10417-10422.

97. Nagel, T., S.M. Wasserman, N. Resnick, J.N. Topper, and M.E. Gerritsen. 1996. Transcriptional upregulation of endothelial ICAM-1 by laminar shear stress. *J Vasc Res* 33(Suppl 1):71.

98. Ledebur, H.C. and T.P. Parks. 1995. Transcriptional regulation of the intercellular adhesion

molecule-1 gene by inflammatory cytokines in human endothelial cells. *J Biol Chem* 270(2):933-943.

99. Jahnke, A., A. van de Stolpe, E. Caldenhoven, and J.P. Johnson. 1995. Constitutive expression of human intercellular adhesion molecule-1 (ICAM-1) is regulated by differentially active enhancing and silencing elements. *Eur J Biochem* 228:439-446.

100. Nagel, T., N. Resnick, W.J. Atkinson, C.F. Dewey, Jr., and M.A. Gimbrone, Jr. 1994. Shear stress selectively upregulates intercellular adhesion molecule-1 expression in cultured human vascular endothelial cells. *J Clin Invest* 94(2):885-91.

101. Tsuboi, H., J. Ando, R. Korenaga, Y. Takada, and A. Kamiya. 1995. Flow stimulates ICAM-1 expression time and shear stress dependently in cultured human endothelial cells. *Biochem Biophys Res Commun* 206(3):988-96.

102. Morigi, M., C. Zoja, M. Figliuzzi, M. Foppolo, G. Micheletti, M. Bontempelli, M. Saronni, G. Remuzzi, and A. Remuzzi. 1995. Fluid shear stress modulates surface expression of adhesion molecules by endothelial cells. *Blood* 85(7):1696-703.

103. Sampath, R., G.L. Kukielka, C.W. Smith, S.G. Eskin, and L.V. McIntire. 1995. Shear stress-mediated changes in the expression of leukocyte adhesion receptors on human umbilical vein endothelial cells *in vitro*. *Ann Biomed Eng* 23(3):247-56.

104. Bevilacqua, M.P., R.M. Nelson, G. Mannori, and O. Cecconi. 1994. Endothelial-leukocyte adhesion molecules in human disease. *Annu Rev Med* 45:361-78.

105. Chappell, D.C., R.M. Nerem, R.M. Medford, and R.W. Alexander. 1996. Oscillatory flow upregulates adhesion molecule expression in human endothelial cells. *J Vasc Res* 33(Suppl 1):14.

106. Ohtsuka, A., J. Ando, R. Korenaga, A. Kamiya, N. Toyama-Sorimachi, and M. Miyasaka. 1993. The effect of flow on the expression of vascular adhesion molecule-1 by cultured mouse endothelial cells. *Biochem Biophys Res Commun* 193(1):303-10.

107. Ando, J., H. Tsuboi, R. Korenaga, Y. Takada, N. Toyama-Sorimachi, M. Miyasaka, and A. Kamiya. 1994. Shear stress inhibits adhesion of cultured mouse endothelial cells to lymphocytes by downregulating VCAM-1 expression. *Am J Physiol* 267(3 Pt 1):C679-87.

108. Korenaga, R., K. Kosaki, M. Isshiki, J. Ando, and A. Kamiya. 1997. Negative transcriptional regulation of the VCAM-1 gene by fluid shear stress in mouse endothelial cells. *FASEB J* 11(3):A223.

109. Varner, S.E., R.M. Nerem, R.M. Medford, and R.W. Alexander. 1994. Laminar shear stress regulates VCAM-1 gene expression and transcription in human vascular endothelial cells. *Ann Biomed Eng* 22(Suppl 1):40.

110. Tsao, P.S., R. Buitrago, J.R. Chan, and J.P. Cooke. 1996. Fluid flow inhibits endothelial adhesiveness. Nitric oxide and transcriptional regulation of VCAM-1. *Circulation* 94(7):1682-9.

111. Gonzales, R.S. and T.M. Wick. 1996. Hemodynamic modulation of monocytic cell adherence to vascular endothelium. *Ann Biomed Eng* 24(3):382-93.

112. Walpola, P.L., A.I. Gotlieb, M.I. Cybulsky, and B.L. Langille. 1995. Expression of ICAM-1 and VCAM-1 and monocyte adherence in arteries exposed to altered shear stress [published erratum appears in *Arterioscler Thromb Vasc Biol* 1995 Mar;15(3):429]. *Arterioscler Thromb Vasc Biol* 15(1):2-10.

113. Karino, T., T. Asakura, and S. Mabuchi. 1988. Flow patterns and preferred sites of

atherosclerosis in human coronary and cerebral arteries. *In* Role of Blood Flow in Atherogenesis. Yoshida, Y., T. Yamaguchi, C. G. Caro, S. Glagov, and R. M. Nerem, editors. Springer-Verlag: Tokyo. p. 67-72.

114. Wang, N., J.P. Butler, and D.E. Ingber. 1993. Mechanotransduction across the cell surface and through the cytoskeleton. *Science* 260:1124-1127.

115. Texon, M. 1957. A hemodynamic concept of atherosclerosis, with particular reference to coronary occlusion. *Arch Intern Med* 99:418-427.

116. Imparato, A.M., J.W. Lord, Jr., M. Texon, and M. Helpern. 1961. Experimental atherosclerosis produced by alteration of blood vessel configuration. *Surg Forum* 12:245-247.

117. Gyurko, G. and M. Szabo. 1969. Experimental investigations of the role of hemodynamic factors in formation of intimal changes. *Surgery* 66(5):871-874.

118. Caro, C.G., J.M. Fitz-Gerald, and R.C. Schroter. 1969. Arterial wall shear and distribution of early atheroma in man. *Nature* 223:1159-1161.

119. Friedman, M.H., V. O'Brien, and L.W. Ehrlich. 1975. Calculations of pulsatile flow through a branch: implications for the hemodynamics of atherogenesis. *Circ Res* 36(2):277-85.

120. Friedman, M.H., G.M. Hutchins, C.B. Bargeron, O.J. Deters, and F.F. Mark. 1981. Correlation between intimal thickness and fluid shear in human arteries. *Atherosclerosis* 39(3):425-36.

121. Friedman, M.H., G.M. Hutchins, C.B. Bargeron, O.J. Deters, and F.F. Mark. 1981. Correlation of human arterial morphology with hemodynamic measurements in arterial casts. *J Biomech Eng* 103(3):204-7.

122. Zarins, C.K., D.P. Giddens, B.K. Bharadvaj, V.S. Sottiurai, R.F. Mabon, and S. Glagov. 1983. Carotid bifurcation atherosclerosis. Quantitative correlation of plaque localization with flow velocity profiles and wall shear stress. *Circ Res* 53(4):502-14.

123. Ku, D.N., D.P. Giddens, C.K. Zarins, and S. Glagov. 1985. Pulsatile flow and atherosclerosis in the human carotid bifurcation. Positive correlation between plaque location and low oscillating shear stress. *Arteriosclerosis* 5(3):293-302.

124. Anayiotos, A.S., S.A. Jones, D.P. Giddens, S. Glagov, and C.K. Zarins. 1994. Shear stress at a compliant model of the human carotid bifurcation. *J Biomech Eng* 116(1):98-106.

125. Ku, D.N., S. Glagov, J.E.J. Moore, and C.K. Zarins. 1989. Flow patterns in the abdominal aorta under simulated postprandial and exercise conditions: an experimental study. *J Vasc Surg* 9(2):309-16.

126. Moore, J.E., Jr., D.N. Ku, C.K. Zarins, and S. Glagov. 1992. Pulsatile flow visualization in the abdominal aorta under differing physiologic conditions: implications for increased susceptibility to atherosclerosis [published erratum appears in *J Biomech Eng* 1993 Feb;115(1):12]. *J Biomech Eng* 114(3):391-7.

127. Pedersen, E.M., H.W. Sung, A.C. Burlson, and A.P. Yoganathan. 1993. Two-dimensional velocity measurements in a pulsatile flow model of the normal abdominal aorta simulating different hemodynamic conditions. *J Biomech* 26(10):1237-47.

128. Karino, T. and M. Motomiya. 1983. Flow visualization in isolated transparent natural blood vessels. *Biorheology* 20(2):119-27.

129. Motomiya, M. and T. Karino. 1984. Flow patterns in the human carotid artery bifurcation.

Stroke 15(1):50-6.

130. Fukushima, T., T. Karino, and H.L. Goldsmith. 1985. Disturbances of flow through transparent dog aortic arch. *Heart Vessels* 1(1):24-8.

131. Karino, T. 1986. Microscopic structure of disturbed flows in the arterial and venous systems, and its implication in the localization of vascular diseases. *Int Angiol* 5(4):297-313.

132. Asakura, T. and T. Karino. 1990. Flow patterns and spatial distribution of atherosclerotic lesions in human coronary arteries. *Circ Res* 66(4):1045-66.

133. Karino, T., M. Motomiya, and H.L. Goldsmith. 1990. Flow patterns at the major T-junctions of the dog descending aorta. *J Biomech* 23(6):537-48.

134. Perktold, K., H. Florian, D. Hilbert, and R. Peter. 1988. Wall shear stress distribution in the human carotid siphon during pulsatile flow. *J Biomech* 21(8):663-671.

135. Perktold, K. and R. Peter. 1990. Numerical 3D-stimulation of pulsatile wall shear stress in an arterial T-bifurcation model. *J Biomed Eng* 12(1):2-12.

136. Perktold, K., M. Resch, and R.O. Peter. 1991. Three-dimensional numerical analysis of pulsatile flow and wall shear stress in the carotid artery bifurcation. *J Biomech* 24(6):409-20.

137. Perktold, K., R.M. Nerem, and R.O. Peter. 1991. A numerical calculation of flow in a curved tube model of the left main coronary artery. *J Biomech* 24(3-4):175-89.

138. Perktold, K., M. Resch, and H. Florian. 1991. Pulsatile non-Newtonian flow characteristics in a three-dimensional human carotid bifurcation model. *J Biomech Eng* 113(4):464-75.

139. Perktold, K., E. Thurner, and T. Kenner. 1994. Flow and stress characteristics in rigid walled and compliant carotid artery bifurcation models. *Med Biol Eng Comput* 32(1):19-26.

140. Perktold, K. and M. Resch. 1990. Numerical flow studies in human carotid artery bifurcations: basic discussion of the geometric factor in atherogenesis. *J Biomed Eng* 12:111-123.

141. Perktold, K., R.O. Peter, M. Resch, and G. Langs. 1991. Pulsatile non-Newtonian blood flow in three-dimensional carotid bifurcation models: a numerical study of flow phenomena under different bifurcation angles. *J Biomed Eng* 13(6):507-15.

142. DeSyo, D. 1989. Radiogrammetric analysis of carotid bifurcation: Hemodynamic-atherogenetic repercussions on surgical practice. *In* Proceedings of the 2nd International Symposium on Biofluid Mechanics and Biorheology. Munich.

143. Bargeron, C.B., G.M. Hutchins, G.W. Moore, O.J. Deters, F.F. Mark, and M.H. Friedman. 1986. Distribution of the geometric parameters of human aortic bifurcations. *Arteriosclerosis* 6(1):109-13.

144. Ku, D.N., C.L. Biancheri, R.I. Pettigrew, J.W. Peifer, C.P. Markou, and H. Engels. 1990. Evaluation of magnetic resonance velocimetry for steady flow. *J Biomech Eng* 112:464-472.

145. Klanchar, M., J.M. Tarbell, and D.M. Wang. 1990. *In vitro* study of the influence of radial wall motion on wall shear stress in an elastic tube model of the aorta. *Circ Res* 66(6):1624-35.

146. Dutta, A., D.M. Wang, and J.M. Tarbell. 1992. Numerical analysis of flow in an elastic artery model. *J Biomech Eng* 114(1):26-33.

147. Reidy, M.A. and D.E. Bowyer. 1977. Scanning electron microscopy of arteries. The morphology of aortic endothelium in haemodynamically stressed areas associated with

branches. *Atherosclerosis* 26(2):181-94.

148. Greenhill, N.S. and W.E. Stehbens. 1981. Scanning electron-microscopic study of the anastomosed vein of arteriovenous fistulae. *Atherosclerosis* 39(3):383-93.

149. Hutchison, K.J. 1991. Endothelial cell morphology around graded stenoses of the dog common carotid artery. *Blood Vessels* 28(5):396-406.

150. Okano, M. and Y. Yoshida. 1992. Endothelial cell morphometry of atherosclerotic lesions and flow profiles at aortic bifurcations in cholesterol fed rabbits. *J Biomech Eng* 114(3):301-8.

151. Bender, J.R., M.M. Sadeghi, C. Watson, S. Pfau, and R. Pardi. 1994. Heterogeneous activation thresholds to cytokines in genetically distinct endothelial cells: evidence for diverse transcriptional responses. *Proc Natl Acad Sci U S A* 91(9):3994-8.

152. Varner, S.E., R.M. Nerem, R.W. Alexander, and R.M. Medford. 1996. Differential suppression of inducible endothelial VCAM-1 gene expression and NF-κB activation by laminar shear stress. *J Vasc Res* 33(Suppl 1):103.

153. Siebenlist, U., G. Franzoso, and K. Brown. 1994. Structure, regulation and function of NF-κB. *Annu Rev Cell Biol* 10:405-455.

154. Du, W., I. Mills, and B.E. Sumpio. 1995. Cyclic strain causes heterogeneous induction of transcription factors, AP-1, cre binding protein and NF-κB in endothelial cells - species and vascular bed diversity. *J Biomech* 28(12):1485-1491.

155. Lindner, V. and T. Collins. 1996. Expression of NF-κB and IκB-α by aortic endothelium in an arterial injury model. *Am J Pathol* 148(2):427-38.

156. Ueberla, K., Y. Lu, E. Chung, and W.A. Haseltine. 1993. The NF-κB p65 promoter. *J Acquir Immune Defic Syndr* 6(3):227-30.

157. Read, M.A., M.Z. Whitley, A.J. Williams, and T. Collins. 1994. NF-κB and IκB-α: an inducible regulatory system in endothelial activation. *J Exp Med* 179(2):503-12.

158. Henkel, T., R. Zabel, K. vanZee, J.M. Muller, E. Fanning, *et al.* 1992. Intramolecular masking of the nuclear localization signal and dimerization domain in the precursor for the p50 NF-κB subunit. *Cell* 68:1121-1133.

159. Ganchi, P.A., S.-C. Sun, W.C. Greene, and D.W. Ballard. 1992. IκB/MAD-3 masks the nuclear localization signal of NF-κB p65 and requires the transactivation domain to inhibit NF-κB p65 DNA binding. *Mol Cell Biol* 3:1339-1352.

160. Henkel, T., I. Alkalay, T. Machleidt, M. Kronke, Y. Ben-Neriah, *et al.* 1993. Rapid proteolytic degradation of IκB-α induced by stimulation of cells with phorbol ester, cytokines, and lipopolysaccharide is a necessary step in the activation of NF-κB. *Nature* 365:182-185.

161. Miyamoto, S., M. Maki, M.J. Schmitt, M. Hatanaka, and I.M. Verma. 1994. Tumor necrosis factor-α-induced phosphorylation of IκB-α is a signal for its degradation but not dissociation from NF-κB. *Proc Natl Acad Sci U S A* 91:12740-12744.

162. Lin, Y.-C., K. Brown, and U. Siebenlist. 1995. Activation of NF-κB requires proteolysis of the inhibitor IκB-α: signal-induced phosphorylation of IκB-α alone does not release active NF-κB. *Proc Natl Acad Sci U S A* 92:552-556.

163. Read, M.A., A.S. Neish, F.W. Luscinskas, V.J. Palombella, T. Maniatis, and T. Collins. 1995. The proteasome pathway is required for cytokine-induced endothelial-leukocyte adhesion molecule expression. *Immunity* 2(5):493-506.

164. Matthews, J.R., N. Wakasugi, J.L. Virelizier, J. Yodoi, and R.T. Hay. 1992. Thioredoxin regulates the DNA binding activity of NF-κB by reduction of a disulphide bond involving cysteine 62. *Nucleic Acids Res* 20(15):3821-30.

165. Toledano, M.B., D. Ghosh, F. Trinh, and W.J. Leonard. 1993. N-terminal DNA-binding domains contribute to differential DNA-binding specificities of NF-κB p50 and p65. *Mol Cell Biol* 13(2):852-60.

166. Shono, T., M. Ono, H. Izumi, S.I. Jimi, K. Matsushima, T. Okamoto, K. Kohno, and M. Kuwano. 1996. Involvement of the transcription factor NF-κB in tubular morphogenesis of human microvascular endothelial cells by oxidative stress. *Mol Cell Biol* 16(8):4231-9.

167. Das, K.C., Y. Lewis-Molock, and C.W. White. 1995. Thiol modulation of TNF-α and IL-1 induced MnSOD gene expression and activation of NF-κB. *Mol Cell Biochem* 148(1):45-57.

168. Mitomo, K., K. Nakayama, K. Fujimoto, X. Sun, S. Seki, and K. Yamamoto. 1994. Two different cellular redox systems regulate the DNA-binding activity of the p50 subunit of NF-κB *in vitro*. *Gene* 145(2):197-203.

169. Xanthoudakis, S., G. Miao, F. Wang, Y.C. Pan, and T. Curran. 1992. Redox activation of Fos-Jun DNA binding activity is mediated by a DNA repair enzyme. *EMBO J* 11(9):3323-35.

170. Resnick, N. and M.A. Gimbrone, Jr. 1995. Hemodynamic forces are complex regulators of endothelial gene expression. *FASEB J* 9(10):874-82.

171. Lan, Q., K.O. Mercurius, and P.F. Davies. 1994. Stimulation of transcription factors NF-κB and AP1 in endothelial cells subjected to shear stress. *Biochem Biophys Res Commun* 201(2):950-6.

172. Bonventre, J.V., V.P. Sukhatme, M. Bamberger, A.J. Ouellette, and D. Brown. 1991. Localization of the protein product of the immediate early growth response gene, Egr-1, in the kidney after ischemia and reperfusion. *Cell Regul* 2(3):251-60.

173. Petersohn, D. and G. Thiel. 1996. Role of zinc-finger proteins Sp1 and zif268/egr-1 in transcriptional regulation of the human synaptobrevin II gene. *Eur J Biochem* 239(3):827-34.

174. Thiel, G., S. Schoch, and D. Petersohn. 1994. Regulation of synapsin I gene expression by the zinc finger transcription factor zif268/egr-1. *J Biol Chem* 269(21):15294-301.

175. Brand, T., H.S. Sharma, K.E. Fleischmann, D.J. Duncker, E.O. McFalls, P.D. Verdouw, and W. Schaper. 1992. Proto-oncogene expression in porcine myocardium subjected to ischemia and reperfusion. *Circ Res* 71(6):1351-60.

176. Gupta, M.P., M. Gupta, R. Zak, and V.P. Sukhatme. 1991. Egr-1, a serum-inducible zinc finger protein, regulates transcription of the rat cardiac a-myosin heavy chain gene. *J Biol*

Chem 266(20):12813-6.

177. Sadoshima, J., L. Jahn, T. Takahashi, T.J. Kulik, and S. Izumo. 1992. Molecular characterization of the stretch-induced adaptation of cultured cardiac cells. An *in vitro* model of load-induced cardiac hypertrophy. *J Biol Chem* 267(15):10551-60.

178. Nose, K. and M. Ohba. 1996. Functional activation of the egr-1 (early growth response-1) gene by hydrogen peroxide. *Biochem J* 316(Pt 2):381-3.

179. McMahon, S.B. and J.G. Monroe. 1996. The role of early growth response gene 1 (egr-1) in regulation of the immune response. *J Leukoc Biol* 60(2):159-66.

180. Khachigian, L.M., V. Lindner, A.J. Williams, and T. Collins. 1996. Egr-1-induced endothelial gene expression: a common theme in vascular injury. *Science* 271(5254):1427-31.

181. Cao, X.M., G.R. Guy, V.P. Sukhatme, and Y.H. Tan. 1992. Regulation of the Egr-1 gene by tumor necrosis factor and interferons in primary human fibroblasts. *J Biol Chem* 267(2):1345-9.

182. Puri, P.L., M.L. Avantaggiati, V.L. Burgio, P. Chirillo, D. Collepardo, G. Natoli, C. Balsano, and M. Levrero. 1995. Reactive oxygen intermediates (ROIs) are involved in the intracellular transduction of angiotensin II signal in C2C12 cells. *Ann N Y Acad Sci* 752:394-405.

183. Rothman, A., B. Wolner, D. Button, and P. Taylor. 1994. Immediate-early gene expression in response to hypertrophic and proliferative stimuli in pulmonary arterial smooth muscle cells. *J Biol Chem* 269(9):6399-404.

184. Datta, R., N. Taneja, V.P. Sukhatme, S.A. Qureshi, R. Weichselbaum, and D.W. Kufe. 1993. Reactive oxygen intermediates target CC(A/T)6GG sequences to mediate activation of the early growth response 1 transcription factor gene by ionizing radiation. *Proc Natl Acad Sci U S A* 90(6):2419-22.

185. Huang, R.P. and E.D. Adamson. 1993. Characterization of the DNA-binding properties of the early growth response-1 (Egr-1) transcription factor: evidence for modulation by a redox mechanism. *DNA Cell Biol* 12(3):265-73.

186. Ohba, M., M. Shibanuma, T. Kuroki, and K. Nose. 1994. Production of hydrogen peroxide by transforming growth factor-beta 1 and its involvement in induction of egr-1 in mouse osteoblastic cells. *J Cell Bio* 126(4):1079-88.

187. Wollnik, B., C. Kubisch, A. Maass, H. Vetter, and L. Neyses. 1993. Hyperosmotic stress induces immediate-early gene expression in ventricular adult cardiomyocytes. *Biochem Biophys Res Commun* 194(2):642-6.

188. Akai, Y., T. Homma, K.D. Burns, T. Yasuda, K.F. Badr, and R.C. Harris. 1994. Mechanical stretch/relaxation of cultured rat mesangial cells induces protooncogenes and cyclooxygenase. *Am J Physiol* 267(2 Pt 1):C482-90.

189. Yamazaki, T., I. Komuro, and Y. Yazaki. 1995. Molecular mechanism of cardiac cellular hypertrophy by mechanical stress. *J Mol Cell Cardiol* 27(1):133-40.

190. Skerka, C., E.L. Decker, and P.F. Zipfel. 1995. A regulatory element in the human interleukin 2 gene promoter is a binding site for the zinc finger proteins Sp1 and EGR-1. *J Biol Chem* 270(38):22500-6.

191. Chaudhary, L.R., S.L. Cheng, and L.V. Avioli. 1996. Induction of early growth response-1 gene by interleukin-1ß and tumor necrosis factor-α in normal human bone marrow stromal

an osteoblastic cells: regulation by a protein kinase C inhibitor. *Mol Cell Biochem* 156(1):69-77.

192. Liebermann, D.A. and B. Hoffman. 1994. Differentiation primary response genes and proto-oncogenes as positive and negative regulators of terminal hematopoietic cell differentiation. *Stem Cells* 12(4):352-69.

193. Krishnaraju, K., H.Q. Nguyen, D.A. Liebermann, and B. Hoffman. 1995. The zinc finger transcription factor Egr-1 potentiates macrophage differentiation of hematopoietic cells. *Mol Cell Biol* 15(10):5499-507.

194. Maltzman, J.S., J.A. Carmen, and J.G. Monroe. 1996. Transcriptional regulation of the ICAM-1 gene in antigen receptor- and phorbol ester-stimulated B lymphocytes: role for transcription factor EGR1. *J Exp Med* 183(4):1747-59.

195. Maltzman, J.S., J.A. Carman, and J.G. Monroe. 1996. Role of EGR1 in regulation of stimulus-dependent CD44 transcription in B lymphocytes. *Mol Cell Biol* 16(5):2283-94.

196. Seyfert, V.L., V.P. Sukhatme, and J.G. Monroe. 1989. Differential expression of a zinc finger-encoding gene in response to positive versus negative signaling through receptor immunoglobulin in murine B lymphocytes. *Mol Cell Biol* 9(5):2083-8.

197. Seyfert, V.L., S.B. McMahon, W.D. Glenn, A.J. Yellen, V.P. Sukhatme, X.M. Cao, and J.G. Monroe. 1990. Methylation of an immediate-early inducible gene as a mechanism for B cell tolerance induction. *Science* 250(4982):797-800.

198. Khachigian, L.M., A.J. Williams, and T. Collins. 1995. Interplay of Sp1 and Egr-1 in the proximal platelet-derived growth factor A-chain promoter in cultured vascular endothelial cells. *J Biol Chem* 270(46):27679-86.

199. Cui, M.Z., G.C. Parry, P. Oeth, H. Larson, M. Smith, R.P. Huang, E.D. Adamson, and N. Mackman. 1996. Transcriptional regulation of the tissue factor gene in human epithelial cells is mediated by Sp1 and EGR-1. *J Biol Chem* 271(5):2731-9.

200. Mackman, N. 1995. Regulation of the tissue factor gene. *FASEB J* 9(10):883-9.

201. Kramer, B., A. Meichle, G. Hensel, P. Charnay, and M. Kronke. 1994. Characterization of an Krox-24/Egr-1-responsive element in the human tumor necrosis factor promoter. *Biochim Biophys Acta* 1219(2):413-21.

202. Shingu, T. and P. Bornstein. 1994. Overlapping Egr-1 and Sp1 sites function in the regulation of transcription of the mouse thrombospondin 1 gene. *J Biol Chem* 269(51):32551-7.

203. Sakamoto, K.M., C. Bardeleben, K.E. Yates, M.A. Raines, D.W. Golde, and J.C. Gasson. 1991. 5' upstream sequence and genomic structure of the human primary response gene, EGR-1/TIS8. *Oncogene* 6(5):867-71.

204. Huang, R.P. and E.D. Adamson. 1994. The phosphorylated forms of the transcription factor, Egr-1, bind to DNA more efficiently than non-phosphorylated. *Biochem Biophys Res Commun* 200(3):1271-6.

205. Bernstein, S.H., S.M. Kharbanda, M.L. Sherman, V.P. Sukhatme, and D.W. Kufe. 1991. Posttranscriptional regulation of the zinc finger-encoding EGR-1 gene by granulocyte-macrophage colony-stimulating factor in human U-937 monocytic leukemia cells: involvement of a pertussis toxin-sensitive G protein. *Cell Growth Differ* 2(6):273-8.

206. Kaetzel, D.M., Jr., R.S. Maul, B. Liu, D. Bonthron, R.A. Fenstermaker, and D.W. Coyne. 1994. Platelet-derived growth factor A-chain gene transcription is mediated by positive and

negative regulatory regions in the promoter. *Biochem J* 301(Pt 2):321-7.

207. Ebert, S.N. and D.L. Wong. 1995. Differential activation of the rat phenylethanolamine N-methyltransferase gene by Sp1 and Egr-1. *J Biol Chem* 270(29):17299-305.

208. Mutero, A., S. Camp, and P. Taylor. 1995. Promoter elements of the mouse acetylcholinesterase gene. Transcriptional regulation during muscle differentiation. *J Biol Chem* 270(4):1866-72.

209. Shyy, J.-Y. and S. Chien. 1996. The shear-induced tissue factor gene is regulated by the phosphorylation of Sp1. *Circulation* 94:I-345:A2008.

210. Innis, J.W., D.J. Moore, S.F. Kash, V. Ramamurthy, M. Sawadogo, and R.E. Kellems. 1991. The murine adenosine deaminase promoter requires an atypical TATA box which binds transcription factor IID and transcriptional activity is stimulated by multiple upstream Sp1 binding sites. *J Biol Chem* 266(32):21765-72.

211. Ackerman, S.L., A.G. Minden, G.T. Williams, C. Bobonis, and C.Y. Yeung. 1991. Functional significance of an overlapping consensus binding motif for Sp1 and Zif268 in the murine adenosine deaminase gene promoter. *Proc Natl Acad Sci U S A* 88(17):7523-7.

212. Dusing, M.R. and D.A. Wiginton. 1994. Sp1 is essential for both enhancer-mediated and basal activation of the TATA-less human adenosine deaminase promoter. *Nucleic Acids Res* 22(4):669-77.

213. Hamilton, T.B., K.C. Barilla, and P.J. Romaniuk. 1995. High affinity binding sites for the Wilms' tumour suppressor protein WT1. *Nucleic Acids Res* 23(2):277-84.

214. Lee, Y.I. and S.J. Kim. 1996. Transcriptional repression of human insulin-like growth factor-II P4 promoter by Wilms' tumor suppressor WT1. *DNA Cell Biol* 15(2):99-104.

215. Dey, B.R., V.P. Sukhatme, A.B. Roberts, M.B. Sporn, F.J.r. Rauscher, and S.J. Kim. 1994. Repression of the transforming growth factor-beta 1 gene by the Wilms' tumor suppressor WT1 gene product. *Mol Endocrinol* 8(5):595-602.

216. Rupprecht, H.D., I.A. Drummond, S.L. Madden, F.J.R. Rauscher, and V.P. Sukhatme. 1994. The Wilms' tumor suppressor gene WT1 is negatively autoregulated. *J Biol Chem* 269(8):6198-206.

217. Rackley, R.R., P.M. Kessler, C. Campbell, and B.R. Williams. 1995. In situ expression of the early growth response gene-1 during murine nephrogenesis. *J Urol* 154(2 Pt 2):700-5.

218. Russo, M.W., B.R. Sevetson, and J. Milbrandt. 1995. Identification of NAB1, a repressor of NGFI-A- and Krox20-mediated transcription. *Proc Natl Acad Sci U S A* 92(15):6873-7.

219. Svaren, J., B.R. Sevetson, E.D. Apel, D.B. Zimonjic, N.C. Popescu, and J. Milbrandt. 1996. NAB2, a corepressor of NGFI-A (Egr-1) and Krox20, is induced by proliferative and differentiative stimuli. *Mol Cell Biol* 16(7):3545-53.

220. Nagel, T., K.R. Anderson, J.N. Topper, and M.A. Gimbrone, Jr. 1997. Induction of Egr-1 gene expression and nuclear localization in cultured vascular endothelial cells axposed to laminar shear stress. *Microcirculation* 4(1):A167.

221. Sachinidis, A., K. Schulte, Y. Ko, M.K. Meyer zu Brickwedde, V. Hoppe, J. Hoppe, and H. Vetter. 1993. The induction of early response genes in rat smooth muscle cells by PDGF-AA is not sufficient to stimulate DNA-synthesis. *FEBS Lett* 319(3):221-4.

222. Feldman, S.T., D. Gately, A. Schonthal, and J.R. Feramisco. 1992. Fos expression and growth regulation in bovine corneal endothelial cells. *Invest Ophthalmol Vis Sci*

33(12):3307-14.

223. Matsuda, T., K. Okamura, Y. Sato, A. Morimoto, M. Ono, K. Kohno, and M. Kuwano. 1992. Decreased response to epidermal growth factor during cellular senescence in cultured human microvascular endothelial cells. *J Cell Physiol* 150(3):510-6.

224. Badimon, L., J.J. Badimon, W. Penny, M.W. Webster, J.H. Chesebro, and V. Fuster. 1992. Endothelium and atherosclerosis. *J Hypertens (Suppl)* 10(2):S43-50.

225. Herman, W.H. and M.S. Simonson. 1995. Nuclear signaling by endothelin-1. A Ras pathway for activation of the c-*fos* serum response element. *J Biol Chem* 270(19):11654-61.

226. Naftilan, A.J., G.K. Gilliland, C.S. Eldridge, and A.S. Kraft. 1990. Induction of the proto-oncogene c-*jun* by angiotensin II. *Mol Cell Biol* 10(10):5536-40.

227. Taubman, M.B., B.C. Berk, S. Izumo, T. Tsuda, R.W. Alexander, and B. Nadal-Ginard. 1989. Angiotensin II induces c-*fos* mRNA in aortic smooth muscle. Role of Ca2+ mobilization and protein kinase C activation. *J Biol Chem* 264(1):526-30.

228. Laniado-Schwartzman, M., Y. Lavrovsky, R.A. Stoltz, M.S. Conners, J.R. Falck, K. Chauhan, and N.G. Abraham. 1994. Activation of nuclear factor-κB and oncogene expression by 12(R)-hydroxyeicosatrienoic acid, an angiogenic factor in microvessel endothelial cells. *J Biol Chem* 269(39):24321-7.

229. Bierhaus, A., Y. Zhang, Y. Deng, N. Mackman, P. Quehenberger, M. Haase, T. Luther, M. Muller, H. Bohrer, J. Greten, and et al. 1995. Mechanism of the tumor necrosis factor-α-mediated induction of endothelial tissue factor. *J Biol Chem* 270(44):26419-32.

230. Rao, G.N. and M.S. Runge. 1996. Cyclic AMP inhibition of thrombin-induced growth in vascular smooth muscle cells correlates with decreased JNK1 activity and c-Jun expression. *J Biol Chem* 271(34):20805-10.

231. Allen, S.P., H.M. Liang, M.A. Hill, and R.L. Prewitt. 1996. Elevated pressure stimulates protooncogene expression in isolated mesenteric arteries. *Am J Physiol* 271(4 Pt 2):H1517-23.

232. Graham, J.C., G.E. Hoffman, and A.F. Sved. 1995. c-Fos expression in brain in response to hypotension and hypertension in conscious rats. *J Auton Nerv Syst* 55(1-2):92-104.

233. Sumpio, B.E., W. Du, and W.-J. Xu. 1994. Exposure of endothelial cells to cyclic strain induced c-*fos*, *fos* B and c-*jun* but not *jun* B or *jun* D and increases the transcription factor AP-1. *Endothelium* 2:149-156.

234. Lyall, F., M.R. Deehan, I.A. Greer, F. Boswell, W.C. Brown, and G.T. McInnes. 1994. Mechanical stretch increases proto-oncogene expression and phosphoinositide turnover in vascular smooth muscle cells. *J Hypertens* 12(10):1139-45.

235. Hsieh, H.J., N.Q. Li, and J.A. Frangos. 1993. Pulsatile and steady flow induces c-*fos* expression in human endothelial cells. *J Cell Physiol* 154(1):143-51.

236. Ranjan, V., R. Waterbury, Z.H. Xiao, and S.L. Diamond. 1996. Fluid shear stress induction of the transcriptional activator c-*fos* in human and bovine endothelial cells, hela, and chinese hamster ovary cells. *Biotechnol Bioeng* 49(4):383-390.

237. Yao, K.S., S. Xanthoudakis, T. Curran, and P.J. O'Dwyer. 1994. Activation of AP-1 and of a nuclear redox factor, Ref-1, in the response of HT29 colon cancer cells to hypoxia. *Mol Cell Biol* 14(9):5997-6003.

238. Rupec, R.A. and P.A. Baeuerle. 1995. The genomic response of tumor cells to hypoxia and

reoxygenation. Differential activation of transcription factors AP-1 and NF-κB. *Eur J Biochem* 234(2):632-40.

239. Webster, K.A., D.J. Discher, and N.H. Bishopric. 1994. Regulation of fos and jun immediate-early genes by redox or metabolic stress in cardiac myocytes. *Circ Res* 74(4):679-86.

240. Beiqing, L., M. Chen, and R.L. Whisler. 1996. Sublethal levels of oxidative stress stimulate transcriptional activation of c-*jun* and suppress IL-2 promoter activation in Jurkat T cells. *J Immunol* 157(1):160-9.

241. Rao, G.N., W.C. Glasgow, T.E. Eling, and M.S. Runge. 1996. Role of hydroperoxyeicosatetraenoic acids in oxidative stress-induced activating protein 1 (AP-1) activity. *J Biol Chem* 271(44):27760-4.

242. Miano, J.M., R.R. Tota, N. Vlasic, K.J. Danishefsky, and M.B. Stemerman. 1990. Early proto-oncogene expression in rat aortic smooth muscle cells following endothelial removal. *Am J Pathol* 137(4):761-5.

243. Indolfi, C., G. Esposito, E. Di Lorenzo, A. Rapacciuolo, A. Feliciello, A. Porcellini, V.E. Avvedimento, M. Condorelli, and M. Chiariello. 1995. Smooth muscle cell proliferation is proportional to the degree of balloon injury in a rat model of angioplasty. *Circulation* 92(5):1230-5.

244. Van Belle, E., C. Bauters, N. Wernert, C. Delcayre, E.P. McFadden, B. Dupuis, J.M. Lablanche, M.E. Bertrand, and B. Swynghedauw. 1995. Angiotensin converting enzyme inhibition prevents proto-oncogene expression in the vascular wall after injury. *J Hypertens* 13(1):105-12.

245. Moggio, R.A., J.Z. Ding, C.J. Smith, R.R. Tota, M.B. Stemerman, and G.E. Reed. 1995. Immediate-early gene expression in human saphenous veins harvested during coronary artery bypass graft operations. *J Thorac Cardiovasc Surg* 110(1):209-13.

246. Karin, M. 1995. The regulation of AP-1 activity by mitogen-activated protein kinases. *J Biol Chem* 270(28):16483-16486.

247. Oehler, T., A. Pintzas, S. Stumm, A. Darling, D. Gillespie, and P. Angel. 1993. Mutation of a phosphorylation site in the DNA-binding domain is required for redox-independent transactivation of AP1-dependent genes by v-Jun. *Oncogene* 8(5):1141-7.

248. Cobb, M.H. and E.J. Goldsmith. 1995. How MAP kinases are regulated. *J Biol Chem* 270(25):14843-14836.

249. Canman, C.E. and M.B. Kastan. 1996. Three paths to stress relief. *Nature* 384:213-214.

250. Deng, T. and M. Karin. 1994. *Nature* 371:171-175.

251. Smeal, T., B. Binetruy, D. Mercola, M. Birrer, and M. Karin. 1991. Phosphorylation of c-Jun and serines 63 and 73 is required for oncogenic and transcriptional cooperation with Ha-Ras. *Nature* 354:494-496.

252. Smeal, T., B. Binetruy, D. Mercola, A. Grover-Bardwick, G. Heidecker, U.R. Rapp, and M. Karin. 1992. Oncoprotein-mediated signalling cascade stimulates c-Jun activity by phosphorylation of serines 63 and 73. *Mol Cell Biol* 12:3507-3513.

253. Karin, M. 1994. Signal transduction from the cell surface to the nucleus through the phosphorylation of transcription factors. *Curr Opin Cell Biol* 6:415-424.

254. Xanthoudakis, S. and T. Curran. 1992. Identification and characterization of Ref-1, a

nuclear protein that facilitates AP-1 DNA-binding activity. *EMBO J* 11(2):653-65.

255. Walker, L.J., C.N. Robson, E. Black, D. Gillespie, and I.D. Hickson. 1993. Identification of residues in the human DNA repair enzyme HAP1 (Ref-1) that are essential for redox regulation of Jun DNA binding. *Mol Cell Biol* 13(9):5370-6.

256. Gomez del Arco, P., S. Martinez-Martinez, V. Calvo, A.L. Armesilla, and J.M. Redondo. 1996. JNK (c-Jun NH2-terminal kinase) is a target for antioxidants in T lymphocytes. *J Biol Chem* 271(42):26335-40.

257. Ranjan, V. and S.L. Diamond. 1993. Fluid shear stress induces synthesis and nuclear localization of c-Fos in cultured human endothelial cells. *Biochem Biophys Res Commun* 196(1):79-84.

258. Li, Y.S., J.Y. Shyy, S. Li, J. Lee, B. Su, M. Karin, and S. Chien. 1996. The Ras-JNK pathway is involved in shear-induced gene expression. *Mol Cell Biol* 16(11):5947-54.

259. Davies, P.F., H.G. Rennke, and R.S. Cotran. 1981. Influence of molecular charge upon the endocytosis and intracellular fate of peroxidase activity in cultured arterial endothelium. *J Cell Sci* 49:69-86.

260. Davies, P.F. 1981. Microcarrier culture of vascular endothelial cells on solid plastic beads. *Exp Cell Res* 134(2):367-76.

261. Barbee, K.A., P.F. Davies, and R. Lal. 1994. Shear stress-induced reorganization of the surface topography of living endothelial cells imaged by atomic force microscopy. *Circ Res* 74(1):163-71.

262. Barbee, K.A. 1995. Changes in surface topography in endothelial monolayers with time at confluence - influence on subcellular shear stress distribution due to flow. *Biochem Cell Biol* 73(7-8):501-505.

263. Hayashi, T., Y. Ueno, and T. Okamoto. 1993. Oxidoreductive regulation of nuclear factor-κB. Involvement of a cellular reducing catalyst thioredoxin. *J Biol Chem* 268(15):11380-8.

264. Ammendola, R., F. Fiore, F. Esposito, G. Caserta, M. Mesuraca, T. Russo, and F. Cimino. 1995. Differentially expressed mRNAs as a consequence of oxidative stress in intact cells. *FEBS Lett* 371(3):209-13.

265. Helmlinger, G., R.V. Geiger, S. Schreck, and R.M. Nerem. 1991. Effects of pulsatile flow on cultured vascular endothelial cell morphology. *J Biomech Eng* 113(2):123-31.

266. Bao, X. and F.J. A. 1996. Camparison of ramp, step and impulsive flow-induced signal transduction and gene expression in cultured human endothelial cells. *Circulation (Suppl)* 94(8):I-443.

267. Klein-Nulend, J., A. Van der Plas, C.M. Semeins, N.E. Ajubi, J.A. Frangos, P.J. Nijweide, and E.H. Burger. 1995. Sensitivity of osteocytes to biomechanical stress *in vitro*. *FASEB J* 9:441-445.

Appendices: Oncor Image Macros

In order to perform quantitative analyses of fluorescently stained endothelial monolayers (Chapter 4), it was necessary to develop image acquisition and analysis macros with the Oncor Image software package. Such automation allowed for analysis of numerous images (each experiment routinely involved over 700 images) as well as standardization of quantitation. The basic structure of each macro was composed by Lou Marek (Oncor, Inc., Gaithersburg, MD), based on my design specifications, and I subsequently extensively modified the analysis macros (NLTF.tip, Confl.tip, and NLhisto.tip). These acquisition and analysis macros are shown in detail in Appendices A - F, and the basic functions performed by each are summarized below.

Acquisition Macros

SetStageList.tip

This macro calculates and programs the stage positions necessary for acquiring images successively in a single strip (e.g., beginning at the bar within the disturbed flow field and moving toward the uniform flow region). It prompts the user to input information necessary to perform these tasks, including the objective magnification, the orientation of the strip (X or Y direction), and the number of images desired. In addition, it displays the exact image dimension (based on the objective magnification), to aid the user in determining the number of stage positions desired, and prompts the user to log that number of stage positions.

GetStrip.tip and mTimeLapseStart_Tobi.tip

Together, these two macros automate the sequential acquisition of multiple images (e.g., DAPI and Texas Red) for each image field in a strip. Before beginning these macros, the user must designate the acquisition times and filenames to which the images should be saved (SetUp menu, Modify all Modes), indicate the filters to be used (Acquire menu, MultiMode Settings), calculate the stage list (SetStageList.tip), and position the stage at the first position on the coverslip. Each image is saved under the designated filename appended with a series of numbers indicating the image position (e.g., <filename --1 ---2.dat> would refer to the first image in the second strip).

Analysis Macros

NLTF.tip

This macro computes both the average total fluorescence and average nuclear fluorescence per image for a series of image strips. The user is prompted to indicate the first DAPI image in the first image strip to be analyzed and the last Texas Red image in the last image strip. The resulting data is stored in two separate data files (total fluorescence data and nuclear localization data), and the user is prompted to designate these filenames. These files can then be opened in Microsoft Excel for final analysis and presentation of data. Note that the total fluorescence data does not exclude subconfluent images; that exclusion function is subsequently performed by Confl.tip.

Confl.tip

This macro determines whether each image is 95% confluent or not. Within an image, pixels having values below background fluorescence levels are considered devoid of cells and counted as non-confluent areas. Background fluorescence was determined from the average fluorescence of monolayers stained with rabbit IgG as the primary antibody. If an image is greater than 95% confluent, the total fluorescence value for that image is entered into the data file; if less than 95% confluent, a value of 0 is recorded.

NLhisto.tip

This macro computes the average nuclear fluorescence for individual nuclei in each image and places the resulting data into a data file designated by the user. Note that this calculation is slightly different from that performed by NLTF.tip, since NLTF.tip calculates the average nuclear fluorescence for an entire image, rather than for each individual nucleus.

Appendix A: SetStageList.tip

```
! Declare variables
decl mag float
decl/init=0.10000 stagecal float
decl/init=1.25 intermedmag float
decl numpoints int
decl ii int
decl onestep float

! Prompt user for required variables
write "Enter Objective Magnification"
read mag
du ((ccdxsize*ccdxbinning*6.8)/(intermedmag*mag*stagecal)) onestep
write "Going in X or Y direction?"
read str1
write/outst=str(0)/f="One field is %5.2f microns" (onestep*stagecal)
write str(0)
write "Enter Number of Stage Positions"
read numpoints
write/f="Have you logged %d stage positions? (y or n)"/outstring=str2 numpoints
write str2
read str2
if ((str2=="n") || (str2 == "N"))
        Say "You must log the dummy stage postions and rerun this program."
        return
endif

! Declare additional variables
decl xcoords long (numpoints)
decl ycoords long (numpoints)

! Calculate and store stage coordinates
if ((str1 == "x") || (str1 == "X"))
        for ii 1 to (numpoints-1)
                du (ii*onestep) xcoords(ii)
        endfor
else if ((str1 == "y") || (str1 == "Y"))
        for ii 1 to (numpoints-1)
                du (ii*onestep) ycoords(ii)
        endfor
else
        say "wrong answer for x or y direction"
endif

write "Coordinate List"
for ii 0 to (numpoints-1)
write (ii + 1) xcoords(ii) ycoords(ii)
endfor
```

```
for ii 0 to (numpoints-1)
        relog (ii+1) xcoords(ii) ycoords(ii) 0
endfor

savestagelist
```

Appendix B: GetStrip.tip

```
decl isit logical
vartst/exist zhere isit
if (!isit)
        decl/w zhere long
endif

say "Move to starting position"
stage/here 0 0
focus/inq zhere


! Call mTimeLapseStart_Tobi.tip
mtimelapsestart_tobi
```

Appendix C: mTimeLapseStart_Tobi.tip

```
copy 0 choice
copy keepiPar(1) choice(0)     ! continuous acq
copy keepiPar(2) choice(2)     ! process later to save time
if (choice(2) == 0) then
        copy 1 choice(1)       ! update the radio button
endif
copy keepiPar(3) choice(6)     ! save to disk
copy keepiPar(4) choice(7)     ! display images
copy cycletime par1
copy keepiPar(5) par2
copy keepiPar(6) par3
decl/l rescode int

if ((ExpName == "") && (warnCount(6) == 0)) then
        Say $
'You have not yet selected a destination for your experiment. See File Menu'
        Say $
'By default, images will be stored in the "Oncor Image:Output:" Folder'
        incr warnCount(6)
endif

! Prompt user for input
DoDialog 10049 result
if (eq result,"Cancel") then
        return
endif

if (choice(6) == 1) then
        copy .true. SaveFlag
        * Saving image to disk
else
        DoAlert/stop 'Are you sure you do not want to save' $
        'your image data to disk?' $
        ' ' ,,  rescode
        !pb rescode
        if (eq rescode,2) then
                return
        endif
        copy .false. SaveFlag
endif

if (choice(5) == 1) then
        * Saving images in Macintosh memory
        copy .true. SaveMacMem
else
        copy .false. SaveMacMem
endif
```

```
if (choice(4) == 1) then
        * Saving images in Video Bulk Memory card
        copy .true. SaveVideoMem
        du 1 BulkCount
else
        copy .false. SaveVideoMem
endif

if (choice(3) == 1) then
        DoAlert/caution 'Sorry, This system does not support an OMDR' $
        '(Real Time Opto Magnetical Disk Recorder).' $
        'Please select another option' ,,rescode
        if (eq rescode,1) then
                return
        endif
        copy .false. SaveOMDR
else
        copy .false. SaveOMDR
endif

if (choice(0)==1) then
        copy 30000 par2
endif

if (choice(7) == 1) then
        copy .true. DispIndivids
else
        copy .false. DispIndivids
endif

pb par1
du par1 cycletime
if (cycletime < 1) then
        copy 1 cycletime
endif

copy choice(0)  keepiPar(1)     ! continuous acq
copy choice(2) keepiPar(2)      ! process later to save time
copy choice(6) keepiPar(3)      ! save to disk
copy choice(7) keepiPar(4)      ! display images
copy par2 keepiPar(5)
copy par3 keepiPar(6)

do_nTimeLapse_tobi  par2 par3

if (SaveVideoMem == .true.)
        Write/f='Time lapse Movie of %d frames is stored in Movie Projector' par2
        Write/f='%s' 'Use <Save Movie> to save this movie to disk'
        OMkillobj/all 3
        OMnewobject "TLapse" 512 512 par2 3 str(0)
endif
```

Appendix D: NLTF.tip

```
! Declare variables
decl types long 4
decl ext string 2

filetype 'IMAG' types(0)
filetype 'PICT' types(1)
filetype 'TIFF' types(2)
filetype 'TEXT' types(3)

decl avgexp float
decl nucleus string
decl experimental string
decl thepath string
decl dum string
decl firststagepos int
decl laststagepos int
decl firststrip int
decl laststrip int
decl output string
decl label int
decl pixcount long
decl pixsum long

decl ii int
decl jj int
decl kk int

! Prompt user to indicate images to analyze
SFGetFile 'Pick First Strip, First Sequence, Nuclear Image' $
        str1 thePath  4 types success
if (not success) then
        return
endif
parsenm @str1 firststagepos firststrip  ext(0) nucleus

SFGetFile 'Pick Last Strip, Last Sequence, Experimental Image' $
        str1 thePath  4 types success
if (not success) then
        return
endif
parsenm @str1 laststagepos laststrip  ext(1) experimental

pb firststrip
pb laststrip
pb firststagepos
pb laststagepos
pb nucleus
pb experimental
```

```
! Declare additional variables
decl avgexps float (laststagepos) (laststrip)
decl nuclei float (laststagepos) (laststrip)
decl avgfgd float (laststagepos) (laststrip)

! Open each image in sequence and perform analyses
for ii firststagepos to laststagepos
        for jj firststrip to laststrip
                makenm @nucleus ii jj @ext(0) str(0)
                makenm @experimental ii jj @ext(1) str(1)
                write "Reading " @str(0) " and " @str(1)
        imread (@thepath//@str(0)) r1 dum dum dum
        imread (@thepath//@str(1)) r2 dum dum dum

! Compute average total fluorescence per image
saver r2 avgexps((ii-1),(jj-1))

! Compute average nuclear fluorescence per image
changeb0 512 517
gredu/autoscale r1 r1 256
thresh r1 bit8 entropy ,,
beros bit8 bit8 2 8 0
bcount bit8 pixcount
blabel bit8 r1 8 label
div label avgexps((ii-1),(jj-1)) nuclei((ii-1),(jj-1))
mul bit8 r2 r2
ssum r2 pixsum
div pixcount pixsum avgfgd((ii-1),(jj-1))

endfor
endfor

! Prompt user to input filenames and create headers for each file
write "Enter file name to save NucLoc data (without .dat)"
read str1
write/outf=@str1 "Strip" $
                "Stage" "AvgFgd"

for jj firststrip to laststrip
        for ii firststagepos to laststagepos
        write/outf=@str1/append/f="%d %d %f" jj $
                ii avgfgd((ii-1),(jj-1))

endfor
endfor

write "Enter file name to save TotFluor data (without .dat)"
read output
write/outf=@output "Strip" $
                "Stage" "AverFluor" "AvgFl/Nuc"
```

```
for jj firststrip to laststrip
        for ii firststagepos to laststagepos
        write/outf=@output/append/f="%d %d %f %f" jj $
                ii avgexps((ii-1),(jj-1)) nuclei((ii-1),(jj-1))

endfor
endfor
```

Appendix E: Confl.tip

```
! Declare variables
decl types long 4
decl okflg logical
decl ext string 2

filetype 'IMAG' types(0)
filetype 'PICT' types(1)
filetype 'TIFF' types(2)
filetype 'TEXT' types(3)

decl avgexp float
decl nucleus string
decl experimental string
decl thepath string
decl dum string
decl firststagepos int
decl laststagepos int
decl firststrip int
decl laststrip int
decl output string
decl threshout sbit/plane=5 512 517
decl pixcount long
decl confl float
decl ninety long
decl imgperc long

! Create set point of 95%
mul 0 ninety ninety
add ninety 95 ninety

! Declare additional variables
decl ii int
decl jj int
decl kk int

! Prompt user to indicate images to analyze
SFGetFile 'Pick First Strip, First Sequence, Nuclear Image' $
        str1 thePath  4 types success
if (not success) then
        return
endif
parsenm @str1 firststagepos firststrip  ext(0) nucleus

SFGetFile 'Pick Last Strip, Last Sequence, Experimental Image' $
        str1 thePath  4 types success
if (not success) then
        return
endif
```

```
parsenm @str1 laststagepos laststrip  ext(1) experimental
pb firststrip
pb laststrip
pb firststagepos
pb laststagepos
pb nucleus
pb experimental

! Declare additional variables
decl avgexps float (laststagepos) (laststrip)
decl conflTF float (laststagepos) (laststrip)
decl mult float (laststagepos) (laststrip)

! Open each image in sequence and perform analyses
for ii firststagepos to laststagepos
        for jj firststrip to laststrip
                makenm @nucleus ii jj @ext(0) str(0)
                makenm @experimental ii jj @ext(1) str(1)
                write "Reading " @str(0) " and " @str(1)
        imread (@thepath//@str(0)) r1 dum dum dum
        imread (@thepath//@str(1)) r2 dum dum dum

! Determine the percentage of pixels with values below background fluorescence
thresh r2 threshout f 250
bcount threshout pixcount
div 264704 pixcount confl 100
mul confl 1 imgperc

! Output 1 for each confluent image, 0 for each subconfluent image
if (GE imgperc ninety) then
        mul 1 1 conflTF((ii-1),(jj-1))
elseif (LE imgperc ninety)
        mul 1 0 conflTF((ii-1),(jj-1))
end

! Multiply each 1 and 0 by the average total fluorescence of that image
saver r2 avgexps((ii-1),(jj-1))
mul conflTF((ii-1),(jj-1)) $
        avgexps((ii-1),(jj-1)) mult((ii-1),(jj-1))

endfor
endfor

! Prompt user to input filenames and create headers for each file
write "Enter file name to save Confl & TF data (without .dat)"
read str1
write/outf=@str1 "Strip" $
                "Stage" ">95%_Confl" "Tot_Fluor" "ConflxTF"
```

```
for jj firststrip to laststrip
        for ii firststagepos to laststagepos
        write/outf=@str1/append/f="%d %d %f %f %f" jj $
                ii conflTF((ii-1),(jj-1)) avgexps((ii-1),(jj-1)) $
                mult((ii-1),(jj-1))

endfor
endfor
```

Appendix F: NLhisto.tip

```
! Declare variables
decl types long 4
decl ext string 2

filetype 'IMAG' types(0)
filetype 'PICT' types(1)
filetype 'TIFF' types(2)
filetype 'TEXT' types(3)

decl sumnuc float
decl avgexp float
decl nucleus string
decl experimental string
decl thepath string
decl dum string
decl firststagepos int
decl laststagepos int
decl firststrip int
decl laststrip int
decl output string
decl label int

decl ii int
decl jj int
decl kk int

! Prompt user to indicate images to analyze
SFGetFile 'Pick First Strip, First Sequence, Nuclear Image' $
        str1 thePath  4 types success
if (not success) then
        return
endif
parsenm @str1 firststagepos firststrip  ext(0) nucleus

SFGetFile 'Pick Last Strip, Last Sequence, Experimental Image' $
        str1 thePath  4 types success
if (not success) then
        return
endif
parsenm @str1 laststagepos laststrip  ext(1) experimental

pb firststrip
pb laststrip
pb firststagepos
pb laststagepos
pb nucleus
pb experimental
```

```
! Declare additional variables
decl sumnucs float (laststagepos) (laststrip)
decl avgexps float (laststagepos) (laststrip)

! Prompt user to input filenames and create headers for each file
write "Enter filename to save NuclLoc data (without .dat)"
read output

write/append/outfile=@output "Particle#" $
        "X-Coord" "Y-Coord" "TotDens" "Size" "Ratio"

! Open each image in sequence and perform analyses
for ii firststagepos to laststagepos
        for jj firststrip to laststrip
                makenm @nucleus ii jj @ext(0) str(0)
                makenm @experimental ii jj @ext(1) str(1)
                write "Reading " @str(0) " and " @str(1)
        imread (@thepath//@str(0)) r1 dum dum dum
        imread (@thepath//@str(1)) r2 dum dum dum

        ssum r1 sumnucs((ii-1),(jj-1))
        saver r2 avgexps((ii-1),(jj-1))
        write/outstrin=str(2)/f="%15.4f %15.4f %15.4f" sumnuc avgexp (sumnuc/avgexp)
        write str(2)

! Compute average nuclear fluorescence for each nucleus
changeb0 512 517
gredu/autoscale r1 r1 256
thresh r1 bit8 entropy ,,
beros bit8 bit8 2 8 0
blabel bit8 r1 8 label
mul bit8 r2 r2
dens/append r1 r2 @output

endfor
endfor
```